UNIVERSITY OF CALIFORNIA

Santa Barbara

Genetic and epigenetic regulation of a core embryonic gene regulatory network

A dissertation submitted in partial satisfaction of the

requirements for the degree Doctor of Philosophy

in Molecular, Cellular and Developmental Biology

by

Chee Kiang Ewe

Committee in charge:

Professor Joel H. Rothman, Chair

Professor Denise J. Montell

Professor William Smith

Professor Siddharth Dey

March 2022

The dissertation of Chee Kiang Ewe is approved.

_____
Denise J. Montell

_____
William Smith

_____
Siddharth Dey

_____
Joel H. Rothman, Committee Chair

January 2022

Genetic and epigenetic regulation of a core embryonic gene regulatory network

by

Chee Kiang Ewe

Acknowledgements

This dissertation would not have been possible without the help of my adviser, Joel Rothman. He provided essential guidance and expertise and has helped me to grow as a scientist. I truly appreciate that he promoted autonomy, allowing me to freely explore various and, at times, wild ideas. His passion for science is contagious. I especially enjoyed our biweekly journal club where everyone in the lab, including Joel, engaged in thought-provoking debates with unflagging curiosity.

Growing up, I had not considered pursuing a career in academia was an option for myself until I met Yamila (Yami) Torres Cleuren one evening in 2014 at the Auckland Philharmonic Orchestra concert in New Zealand. She introduced me to *C. elegans* research, and I am hooked ever since. Much to my great fortune, Joel offered me a position at UCSB as I completed my undergraduate degree at the University of Auckland. Thank you, Joel and Yami, for your unwavering support and belief in me!

I am grateful to my committee members, Denise Montell, Bill Smith, and Sid Dey for providing helpful feedback and advice on my research. I would also like to offer my heartfelt gratitude to all Rothman lab members, past and present, for being great colleagues and friends: Sage Flowers, Geneva Alok, Pradeep Joshi (PJ), Cricket Wood, Caroline Ackley, Tsunghan Yeh, Melissa Alcorn, Erik Spikard, Eric Terry, Pan Young Jeong and Sam Fiallo. And, of course, many thanks to my dedicated mentees for experimental assistance: Danny Conrad, Jessica Abesamis, Sabina Menzhausen, Grace Mellor, Austin Arnold, and David Jeong. I also want to thank all my friends in

the MCDB department and UCSB for making my time in graduate school a memorable and an enjoyable one.

I am fortunate to have three older brothers, Chee Teong, Chee Yeng and Chee Kuang, who are incredibly caring, patient, and supportive all my life. I thank you wholeheartedly! Lastly, I would like to thank my parents, Chau Hock Ewe and Soo Gnoh Chua, without whom I would be nowhere. I devoted the past five years to understanding how life begins and evolves. My life started from you, your DNA, your care, support and unconditionally love. I am forever in your debt.

Vita of Chee Kiang Ewe

January 2022

Education

Bachelor of Science (with First Class Honors in Biomedical Science), University of Auckland, New Zealand, May 2016
Doctor of Philosophy in Molecular, Cellular, and Developmental Biology, University of California, Santa Barbara, March 2022 (expected)

Professional Employment

2012-2015: Teaching Assistant, Faculty of Medical and Health Sciences and Department of Statistics, University of Auckland, New Zealand
June 2016-May 2017: Junior Specialist, Neuroscience Research Institute, University of California, Santa Barbara
September 2017-2022: Teaching Assistant, Department of MCD Biology, University of California, Santa Barbara

Publications

Torres Cleuren YN, Ewe CK, Chipman KC, Mears ER, Wood CG, Al-Alami CEA, Alcorn MR, Turner TL, Joshi PM, Snell RG, Rothman JH. Extensive intraspecies cryptic variation in an ancient embryonic gene regulatory network. Elife. 2019 Aug 15;8:e48220. doi: 10.7554/eLife.48220

Ewe CK, Torres Cleuren Y, Alok G, Rothman J. ICD-1/BTF3 antagonizes SKN-1-mediated endoderm specification in *Caenorhabditis elegans*. MicroPubl Biol. 2019 Oct 4; doi:10.17912/micropub.biology.000167

Ewe CK, Torres Cleuren YN, Rothman JH. Evolution and developmental system drift in the endoderm gene regulatory network of *Caenorhabditis* and other nematodes. Front Cell Dev Biol. 2020 Mar 18;8:170. doi:10.3389/fcell.2020.00170

Ewe CK, Torres Cleuren YN, Flowers SE, Alok G, Snell RG, Rothman JH. Natural cryptic variation in epigenetic modulation of an embryonic gene regulatory network. Proc Natl Acad Sci U S A. 2020 Jun 16;117(24):13637-13646. doi:10.1073/pnas.1920343117

Ewe CK. Dare to be different. Science. 2020 Dec 11; 370(6522):1366. doi:10.1126/science.370.6522.1366

Ewe CK, Alok G, Rothman JH. Stressful development: integrating endoderm development, stress, and longevity. Dev Biol. 2021 Mar; 471:34-48. doi:10.1016/j.ydbio.2020.12.002

Ewe CK†, Sommermann EM†, Kenchel J, Flowers SE, Maduro MF, Rothman JH. Recursive feedforward regulatory logic underlies robustness of the specification-to-differentiation transition and fidelity of terminal cell fate during C. elegans endoderm development. BioRxiv. 2021 Aug 25; doi: 10.1101/2021.08.24.457588

Flowers SE, Kothari R, Torres Cleuren YN, Alcorn MR, Ewe CK, Alok G, Joshi PM, Rothman JH. Regulation of defective mitochondrial DNA accumulation and transmission in C. elegans by the programmed cell death and aging pathways. BioRxiv. 2021 Oct 28; doi: 10.1101/2021.10.27.466108

Awards and Fellowships

The Tan Sri Dato' Seri Dr Jeffrey Cheah Entrance Scholarship, Sunway College, Malaysia, 2009
First-in-Class Award (Data Analysis), 2013
Summer Research Scholarship, University of Auckland, New Zealand, 2014
First-in-Class Award (Molecular Cell Biology and Biomedicine), 2015
Summer Research Scholarship, Australian National University, Australia, 2016
Devlin Fellowship, 2019
UCSB MCDB/BMSE Retreat & Symposium Best Poster Award, 2019
Neuroscience Research Institute Travel Award, 2020
Academic Senate Doctoral Student Travel Grant, 2020
Keystone Symposia Future of Science Fund Scholarship, 2020
UCSB Graduate Division Dissertation Fellowship, 2020
Genetic Society of America (GSA) DeLill Nasser Award, 2021
Academic Senate Doctoral Student Travel Grant, 2022
Keystone Symposia Scholarship, 2022
Tel Aviv University Postdoctoral Scholarship, 2022

Field of study

Major Field: Developmental Biology

Investigating the effects of genetic and epigenetic variations on caste determination in Honeybee (*Apis mellifera*) with (vale) Dr. Sylvain Foret and Professor Ryszard Maleszka, Australian National University

Investigating the anti-inflammatory effects of New Zealand honeys with Dr. John Taylor, University of Auckland

Abstract

Development is driven by progressive installation of transcriptional programs and complex interactions between genetic factors that constitute gene regulatory networks (GRNs). How are GRNs structured and deployed to avoid frequent catastrophic failure resulting from environmental and genetic variation? How are GRNs modified during evolution to engender Charles Darwin's "endless forms most beautiful"? In the nematode *C. elegans*, the SKN-1/Nrf transcription factor activates a GATA transcription factor-driven cascade that modulates specification and differentiation of the endoderm. We found that six GATA factors (MED-1/2, END-1/3, and ELT-2/7) form a recursive series of interlocked feedforward loops to mediate robust lockdown of endodermal cell fate. We further found that the specification-to-differentiation transition is linked through END-1 that straddles the two processes. Further, we uncovered additional role for key GATA factors as transcriptional repressors in establishing spatial gene expression domains that appear to define the boundaries of the digestive tract (Chapter 2).

With the molecular details of the endoderm GRN in hand, we subsequently explored the evolutionary diversification of the regulatory network by exploiting natural genetic variation in the *C. elegans* wild isotypes. Remarkably, we uncovered extensive intraspecies variation in SKN-1 requirement: some isotypes absolutely require SKN-1 during endoderm development, while in others most embryos differentiate endoderm in its absence. We showed that this polymorphism results from accumulation of cryptic genetic variations, including a missense variant in the transcriptional activator Pur-α

homolog, PLP-1 (Appendix II). In addition to the genetic plasticity of the GRNs, we found that SKN-1 requirement can be further tuned by a heritable epigenetic effect triggered by nutritional stress. This transgenerational epigenetic inheritance involves Piwi Argonaute, the nuclear RNAi pathway, and H3K9 methyltransferases (Chapter 3). Our results therefore demonstrate that the substantial plasticity in *C. elegans* endoderm GRN is driven by both genetic and epigenetic mechanisms.

Table of Contents

List of Figures

List of Tables

Chapter 1 : Introduction[1]

"The known is finite, the unknown infinite. Intellectually we stand on an islet in the midst of an illimitable ocean of inexplicability. Our business every generation is to reclaim a little more land"- Thomas H. Huxley

[1] Alternate form of this chapter has been published in Ewe et al., Front Cell Dev Biol (2020) and Ewe et al., Dev Biol (2021) with minor modifications.

From the moment of fertilization, embryos must follow a highly regulated script that ensures reproducible outcomes, while remaining plastic to accommodate changes that generate morphological diversity. The architectures of the gene regulatory networks (GRNs) are sculpted by, and can greatly influence, evolutionary trajectory. How are gene networks wired in ways that ensure developmental robustness? Which nodes are plastic and which nodes are more rigidly fixed? How does environmental perturbation influence developmental programs? These are questions of large significance to developmental and evolutionary biology.

As was first recognized with the nematode *Ascaris megalocephala* by Theodor Boveri over a century ago (Boveri, 1899), early *C. elegans* embryogenesis is essentially invariant, resulting in generation of six founder cells (AB, MS, E, C, D, and P_4) through a series of asymmetrical cleavages (Sulston et al., 1983), providing a unique opportunity to study the molecular mechanism underlying developmental robustness and fidelity.

The *C. elegans* Intestine

The entire *C. elegans* intestine, is derived clonally from the E blastomere (Sulston et al., 1983), providing a highly tractable system to study cell specification, differentiation and organogenesis. Studies over the past three decades have provided a high-resolution description of the endoderm GRN (Maduro, 2015, 2017; Maduro and Rothman, 2002; McGhee, 2007). In brief, maternally provided SKN-1/Nrf activates a zygotically expressed transcriptional cascade comprising a series of GATA-like transcription factors, including the GATA-like factors MED (MesEnDoderm)-1 and MED-2, which bind to a non-canonical RRRAGTATAC site (Broitman-Maduro et al.,

2005), and the canonical GATA factors END-3 and END-1. This leads to the activation of ELT-7 and ELT-2, which, together, drive activation of thousands of gut-expressed genes and morphological differentiation of the intestine (Dineen et al., 2018; Fukushige et al., 1998; McGhee et al., 2009; Sommermann et al., 2010). SKN-1 and MED-1/2 also function in the sister of E, MS, to activate mesoderm development (Figure 1.1).

Endoderm fate is activated by an inductive cellular interaction: a triply redundant Wnt/MAPK/Src signaling system triggered by signals from the neighboring P_2 cell polarizes the mesendodermal EMS cell and subsequently modifies the nucleocytoplasmic distribution and activity of POP-1/Tcf (Maduro et al., 2002; Owraghi et al., 2010; Phillips et al., 2007; Shetty et al., 2005). In the un-signaled MS cell, POP-1 represses *end-1* and *-3* expression, thereby inhibiting gut fate. In the posterior E cell, the inductive signal results in phosphorylation of POP-1 by LIT-1/Nlk, converting it from a repressor to an activator of E fate. Thus, SKN-1 and POP-1 play a partially redundant role in endoderm specification in *C. elegans* (Figure 1.1). Additionally, Wnt signaling represses MS fate in the E cell in a POP-1 independent manner (Broitman-Maduro et al., 2006).

Evolution of the Endoderm GRN

While orthologs of SKN-1, which is essential for initiating mesendoderm specification in *C. elegans*, are found across divergent nematode species, its action in endoderm development varies dramatically between them. Maternally provided *skn-1* RNA is initially present throughout the *C. elegans* early embryo but becomes differentially lost in somatic blastomeres and is maintained in the germline lineage

(Seydoux and Fire, 1994). In contrast, a very different pattern is observed in *Propanagrolaimus sp.* JU765 (clade 10)[2] and *A. nanus* (clade 11)[2], in which *skn-1* mRNAs, which are presumably zygotic products, accumulate in all somatic blastomeres through much of embryogenesis (Schiffer et al., 2014, 2018; Wiegner and Schierenberg, 1998). These observations suggest differential regulation of *skn-1* expression and that, in addition to activating mesendoderm specification, SKN-1 may perform distinct functions in species from neighboring clades. Remarkably, the requirement for SKN-1 in endoderm specification varies even in closely related *Caenorhabditis* species. In *C. elegans*, eliminating SKN-1 results in a partial penetrant loss-of-endoderm phenotype, as SKN-1 and POP-1 function through an "OR" Boolean logic gate (Figure 1.1). However, in *Caenorhabditis briggsae*, which diverged from *C. elegans* ~20–40 million years ago, both SKN-1 and POP-1 show an absolute requirement in endoderm specification, indicative of an "AND" logic gate (Cutter, 2008; Lin et al., 2009). These observations suggest that the early inputs into the endoderm GRN are rapidly evolving in nematodes.

The gut terminal differentiation factors, including ELT-2/GATA and the FoxO factor PHA-4 are conserved across Nematoda (Maduro, 2020; Schiffer et al., 2014). In contrast, the upstream *med* and *end* orthologs are present only in closely related *Caenorhabditis* species, apparently having arisen as a result of extensive gene duplication events at the base of the Elegans supergroup, as revealed in a recent study that examined the evolutionary variation in the GATA regulatory cascade across

[2] Nematodes are classified into 12 clades based on rDNA sequences (Holterman et al., 2006). *Caenorhabditis* species belongs to clade 9.

24 species spanning the *Caenorhabditis* genus (Maduro, 2020). In two strikingly extreme cases, *Caenorhabditis doughertyi* and *Caenorhabditis brenneri* each contain ~30 copies of the *med* genes (Maduro, 2020). This massive proliferation of protein-coding genes is highly unusual and may reflect adoption of new functions by at least some of the paralogs, as exemplified by the expansion of another class of transcription factors in Caenorhabditis species, the nuclear hormone receptors (NHRs) (Holterman et al., 2006). Most *Caenorhabditis* NHRs appear to have arisen from an ancestral Hepatocyte Nuclear Factor 4 (HNF4)-type NHR and appear to have evolved to perform diverse roles ranging from neural development (Much et al., 2000; Zhou and Walthall, 1998) to metabolic control (Gilst et al., 2005; Wang et al., 2015) to sex determination (Ilil et al., 1998). It is conceivable that changes in the cis-regulatory regions lead to differential expression and subsequent functional divergence of the MED paralogs, leading to retention of gene duplicates (Gissendanner et al., 2004; Taubert et al., 2011; True and Haag, 2001), though the function of MEDs beyond mesendoderm development have not been described. Importantly, functional diversification of duplicate genes can also drive rapid changes in developmental programs and developmental system drift (DSD)[3] (Haag et al., 2018; True and Haag, 2001). For example, the *C. briggsae* translational regulator PUF (PUmilio and FBF)-2 plays a non-redundant role in pharynx and vulva development, in addition to promoting gametogenesis, the sole known role of its paralog PUF-1.2 and its homologs in *C. elegans* (Liu and Haag, 2014; Liu et al., 2012). Although morphologically invariant, the molecular mechanisms underlying vulva development vary across nematodes

[3] Constant morphological features allow the evolution of underlying molecular pathways without compromising fitness (True and Haag, 2001).

(Dichtel-Danjoy and Félix, 2004; Félix, 2007; Félix et al., 2000; Sommer and Sternberg, 1994; Zheng et al., 2005), which may, at least partly, have been caused by DSD resulting from gene duplication.

What might account for the expansion of GATA factors in the *Caenorhabditis* endoderm GRN? The cascade of redundant factors may function to ensure developmental robustness during the rapid embryogenesis characteristic of this clade. In *C. elegans*, and likely in the other *Caenorhabditis* species (Wiesenfahrt et al., 2016), the endoderm GATA factors form recursive feedforward loops, which may provide a rapid, forward-driven activation switch (see Chapter 2). In addition, the small size of the MEDs (174 residues) and ENDs (221–242 residues), compared to ELT-2 (433 residues) and SKN-1 (~600 residues), may allow for more rapid deployment of the cascade and lockdown of gut fate, perhaps owing to more rapid synthesis and access to chromatin (Maeshima et al., 2015). Another potential explanation is that the GATA cascade may allow more robust expression of ELT-2. The provision of maternal factors can vary among individuals (Nuzhdin et al., 2008; Perez et al., 2017; Surkova et al., 2008) especially under conditions of environmental stress, which is mitigated by SKN-1 (see also Pleiotropy may Facilitate the Evolution of the Endoderm GRN) (An and Blackwell, 2003; Crofton et al., 2018; Jordan et al., 2019). Intercession of the MEDs and ENDs in the cascade may therefore free *elt-2* from direct control of SKN-1, thereby buffering against changes in environmental conditions. Finally, redundancy in the system allows for evolutionary experimentation and accumulation of cryptic genetic variants, promoting the evolution of the system (more below) (Félix and Wagner, 2008).

Rapid Developmental System Drift among *C. elegans* Wild Isolates

Most of our understanding of *C. elegans* biology is based on studies on a single genetic background, that of the laboratory reference strain N2. The identification of wild *C. elegans* isolates bearing distinct haplotypes has uncovered considerable phenotypic variation and developmental plasticity in this species (Andersen and Rockman, 2022; Evans et al., 2021). Knocking down essential genes in the wild strains yielded distinct phenotypes and has uncovered substantial cryptic variation between the spectrum of isotypes (Paaby et al., 2015; Torres Cleuren et al., 2019). In addition, while the overall morphology remains constant, the network architecture underlying vulva induction is variable in wild genetic backgrounds (Duveau and Félix, 2012; Milloz et al., 2008). Environmental cues can modulate activities in the vulva signaling network and the sensitivity of the system varies among divergent *C. elegans* isotypes (Braendle and Félix, 2008; Grimbert and Braendle, 2014). Thus, potential incipient changes in developmental regulatory networks, and their robustness to environmental variation, can be revealed by examining the requirement for components in the networks in genetically distinct wild isolates.

We recently uncovered striking variation in the endoderm GRN among the wild isolates, as reflected by the differential requirement of maternal SKN-1 and the endoderm-inducing MOM-2/Wnt (Torres Cleuren et al., 2019). This study revealed in part that the two activating pathways exhibit a partially compensatory relationship, in which a weaker requirement for the SKN-1 input is accompanied by a stronger requirement for the MOM-2 input and vice-versa, which may tune the levels of the activating signals to ensure a constant developmental outcome (Choi et al., 2017;

Maduro et al., 2015; Torres Cleuren et al., 2019). Thus, the accumulation of cryptic genetic variants drives rewiring of the inputs into the endoderm GRN. This rapid DSD may be the result of the extensive redundancy in the system, which permits cryptic genetic variants to arise without diminishing fitness and allows compensatory evolution to occur.

Pleiotropy may Facilitate the Evolution of the Endoderm GRN

Emerging evidence suggests that regulatory factors modulating early endoderm development play pleiotropic roles in regulating gut physiology, stress response, immunity, and lifespan in post-embryonic animals, as discussed in the sections below, based on the component(s) involved. Thus, the remarkable plasticity in the endoderm GRN observed in *C. elegans* isotypes (see above) may be attributable at least in part to differential stress response and pleiotropic interactions that have imposed selective alterations of these regulatory processes.

Pleiotropy is more likely to arise in robust gene networks (e.g., the endoderm GRN owing to extensive redundancy in the signaling inputs) as evolutionary trade-off is relatively small (Guillaume and Otto, 2012; Visser et al., 2003). On the other hand, robustness in one system may be the result of selection for robustness in a different system owing to the existing pleiotropic interactions. For example, a domesticated allele of *nath-10*, the human N-acetyltransferase homolog gene, confers selective advantage in the laboratory *C. elegans* strain (N2) as it increases the age of maturity, brood size, and egg-laying speed by promoting sperm production in the standard laboratory condition. Additionally, the lab-derived allele of *nath-10* enhances the activity of EGF/Ras signaling in vulva development cryptically, revealed only in a

sensitized *let-23(sy1)* mutant background, which shows altered EGF receptor localization and reduced level of vulva cell-fate induction. Hence, selective pressure exerted on gametogenesis could influence the genetic architecture that governs robust vulval cell fate pattern (Duveau and Félix, 2012). Robustness allows accumulation of neutral cryptic genetic variants, which can be revealed in a novel environment, facilitating adaptation.

SKN-1/Nrf: a nexus in development, homeostasis, and aging

SKN-1, an ortholog of vertebrate Nrf1 and 2 transcription factors, is a particularly prominent node linking endoderm specification, stress response, immunity, and lifespan regulation. These transcription factors are characterized by the presence of the DIDLID element, CNC domain, and adjacent basic region (BR). Both Nrf1 and 2 are known to regulate the transcription of antioxidant and phase II enzymes to mitigate oxidative stress; however, unlike Nrf2, which is localized to the cytosol under unstressed conditions, Nrf1 is tethered to the endoplasmic reticulum. The *skn-1* gene encodes three isoforms, SKN-1a, -b and -c, which share the same DNA binding domain. While SKN-1a and SKN-1c are expressed in the intestine, SKN-1b is found in the two ASI sensory neurons (Blackwell et al., 2015).

As described above, SKN-1 was initially found to be important in initiating mesendoderm specification (Figure 1.1) (Bowerman et al., 1992, 1993). In addition, SKN-1 plays a central role in regulating acute oxidative stress, a conserved role of Nrf2. In response to oxidative stress, Nrf2 activates (phase II) detoxification genes. Under normal conditions in mammalian cells, Keap1 binds to Nrf2 to retain it in the cytoplasm, and, in a complex with CUL3, can target Nrf2 for ubiquitination. Upon the

introduction of stress, electrophiles and reactive oxygen species inhibit binding between Keap1 and Nrf2, and Nrf2 is free to translocate into the nucleus to promote the expression of antioxidant genes (Cullinan et al., 2004; Itoh et al., 1999; Keum, 2012). As such, animals lacking functional Nrf2 are hypersensitive to oxidative stress and drug toxicity because they cannot mount the proper transcriptional defense.

Although *C. elegans* lacks a Keap1 orthologue, SKN-1 localization is, in part, modulated via the action of the WD40 Repeat Protein (WDR)-23. Like Keap1, WDR-23 is a cysteine-rich E3 ubiquitin ligase substrate adapter protein that aids in SKN-1 proteasomal degradation (Choe et al., 2009; Lo et al., 2017). Mutants lacking *wdr-23* show an upregulation of SKN-1 transcriptional targets such as glutathione-S-transferases *gst-4* and *gst-30*, along with enhanced stress tolerance and increased lifespan. SKN-1 undergoes numerous post-translational modifications that direct its localization, and evidence suggests that its association with WDR-23 is downstream of other modifications by GSK3β and the p38 MAP kinase pathway (Choe et al., 2009). Upon exposure to oxidative stress, the MAP kinase PMK-1 phosphorylates SKN-1 at Ser164 and Ser430, eventually leading to nuclear accumulation of SKN-1 and activation of antioxidant gene expression (Inoue et al., 2005; Li et al., 2018). Furthermore, MAP kinase signaling activates SKN-1 in response to pathogenic bacterial infection, and removing *skn-1* increases susceptibility of the animals to infection (Papp et al., 2012); however, SKN-1 may also suppress MAP kinase signaling through the activity of RIOK-1, a human RIO kinase homolog, to fine-tune the immune response (Chen et al., 2018).

SKN-1a contains an ER-associated domain and plays an important role in regulating proteostasis and the unfolded protein response (UPR), mechanistically similar to that of vertebrate Nrf1 (Baird et al., 2017; Radhakrishnan et al., 2014; Sha and Goldberg, 2014; Wang and Chan, 2006). SKN-1a in the ER contains glycosylation modifications. It is de-glycosylated and released from the ER, catalyzed by the aspartic protease DDI-1. Under normal conditions, SKN-1a in the cytosol is rapidly degraded; however, in the presence of proteotoxic insults, SKN-1a escapes proteasomal degradation and subsequently translocates into nucleus where it activates target genes to upregulate proteasome function, including *rpt-3*, which codes for the orthologue of human PSMC4 (proteasome 26S subunit, ATPase 4) (Lehrbach and Ruvkun, 2016, 2019).

SKN-1 promotes longevity in part by regulating protein homeostasis as described above (Lehrbach and Ruvkun, 2019). Moreover, in germline-less animals, SKN-1 upregulates lipid metabolism in the intestine, promoting lifespan extension partly by slowing down yolk steatosis (Steinbaugh et al., 2015). Additionally, when IIS is attenuated, SKN-1 accumulates in the intestinal nuclei, along with DAF-16, and activates target genes that extend lifespan (Tullet et al., 2008). Notably, SKN-1b in the ASI neurons has a profound effect on dietary restriction-mediated longevity, independent of the IIS (Bishop and Guarente, 2007). In addition to IIS, the Notch ligand OSM-11 can antagonize SKN-1 signaling and inhibiting *osm-11* leads to increased longevity and resistance to oxidative and heat stress. It is significant to note that loss of *osm-11* also partial rescues embryonic lethality and the loss-of-endoderm

phenotype of *skn-1* deficient embryos, although the detailed molecular mechanism remains to be elucidated (Dresen et al., 2015).

Mechanistic Target of Rapamycin (mTOR) kinase, working through either complex 1 (mTORC1) or complex 2 (mTORC2), has a highly conserved role in growth and aging (Papadopoli et al., 2019). Reducing mTORC1 activity extends lifespan, and in *C. elegans*, this effect requires SKN-1 and DAF-16 (Robida-Stubbs et al., 2012). Remarkably, disrupting mTORC2 by removing *rict-1*, which codes for the Rictor ortholog, produces an opposing effect on lifespan depending on diet. Mutants lacking functional RICT-1 exhibit reduce lifespan when animals are fed on *E. coli* OP50 (B strain); on the other hand, a *rict-1* mutation significantly extends the lifespan of animals fed on the nutrient-dense HT115 (K12 strain). mTORC2 directs SGK-1, the *C. elegans* homolog of the serum- and glucocorticoid-inducible kinase, to phosphorylate and inhibit SKN-1. Hence, in the absence of mTORC2/RICT-1, SKN-1 localizes to the nucleus constitutively. Differential signals from bacterial metabolites generated when the worms are fed on nutrient dense HT115, but not OP50, further modulate the activity SKN-1 (Mizunuma et al., 2014; Reinke et al., 2010; Robida-Stubbs et al., 2012).

SGK-1 is also necessary for IIS-mediated phosphorylation of SKN-1 (Tullet et al., 2008). Thus, two distinct pathways (mTOR and IIS) converge on SGK-1, thereby modulating SKN-1 signaling and longevity. Interestingly, knocking down either *rict-1* or *sgk-1* partially rescues *skn-1(-)*-induced embryonic lethality. Loss of *rict-1* upregulates MED-1 in embryos lacking *skn-1* and promotes mesendoderm specification (Ruf et al., 2013; Torres Cleuren et al., 2019).

Given the interactions between nutrients, mTOR signaling, and SKN-1 regulation, it would be of interest to investigate whether maternal diet influences provision of SKN-1 and other maternal factors in the germline and how it might affect mesendoderm specification. The recently available collection of natural *C. elegans* microbiota (ceMbio) (Dirksen et al., 2020) provides a unique opportunity to probe how maternal dietary composition affects early embryonic development, and perhaps, the evolution of the developmental GRN.

Pleiotropic Actions of Wnt Signaling

The asymmetrical division of EMS is primarily driven by the Wnt/β-catenin asymmetry pathway (Eisenmann, 2005). Unlike canonical Wnt signaling, in which GSK3β phosphorylates β-catenin, thereby targeting it for degradation (Eisenmann, 2005; Korswagen et al., 2002), GSK3β/GSK-3 plays a positive role in endoderm specification in parallel with SKN-1, although the molecular details remain obscure (Bei et al., 2002; Maduro et al., 2001; Schlesinger et al., 1999). At the four-cell stage, the MOM-2 Wnt ligand activates MOM-5/Frizzled. This Wnt receptor is localized to the posterior cell cortex of EMS, along with Dishevelled proteins, DSH-2 and MIG-5, which play partially redundant roles in spindle reorientation and gut specification (Thorpe et al., 1997; Walston et al., 2004). This effectively polarizes the cell, in part by regulating β-catenin/SYS-1 levels, such that it is low in the anterior MS and high in the posterior E cell (Phillips et al., 2007). In addition, LIT-1/NEMO kinase, coupled with WRM-1 (a second β-catenin), phosphorylates POP-1, which is subsequently exported from the E nucleus in a process involving PAR-5 and XPO-1 exportin (Lo et al., 2004; Nakamura et al., 2005; Rocheleau et al., 1999). The low level of modified POP-1 binds

to cofactor SYS-1 and activates specification of endoderm fate (Huang et al., 2007; Maduro et al., 2005a; Yang et al., 2011).

In addition to acting in the Wnt pathway to promote gut fate, GSK-3 modulates the timely oocyte-to-embryo transition by promoting degradation of OMA-1 and -2 (Maduro et al., 2001; Nishi and Lin, 2005). Furthermore, GSK-3 inhibits SKN-1-mediated activation of *med-1/2* to prevent misspecification of the C blastomere mesectoderm progenitor, independent of Wnt activity (Maduro et al., 2001). An interesting parallel is observed postembryonically: in the absence of stress, GSK-3 phosphorylates SKN-1 and inhibits its nuclear accumulation in the intestine (An et al., 2005). It has been shown that phosphorylation by GSK-3 is suppressed by OGT-1-dependent SKN-1 O-GlcNAcylation at Ser470 and Thr493 in response to oxidative stress (Li et al., 2017). Disruption of O-GlcNAcylation reduces nuclear localization of SKN-1, suggesting competitive interactions between GSK-3 and OGT-1 in regulating SKN-1 nucleocytoplasmic distribution and activity through post-translational modifications. The actions of GSK3β typically require priming phosphorylation (Liu et al., 2002), which may be achieved by the AKT kinases in *C. elegans* (Blackwell et al., 2015; Tullet et al., 2008). As mentioned previously, DAF-16 is repressed by IIS-mediated phosphorylation by AKT kinase (Hertweck et al., 2004). Like GSK-3, AKT kinases can also phosphorylate and prevent nuclear accumulation of SKN-1 (Tullet et al., 2008).

In addition to its major role in endoderm development, Wnt signaling appears to negatively regulate longevity and aging. Elevated Wnt signaling accelerates cellular senescence and age-associated tissue fibrosis in mice (Brack et al., 2007; Liu et al.,

2007). In worms, eliminating Wnt ligands, including MOM-2, substantially extends lifespan (although the LIN-44 Wnt appears to play an opposing role) (Lezzerini and Budovskaya, 2014). It has been shown that dietary restriction upregulates *mir-235* which in turn targets the transcript of a Wnt ligand, *cwn-1,* suppressing Wnt signaling though the destruction of the β-catenins HMP-2 and BAR-1 (Xu et al., 2019). While the primary role of HMP-2 is in cadherin-mediated cell adhesion, it may also mediate endoderm fate induction downstream of the Src pathway (see below) (Sumiyoshi et al., 2011). Moreover, in embryos lacking the gene encoding a Fer-type non-Receptor Kinase (FRK)-1, HMP-2 translocates from the cell cortex into the nucleus and provides additional gut-activating input, demonstrating functional redundancy between the divergent β-catenins (Natarajan et al., 2001; Putzke and Rothman, 2010). Hence, Wnt signaling participates in both endoderm specification and regulation of aging.

Pleiotropic Actions of MAP kinase and Src Signaling Pathways

In the endoderm GRN and in many asymmetric divisions throughout *C. elegans* development, MAP kinase and Src signaling work in parallel with the Wnt pathway and converge on POP-1 to mediate its subcellular localization (Figure 1.1). Additionally, the MAP kinase pathway modifies the nucleocytoplasmic distribution of Pur-α PLP-1, which subsequently activates the expression of *end-1* (and perhaps *end-3*) in the E cell (Witze et al., 2009). MAP kinase kinase kinase MOM-4/TAK1 phosphorylates and activates LIT-1 to induce endoderm specification (Meneghini et al., 1999; Shin et al., 1999; Yang et al., 2015). Supporting a conserved role for TAK1 in immune signaling (Ajibade et al., 2013; Ninomiya-Tsuji et al., 1999), MOM-4 is also

found to be required for p38-mediated innate immunity against *P. aeruginosa* infection (Xu et al., 2013), linking regulation of gut development to antimicrobial response.

Tyrosine kinases MES-1 and SRC-1 in the Src signaling pathway activate gut specification by mobilizing HMP-2 and downregulating POP-1 levels in the E cell nucleus (Bei et al., 2002; Sumiyoshi et al., 2011). MES-1 is also required for specification of germline blastomeres. Consequently, animals harboring *mes-1* mutations exhibit a maternal-effect sterile phenotype (Berkowitz and Strome, 2000). The loss of germline in *mes-1* mutants effectively protects the animals from *P. aeruginosa* infection and confers longevity in a DAF-16-dependent manner (Libina et al., 2003; Miyata et al., 2008; Wu et al., 2015).

Endoderm Development and Proteostasis: ICD-1/BTF3/βNAC

ICD (Inhibitor of Cell Death)-1 is a homolog of basal transcription factor 3 (BTF3). In mammals, the gene btf3 encodes two splice isoforms BTF3a and BTF3b. While BTF3a promotes transcription, BTF3b is also the β-subunit of the nascent polypeptide-associated complex (βNAC). The primary function of NAC is assisting co-translational protein folding and transport (Jamil et al., 2015). ICD-1 localizes to mitochondria (Bloss et al., 2003). Knocking down *icd-1* results in a great increase in the number of apoptotic cell corpses in the embryos and larvae (Bloss et al., 2003). It was further demonstrated that ICD-1 inhibits apoptotic cell death through a non-canonical cell death pathway, independent of caspase CED-3, a key effector of apoptosis in *C. elegans* (Bloss et al., 2003).

Consistent with the role of NAC in modulating proteostasis (Kirstein-Miles et al., 2013; Shen et al., 2019), worms lacking *icd-1* upregulate chaperone protein HSP-

4 and the UPR, and show premature sign of aging as indicated by accumulation of enlarged lipofuscin (Arsenovic et al., 2012). On the other hand, eliminating *skn-1* prevents the expression of UPR genes, including *hsp-4*.

The opposing roles of ICD-1 and SKN-1 are also demonstrated in the context of endoderm development. While SKN-1 activates gut development, ICD-1 negatively regulates endoderm specification; knocking down *icd-1* partially rescues the loss-of-gut phenotype of *mom-2/Wnt* and *mom-4/MAPKKK* knockdowns, but not that of *skn-1* mutants, suggesting that ICD-1 antagonizes the activating input of SKN-1 (Ewe et al., 2019), although the detailed molecular mechanisms are currently not clear. Hence, it appears that ICD-1 fine tunes gut-activating signals to promote faithful development, in addition to its conversed role in proteostasis regulation. *Drosophila* βNAC, bicaudal, represses the translation of the (maternally provided) posterior determinant *nanos* in the anterior pole, ensuring proper specification of the anteroposterior axis of the embryo (Markesich et al., 2000). Similarly, ICD-1 may tune the level of endoderm activating input, perhaps, by limiting SKN-1 translation (see Appendix I: ICD-1/BTF3 Antagonizes SKN-1-mediated Endoderm Specification in *C. elegans*).

Conserved Action of Caudal Transcription Factors

The Caudal-like homeodomain protein has been found to play a conserved role in intestine development in fly and mouse models (Hryniuk et al., 2012; Suh et al., 1994; Wu and Lengyel, 1998). In *C. elegans*, Caudal-like PAL-1 is required for specification of P_2 somatic descendants, including the C mesectodermal precursor, which gives rise to epidermis and muscles. During early divisions, localization and translation of maternally provided *pal-1* transcripts in EMS and P_2 are regulated by a

KH domain RNA-binding protein MEX-3 (Hunter and Kenyon, 1996). In P_2, PAL-1 activates a transcriptional program that drives mesectoderm specification. In E and MS, SKN-1 inhibits the activity of PAL-1 (Baugh et al., 2005; Hunter and Kenyon, 1996). Consequently, removing *skn-1* leads to ectopic expression of hypodermal fates (Bowerman et al., 1992). Nonetheless, a minor positive role of PAL-1 in endoderm specification, possibly though the activation of *end-1/3*, is revealed when both SKN-1 and POP-1 are eliminated (Maduro et al., 2005a).

Postembryonic roles of PAL-1 include regulating posterior morphogenesis and the patterning of the sensory rays in the male tail (Gilbert et al., 2020; Waring and Kenyon, 1991). Curiously, many PAL-1 targeted genes also appear to be involved in proteostasis and stress pathways (Baugh et al., 2005). For example, the myogenic factor HLH-1 regulates expression of many chaperones, and loss of *hlh-1* disrupts protein folding (Bar-Lavan et al., 2016). SSP-10/SGP-1 prevents the formation of α-Synuclein Inclusion (Van Ham et al., 2008). Other PAL-1 targets include genes coding for NHR-25 and ELT-3, which are required for immune response against bacterial infection and mitigating oxidative stress, respectively (Hu et al., 2017; Ward et al., 2014). In *Drosophila,* Caudal modulates homeostasis of innate immunity, and its expression is upregulated in response to oxidative stress (Choi et al., 2008; Ryu et al., 2008), suggesting a conserved role of Caudal-like homeobox transcription factor in stress response.

Using network analysis techniques, PAL-1 was predicted to be important for longevity and aging (Witten and Bonchev, 2007), though further functional studies are required to reveal the significance of this observation.

GATA Factors in Endoderm Development, Homeostasis and Aging

ELT-2 and ELT-7 are the major GATA transcription factors driving intestine morphological differentiation (Figure 1.1) (Dineen et al., 2018; McGhee et al., 2009; Sommermann et al., 2010). Animals lacking ELT-2 undergo developmental arrest as first stage larvae in which the morphology of the intestine is disrupted, although the intestinal cells appear to be fully differentiated. Removing both ELT-2 and -7 potently blocks gut differentiation (Sommermann et al., 2010), demonstrating a strongly redundant relationship (see also Chapter 2).

ELT-2 has also been found to function post-embryonically in regulating gut physiology, stress response, and immunity. For example, ELT-2 directly regulates expression of ferritin and metallothionein genes to protect the worms against heavy metal toxicity (Moilanen et al., 1999; Romney et al., 2008). ELT-2 also induces a transcriptional response, including the upregulation of the enzyme Glycerol-3-Phosphate Dehydrogenase (GPDH)-1, which confers adaptation to osmotic stress (Rohlfing et al., 2010). In response to bacterial infection, ELT-2 (and perhaps ELT-7 (Elliott et al., 2011)) upregulates p38 MAP kinase signaling in innate immune response (Block et al., 2015; Shapira et al., 2006). The pathogenic Gram-negative bacterium *Burkholderia pseudomallei* can evade the *C. elegans* immune system by promoting targeted degradation of ELT-2 (Lee et al., 2013), highlighting the central role of ELT-2 in innate immunity.

ELT-2 expression declines during aging. While knocking down *elt-2* in adult animals shortens lifespan, *elt-2* overexpression has been reported to promote longevity (Mann et al., 2016; Zhang et al., 2013). Reduced IIS upregulates ELT-2

independently of SKN-1, which subsequently works collaboratively with DAF-16 to activate pro-longevity transcriptional programs (Mann et al., 2016; McGhee et al., 2009; Zhang et al., 2013). While the activity of DAF-16 is primarily regulated though post-translational modifications, *daf-16* expression can be further tuned by ELT-2 in the intestine (Bansal et al., 2014), revealing ELT-2 as a major regulator of lifespan. Transient hypoxia induces lifespan extension in worms, dependent on mTORC1 regulation of ELT-2 (Schieber and Chandel, 2014). In addition, it has been found that ELT-2 (and SKN-1) promotes the survival and extends the lifespan of mutant animals with proteasome dysfunction (Keith et al., 2016). ELT-2 may act downstream of IIS to modulate protein homeostasis (Florez-Mcclure et al., 2007; Walther et al., 2015). ELT-2 is also required for the lifespan extension of animals overexpressing *lmp-2*, a gene involved in chaperone-mediated autophagy (Mann et al., 2016). Thus, ELT-2 plays pleiotropic roles in endoderm differentiation and longevity.

Regulatory Events Linked through PHA-4/FoxA

HNF3/forkhead (FoxA) is known to cooperate with GATA factors to promote endoderm differentiation across metazoans (Boyle and Seaver, 2008; Martindale et al., 2004; Zaret, 1999). In *C. elegans*, the FoxA homolog PHA-4, is expressed along the digestive tract, including the pharynx, intestine, and the hindgut and functions as an organ selector gene. Animals lacking *pha-4* fail to make pharynx and normal rectum; however, gut development does not appear to be severely affected (Kalb et al., 1998; Mango et al., 1994; McGhee et al., 2009). The expression of *pha-4* is activated by ELT-2 and -7 in the intestine (Kalb et al., 1998; Riddle et al., 2016). PHA-

4 in turn promotes expression of genes involved in metabolic regulation, particularly in response to nutritional stress (Zhong et al., 2010).

PHA-4, a terminal differentiation factor in the gut, is also required for (IIS-independent) diet-restriction-mediated longevity, at least in part by downregulating Wnt signaling through the action of *mir-235* (see above) (Panowski et al., 2007; Xu et al., 2019). When animals experience metabolic stress and reduced TOR signaling, PHA-4 activates transcriptional programs that confer protection against oxidative stress and upregulate autophagy (Hansen et al., 2008; Panowski et al., 2007; Sheaffer et al., 2008; Zhong et al., 2010). RSKS-1/S6K, a major effector of the TOR pathway, antagonizes the activity of PHA-4, and the lifespan extension of *rsks-1* mutants requires PHA-4 (Sheaffer et al., 2008). In the absence of RSKS-1, PHA-4 increases starvation resistance of the animal by elevating lipogenesis (Wu et al., 2018). Indeed, lipogenic genes, including *fasn-1*, *pod-2*, and *dgat-2*, have been shown to be the direct targets of PHA-4 (Wu et al., 2018; Zhong et al., 2010). In addition, germline ablation downregulates TOR signaling, thereby relieving PHA-4 inhibition and leading to upregulation of autophagy and lifespan extension (Lapierre et al., 2011).

Aims of the Present Study

Using *C. elegans* endoderm development as a model system, my research aims to further dissect the molecular basis of for developmental robustness and plasticity. What is the underlying architecture of developmental regulatory networks that directs robust specification and differentiation of progenitor cells during embryogenesis? How is cell differentiated state established and maintained (Chapter 2)? How do the endoderm regulatory inputs respond to environmental perturbation?

What is the molecular mechanism underlying developmental plasticity (Chapter 3)? Overall, these studies will expand our understanding of the influence of genetic and environmental factors on the propensity of developmental defects.

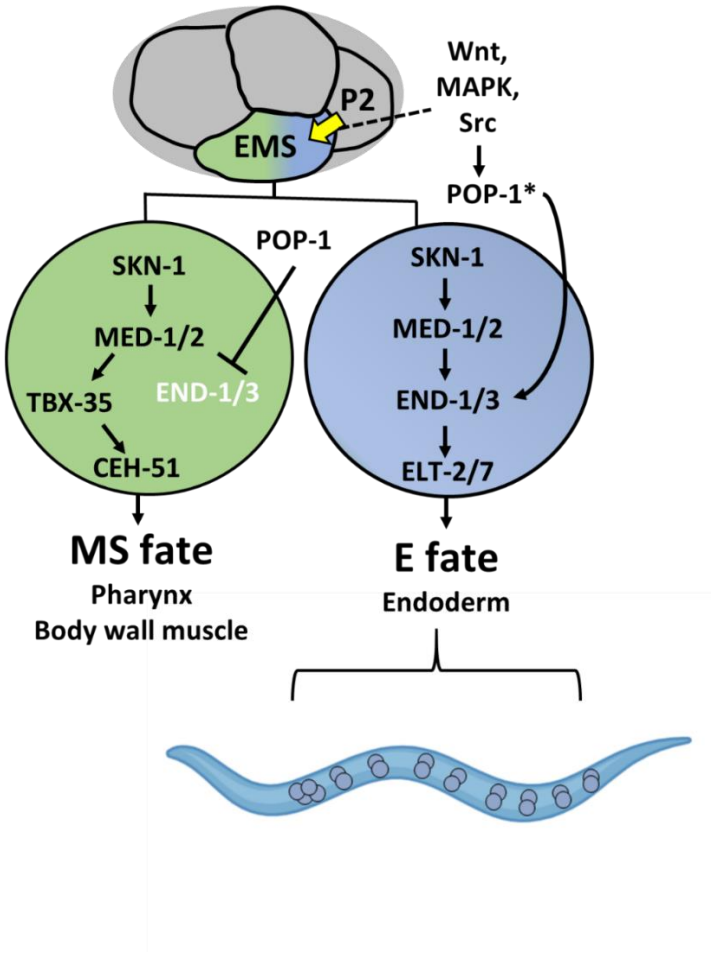

Figure 1.1: The *C. elegans* mesendoderm GRN.
At the four-cell stage, signaling from the posterior P_2 cell (Wnt, MAPK and Src) polarizes the blastomere, leading to POP-1 asymmetry in the descendants of EMS with high levels of nuclear POP-1 in anterior MS and low levels of nuclear POP-1 in the posterior E cell. In the anterior MS cell, high nuclear POP-1 represses *end-1/3*, allowing SKN-1 to induce the MS fate though the actions of TBX-35 and CEH-51. In the posterior E cell, which remains in contact with P_2, POP-1 is converted to an endoderm activator (POP-1*) and along with SKN-1 activates *end-1/3* and *elt-2/7* genes, resulting in the endoderm fate. At hatching, the entire *C. elegans* intestine consists of 20 diploid cells arranged in nine intestinal rings, with four cells in the anterior-most ring and two cells in each of the remaining eight rings.

Chapter 2 : Feedforward Regulatory Logic Underlies Robustness of the Specification-to-differentiation Transition and Fidelity of Terminal Cell Fate during *C. elegans* Endoderm Development[4]

"*Mathematics is the art of the perfect. Physics is the art of the optimal. Biology is the art of the satisfactory*" – Sydney Brenner

[4] This chapter has been published in Ewe, Sommermann et al., BioRvix (2021) with minor modifications.

Summary

Development is driven by gene regulatory networks (GRNs) that progressively dictate specification and differentiation of cell fates. The architecture of GRNs directly determines the specificity and accuracy of developmental outcomes. We report here that the core regulatory circuitry for endoderm development in *C. elegans* is comprised of a recursive series of interlocked feedforward modules linking a cascade of six sequentially expressed GATA-type transcription factors. This structure results in a reiterated sequential redundancy, in which removal of a single factor or alternate factors in the cascade results in no, or a mild, effect on endoderm development and gut differentiation, while elimination of any two factors that are sequentially deployed in the cascade invariably results in a strong phenotype. The strength of the observed phenotypes is successfully predicted by a computational model based on the timing and levels of transcriptional states. The feedforward regulatory logic in the GRN appears to ensure timely onset of terminal differentiation genes and allow rapid and robust lockdown of cell fate during early embryogenesis. We further found that specification-to-differentiation transition is linked through a common regulator, the END-1 GATA factor that straddles the two processes. Finally, we revealed roles for key GATA factors in establishing spatial regulatory state domains by acting as transcriptional repressors that appear to define the boundaries of the digestive tract. Our findings support a comprehensive model of the core gene network that describes how robust endoderm development is achieved during *C. elegans* embryogenesis.

Introduction

Development is driven by progressive activation of transcriptional programs, or gene regulatory networks (GRNs) that direct cell specification and subsequent differentiation (Boveri, 1899; Davidson and Levine, 2008). The sequential restriction of cell identity and developmental potential through dynamic changes in transcriptional states was anticipated by Waddington's epigenetic landscape, a graphic metaphor describing canalization and robustness during development (Waddington, 1957).

The generation of diverse animal forms largely relies on a common genetic toolkit. The GATA transcription factors play a conserved role in the development of diverse cell types, including those of the endoderm, the first of the three germ layers to have evolved during the late Precambrian era (Hashimshony et al., 2015; Rodaway and Patient, 2001). In the diploblastic phyla Poriferans and Cnidarians, GATA factors have been found to be specifically expressed in the endoderm, suggesting that these transcriptional regulators may have driven the invention of the endoderm germ layer and gastrulation at the dawn of metazoan evolution (Martindale et al., 2004; Nakanishi et al., 2014). This association of GATA factors with endoderm development persists throughout metazoan phylogeny, generally through successive deployment of multiple GATA factors. This sequential use of GATA factors is particularly striking in *C. elegans*, in which a cascade of six GATA factor-like transcription factors regulate specification and differentiation of the endoderm (Maduro, 2017; Maduro and Rothman, 2002; McGhee, 2007). In *Drosophila*, the GATA factor Serpent specifies endodermal fate and activates the expression of a second GATA factor, dGATAe, which is essential for the terminal differentiation of the intestine. These factors can act across wide

phylogenetic spans, as first demonstrated with the *C. elegans* END-1 GATA factor, which ectopically activates endoderm development when expressed in the prospective ectoderm of *Xenopus* (Shoichet et al., 2000). Similarly, overexpression of *serpent* or *dGATAe* causes ectopic endoderm differentiation in non-endodermal lineages in *Drosophila*, as well as in *Xenopus*, further supporting the functional conservation of the GATA factors (Murakami et al., 2005; Okumura et al., 2005). In sea urchin, Blimp1/Krox1 activates *otx1*, the product of which activates *gatae* expression (Davidson et al., 2002). Gatae in turn provides a positive input to *otx1*, in addition to activating the transcriptional program for endoderm development, thereby forming a stable circuit in the GRN (Davidson et al., 2002; Yuh et al., 2004). Accordingly, knocking down *gatae* severely blocks endoderm development and gastrulation (Davidson et al., 2002).

The endoderm in *C. elegans*, which arises from a single blastomere born at the 8-cell stage, the E cell (Boveri, 1899; Sulston et al., 1983), provides a highly tractable system for investigating the mechanisms of cell specification, differentiation, and organogenesis. This progenitor cell gives rise to a clone 20 cells comprising the intestine, which are arranged in nine rings (int1-9) spanning the length of the animal (see Figure 1.1). Endoderm development is driven by pairs of duplicated genes encoding GATA-like transcription factors: the divergent MED-1/2 factors and the canonical END-1/3 and ELT-2/7 factors. The maternally provided SKN-1/Nrf transcription factor activates MED-1 and -2, which activate the specification of mesendodermal fate in the EMS blastomere (Bowerman et al., 1992). In the anterior daughter of EMS, the MS cell, the Wnt effector POP-1/Tcf represses the expression

of *end-1/3*, and MED-1 and -2 activate *tbx-35*, whose product specifies mesodermal fate. In the E cell, the posterior daughter of EMS, a triply redundant signaling system (Wnt, Src, and MAPK) leads to the phosphorylation of POP-1 by nemo-like kinase LIT-1 (Bei et al., 2002; Maduro et al., 2002; Meneghini et al., 1999; Shin et al., 1999; Thorpe et al., 1997). Together with MED-1/2, Wnt-signaled POP-1 activates genes encoding the transiently expressed endoderm specification factors END-1 and -3, which in turn activate the expression of *elt-7* and *-2*, orthologues of vertebrate *GATA4/5/6* (Figure 1.1). Expression of the ELT factors is sustained throughout the remainder of the animal's life via a positive autoregulatory loop that "locks down" the differentiated state of the intestine (Maduro, 2017; Maduro and Rothman, 2002; McGhee, 2007). While *elt-7* loss-of-function mutants do not show a discernible phenotype, animals lacking ELT-2 arrest at early larvae stage (L1) owing to severely obstructed gut (Sommermann et al., 2010). Nonetheless, *elt-2(-)* mutant animals contain a well-defined intestinal lumen and the intestinal cells appear to be fully differentiated (Fukushige et al., 1998; Sommermann et al., 2010). In the absence of both ELT-2 and -7, however, the intestinal lumen is completely abolished and differentiation appears to proceed in only a subset of the endoderm-derived cells in a sporadic manner (Sommermann et al., 2010). This suggests that ELT-2 and -7 function synergistically in mediating morphological differentiation of the intestine, and additional input(s) mediate a bistable switch in the endodermal differentiation program in the absence of ELT-2 and -7 (Dineen et al., 2018; Sommermann et al., 2010).

In this study, we sought to decipher the functional requirements and interactions between the GATA transcription factors and how they allow rapid and

faithful deployment of the endoderm GRN. We found that the endoderm GRN consists of a series of interlocking feedforward loops, creating “sequential redundancy” in the cascade and culminating in the rapid lockdown of cell fate. We further report that END-1 acts at a transition point, participating in both specification and differentiation. Finally, we demonstrated the important roles of GATA factors in safeguarding intestinal cell fate and defining the boundaries of the digestive tract. Overall, our findings reveal the nature of the extensive genetic redundancy in the regulatory circuitry and how this GRN architecture dictates robust cell specification and differentiation during embryonic development.

Results

Sequential Redundancy Suggests Feedforward Regulatory Circuitry in the Endoderm GRN

Owing to the extensive genetic redundancy, single mutants of most of the genes throughout the *C. elegans* endoderm GRN either show no overt phenotype (single *med* mutants, *end-1(-)*, *elt-7(-)*) or an extremely weakly penetrant phenotype (*end-3(-)*). Moreover, while the *elt-2(-)* mutant undergoes larval arrest immediately after hatching with a dysfunctional gut, the gut appears fully differentiated and a strong gut differentiation defect requires the removal of both *elt-2* and *elt-7* (Figure 2.1A) (Fukushige et al., 1998; Sommermann et al., 2010). Similarly, strong phenotypes are observed only when both *meds* or both *ends* are removed in pairs. In this study, we sought to examine the basis for this extensive redundancy in the pathway and to illuminate how it might contribute to faithful specification and differentiation in endoderm GRN.

Temporally resolved transcriptomic analyses revealed that the GATA transcription factors are sequentially activated in the mesendoderm regulatory pathway (Baugh et al., 2003; Tintori et al., 2016). This observation suggests that, rather than pairs of factors (MEDs, ENDs, ELTs) acting together at specific tiers in the cascade (Figure 1.1), each factor is redundant with its immediate upstream or downstream factor in a continuously sequential cascade (“sequential redundancy”). For example, as is often seen in forward-driven biological switches, each may act through a feedforward motif in which a given factor activates both its immediate target gene and the target of that gene (Mangan and Alon, 2003).

To test the model that endoderm differentiation is directed by a series of sequentially redundant feedforward regulatory motifs, we constructed a series of double mutants and compared the penetrance of lethality and the extent of gut differentiation. We found that unlike the mild or undetectable phenotypes observed with single mutants, removing pairs of genes that are expressed at sequential steps in the cascade invariably results in severely diminished viability (Figure 2.1A) and defects in endoderm specification/differentiation, as revealed by disrupted gut lumen morphology (Figure 2.1A, B). This effect is associated with sporadic expression, and in some cases, the complete absence of, gut-specific rhabditin granules (Clokey and Jacobson, 1986) (Figure 2.1C). We found that the expression of the gut-specific IFB (Intermediate Filament, B)-2 protein is strongly diminished in the double mutants (Supplemental Figure 2.1A). Moreover, reduced AJM (Apical Junction Molecule)-1 expression suggests gut epithelialization defects in double mutants of sequential members in the endoderm GRN (Supplemental Figure 2.1B).

In the *med-2(-); med-1(-)* double mutants, all embryos die as embryos as MS fails to be specified and its fate is transformed to that of the C mesectodermal progenitor in the early embryo (Figure 2.1A), as is also the case in embryos lacking the initiating, maternally provided SKN-1 transcription factor (Bowerman et al., 1992). The E cell similarly adopt a C cell fate in some, but not all, of the arrested embryos (Maduro et al., 2007). As previously reported (Maduro et al., 2005b), many *end-1(-) end-3(-)* mutants die as embryos owing to transformation of the E cell into a C-like cell (Figure 2.1A). Thus, END-1 and -3 act as redundant selector genes that promote specification of endoderm over other cell fates.

Consistent with the sequential redundancy model, removal of two genes that function at alternate steps in the endoderm cascade does not result in the strong synergistic effect that we observed with removal of pairs of sequentially expressed genes (Figure 2.1A, E, F; Supplemental Figure 2.2). We observed normal expression of IFB-2 and AJM-1 along the length of the gut region in all such double mutants (Supplemental Figure 2.2). Further, while the *end-3(-); med-1(-)* double mutant, in which sequential genes in the cascade are removed, shows severe embryonic lethality, most (89.5%; n = 219) of the *end-1(-); med-1(-)* double mutants, in which alternate genes in the cascade are removed, develop into fertile adults (Figure 2.1A). This observation is also consistent with the reported divergent roles of END-1 and -3 in endoderm specification (Boeck et al., 2011). Moreover, the *elt-7(-) end-3(-)* double mutants are largely viable, in contrast to the *end-3(-); med-1(-)* sequential double mutants, which show a strongly penetrant embryonic lethal phenotype (Figure 2.1A). Of the hatched L1 larvae, 31% of *end-3(-); med-1(-)* sequential double mutant animals exhibit no overt signs of gut differentiation, while only 2% of *elt-7(-) end-3(-)* alternate double mutants completely lack gut (Fisher's exact test; $p < 0.001$) (Figure 2.1D, G). However, many *elt-7(-) end-3(-)* mutants contain a partially differentiated gut (Figure 2.1G). We reasoned that the developmental defects observed in the most affected animals are the result of suboptimal expression of *end-1* in the absence of *end-3* (Maduro et al., 2007).

While neither single mutant shows a discernible phenotype, animals lacking both END-1 and ELT-7 are 100% inviable, and the arrested L1 larvae show a striking gut differentiation defect (Figure 2.1A, Supplemental Figure 2.1). The mutant worms

contain patches of apparently differentiated gut as evidenced by expression of gut granules and immunoreactive IFB-2, similar to *elt-7(-); elt-2(-)* double mutants, which exhibit an all-or-none block to differentiation event along the length of the animals (Figure 2.1B, C; Supplemental Figure 2.1) (Sommermann et al., 2010). However, the differentiation defect observed in *elt-7(-) end-1(-)* double mutants appears to be somewhat milder from that in *elt-7(-); elt-2(-)*: unlike the latter, we observed defined, albeit sporadic, lumen and brush border, and the undifferentiated patches are more frequently interspersed with differentiated patches (Figure 2.1B, C; Supplemental Figure 2.1A) (more below).

Analysis of most alternate and sequential double mutant combinations show similar effects (Figure 2.1): sequential double mutants are invariable much more severely affected than alternate double mutants. Together, our data support a sequentially redundant cascade, comprising a recursive series of feedforward regulatory steps (Figure 2.1H). It is conceivable that such a feedforward system creates a strongly forward-driven, rapidly deployed, switch that ensures timely and robust cell fate commitment and robust lockdown of endoderm cell fate during embryogenesis.

Computational Model Predicts Phenotypes of Sequential and Alternative Double Mutants

We took a complementary approach to testing the sequential feedforward model through a computational strategy. We constructed a mathematical model based on the network topology, in which the interactions between the GATA factors, as well as the additional POP-1-dependent activation of *end-3* and *end-1*, were written as a series of ordinary differential equations and the model parameters were determined

by fitting to published transcriptomics data (Baugh et al., 2003; Tintori et al., 2016) using a custom algorithm that follows an iterative least-squares method. We then carried out *in silico* perturbations of the feedforward circuits to provide predictions of these effects on the relative timing and levels of *elt-2* activation and therefore the final output of the endoderm GRN. Our computed results revealed that the *elt-2* expression is predicted to occur, but its onset delayed in all single mutants and in mutants lacking alternate pairs of GATA factors (Figure 2.1I). However, as observed with the experimental outcomes, *elt-2* expression is completely abrogated in most double mutant combinations in which sequential members of the endoderm cascade are removed (Figure 2.1I), consistent with their pronounced developmental defects (Figure 2.1A). The predicted *elt-2* expression level strikingly correlates (Spearman's Rank Correlation $\rho = 0.96$; $p < 0.001$) with the experimentally observed penetrance of the phenotypes of the single and multiple mutants (Figure 2.1I): single and alternate double mutant combinations, which show no, or weak phenotypes, are predicted to express high levels of *elt-2* early, while sequential double mutants, which show strong defects in gut development and inviability, are predicted not to express *elt-2* at substantial levels at its normal time of onset. These findings, based on modeling with gene expression data, bolster the proposed recursive feedforward structure of the GATA factor cascade.

Variation in Temporal Expression Explains Distinct Functions for MED-1 and -2

It has been shown previously that *end-3* expression is activated slightly earlier than *end-1* (Supplemental Figure 2.3A) (Maduro et al., 2007; Tintori et al., 2016), as is also consistent with our genetic analyses (Figure 2.1). Additionally, the END

paralogues have diverged considerably with variable DNA-binding domains that perform overlapping but distinct functions (Boeck et al., 2011). Unlike the ENDs, MED-1 and -2 are 98% identical (Maduro et al., 2001). Nonetheless, our genetic evidence demonstrates distinguishable contributions of the two nearly identical paralogues, with MED-2 functions preceding MED-1 (Figure 2.1; Supplemental Figure 2.1; Supplemental Figure 2.2). By examining published lineage-resolved single-cell RNA-seq data (Tintori et al., 2016), we observed that *med-2* transcripts are undetectable by the 8-cell stage, while *med-1* expression persists briefly in the endoderm precursors (Supplemental Figure 2.3A). The differential temporal expression of the MEDs was recapitulated using protein-fusion reporters: unlike MED-1, which is expressed in 16E embryos, MED-2 protein is largely diminished by the 8E embryonic stage (Supplemental Figure 2.3B). Together, our data suggest *med-1* and *-2* genes are differentially regulated, and MED-2 functions upstream of MED-1, further supporting the feedforward structure at the top of the endoderm regulatory cascade.

Synergistic Requirements and Cross-regulatory Interactions of END-1, ELT-7, and ELT-2

As described above, while both *elt-7(-)* and *elt-2(-)* single mutants contain a fully differentiated gut, with a contiguous lumen from the pharynx to the rectum surrounded by cells of normal differentiated morphology, *elt-7(-); elt-2(-)* double mutants invariably lack both a defined gut lumen as well as some gut cells, and show a sporadic, all-or-none, block to gut differentiation along the length of the animals (Figure 2.1A-C; Figure 2.2A; Supplemental Figure 2.1; Supplemental Figure 2.4) (Sommermann et al., 2010). Although differentiation is highly defective in the absence of ELT-2 and -7, patches of well-differentiated gut are nonetheless evident. Moreover,

many terminal differentiation genes remain activated in the absence of ELT-2 and -7 (Dineen et al., 2018). For example, eliminating the functions of ELT-2 or -7 has little effect on the expression of *act-5*, a gene encoding an actin isoform required for microvilli formation (Dineen et al., 2018; MacQueen et al., 2005). These observations suggest that at least one additional factor, in addition to the ELTs, may activate gut differentiation. One such candidate is END-1, which acts immediately upstream of the *elt* genes. Indeed, although *end-1(-)* and *elt-7(-)* mutants are both phenotypically silent, we found that the *elt-7(-) end-1(-)* double mutant shows extensive gut differentiation defects, with sporadic expression of rhabditin granules (Figure 2.1A-C; Figure 2.2B) and ifb-2 (Figure 2.2C, D; Supplemental Figure 2.1), as well as reduced number of differentiated gut cells (Figure 2.2E; Supplemental Figure 2.5), reminiscent of *elt-7(-); elt-2(-)* double mutant animals.

We tested whether END-1 could account for the residual gut-promoting activity by removing it from animals also lacking ELT-2/7. Strikingly, simultaneously eliminating END-1, ELT-7, and ELT-2 results in a complete block to intestinal differentiation (Figure 2.2F-I). We found that 19.6% of *elt-7(-) end-1(-); elt-2(-)* mutants undergo embryonic arrest, and the remainder die as L1 larvae (n = 143). The triple mutant animals exhibit no morphological signs of gut differentiation, showing no gut granules (Figure 2.2F, G, H), no detectable intestinal brush border or lumen (Figure 2.2F, G, I), and no differentiated gut nuclei expressing a gut-specific peptidase transporter, OPT-2 (Figure 2.2J; Supplemental Figure 2.6). We found that knocking out *end-1* strongly reduces the expression level of *act-5* (Figure 2.2K, L), and its expression is further downregulated in *elt-7(-) end-1(-)* and *elt-7(-) end-1(-); elt-2(RNAi)*

animals (Figure 2.2K; Supplemental Figure 2.7), suggesting that END-1, ELT-7 and ELT-2 act collaboratively to mediate *act-5* expression, and that END-1 may compensate for the loss of ELT-2 and -7 inputs.

A challenge to the notion of a role for END-1 as the gut-promoting factor in the absence of the ELTs is that its expression in wildtype embryos is transient such that its product is largely undetectable by the 16E embryonic stage (Li et al., 2019; Zhu et al., 1997); yet gut differentiation seen in the differentiated patches in the *elt-7(-); elt-2(-)* double mutant appears strong and robust late in development. These findings led us to hypothesize that ELT-2 and/or ELT-7 may normally repress *end-1* transcription through feedback inhibition and that in the absence of the ELTs, *end-1* may be upregulated and drive differentiation. Indeed, we found that the intensity of an *end-1* endogenous protein fusion reporter is modestly elevated in 8E embryos when *elt-2* is knocked down by RNAi (Figure 2.3A). Moreover, the expression level of *end-1* is upregulated in both 4E and 8E embryos when ELT-7 and -2 are simultaneously depleted (Figure 2.3B). While these findings provide evidence for the hypothesized feedback inhibition, the effect is rather weak, as we did not observe obvious perdurance of *end-1* expression (see Discussion).

Taken together, our results suggest END-1 is poised in the cascade at the interface between specification and differentiation, placing it at the crux of this key transition. END-1, acting with END-3, regulates *specification* of the E lineage, whereas END-1, acting with ELT-7 and ELT-2, controls *differentiation* of the intestine.

ELT-2 and ELT-7 Collaborate to Safeguard Intestinal Cell Fate

When improperly specified, E has been shown to undergo wholesale lineage conversion to either a C-like mesectodermal fate (when SKN-1, the MEDs, or END-1/3 are removed), thereby inappropriately generating epidermis, or an MS-like mesodermal fate (for example, in the absence of Wnt signaling), thereby inappropriately giving rise to pharyngeal tissue (details described in Figure 2.4A). Given that END-1 straddles the transition from specification of the endoderm progenitor and differentiation of the gut, we sought to investigate whether specification and differentiation involve distinct regulatory events by examining non-endodermal (epidermal and pharyngeal) gene activity when differentiation is impaired after this transition is thought to occur. In *end-1(-) end-3(-)* double mutants, misspecification of the E cell and its conversion to a C-like mesectodermal progenitor, results in severe morphological defects as a result of the supernumerary epidermal cells and consequent deformation of the epidermis (Figure 2.4B, Supplemental Figure 2.8) (Maduro et al., 2005b). In contrast, the *elt-7(-) end-1(-); elt-2(-)* triple mutant animals that, like the *end-1(-) end-3(-)* double mutants, do not make a discernible gut, are not substantially defective for overall body morphogenesis (Supplemental Figure 2.8). Consistent with this observation, unlike *end-1(-) end-3(-)* double mutant animals, *elt-7(-) end-1(-); elt-2(-)* triple mutant larvae contain a wildtype number of epidermal cells, implying that E→C misspecification does not occur (Figure 2.4B). These results imply that END-3 alone is sufficient to promote endoderm specification over C-like mesectodermal cell fate. However, we were surprised to observe mis-expression of the pharyngeal muscle-specific myosin gene, *myo-2*, in the mid-gut in many *elt-7(-); elt-2(-)* and *elt-7(-) end-1(-); elt-2(-)* mutants (Figure 2.4C, D). Additionally, knocking

down *elt-7* in *end-1(-); elt-2(-)* results in ectopic expression of *ceh-22*, which encodes a pharynx-specific NK-2-type homeodomain protein, in the intestine (Supplemental Figure 2.9). As the Wnt/POP-1-dependent polarization of EMS is unperturbed in the mutants, we reason that the inappropriate expression of pharyngeal genes is unlikely to be the result of wholesale E→MS transformation, but may reflect later errors in the fidelity of differentiation.

PHA-4/FoxA is the organ selector gene that specifies pharyngeal identity, regulating *myo-2* and *ceh-22* among thousands of other targets in the pharynx (Mango et al., 1994; Zhong et al., 2010). We found that the ectopic expression of *myo-2* in *elt-7(-); elt-2(-)* is at least partially suppressed in *pha-4(RNAi)* animals (Figure 2.4E). In wildtype animals, PHA-4 is expressed at high levels in the pharynx and rectum, and at low levels in the intestine (Figure 2.4F, F') (Horner et al., 1998; Kalb et al., 1998). It was previously found that ELT-2 positively regulates *pha-4* as forced expression of *elt-2* causes widespread activation of *pha-4* (Kalb et al., 1998). Paradoxically, we found that *pha-4* is upregulated in the intestine in *elt-2(-)* animals (Figure 2.4G, G'), and depleting *elt-7* in *elt-2(-)* animals further enhances this effect (Figure 2.4H, H'). Perhaps ELT-2 serves dual roles as both an activator and a repressor depending on its expression level. Thus, it appears that upregulation of *pha-4* in the mid-gut in the absence of ELT-2 and -7 activates sporadic ectopic pharyngeal gene activity. Supporting our model, PHA-4 target genes have been shown to be regulated in part by PHA-4 binding affinity and occupancy (Fakhouri et al., 2010; Gaudet et al., 2004). Taken together, our results show that the boundaries of regulator state domains along

the digestive tract of *C. elegans* are established, at least partly, by transcriptional repression mediated by ELT-2 and -7 in the intestine (Figure 2.4I).

END-1 and ELT-7 Establish the Proper Boundary between the Valve and Intestinal Tubes

The foregoing results suggest that the core regulators involved in gut differentiation (END-1, ELT-2, and ELT-7) regulate the faithful differentiation of cells in the digestive tract. The pharynx and the intestine are linked by the pharyngeal-intestinal valve (vpi), which consists of six cells arranged into three rings (Rasmussen et al., 2013) (Figure 2.5A). In wildtype worms, *ajm-1*::*GFP* (*jcIs1* transgene) is strongly expressed through the adherens junctions lining the lumen of the pharynx and vpi, and the expression drops off sharply to low levels starting at the anteriormost ring of the intestine, and continuing throughout the entire length of the animal (Köppen et al., 2001; Sommermann et al., 2010). However, while *end-1(-)* and *elt-7(-/-) end-1(+/-)* animals show wildtype *ajm-1* expression pattern, *ajm-1* signal is markedly elevated in the anterior intestinal terminus of *elt-7(-/-) end-1(-/-)* animals (Figure 2.5B-E). Additionally, we observed ectopic expression of two vpi markers, *cdf (cation diffusion facilitator)-1* (Figure 2.5F-H) and *hum (heavy chain, unconventional myosin)-1* (Figure 2.5I-K), in the anterior terminus of *end-1(-/-) elt-7(-/-)* larvae.

It has been previously shown that worms lacking *elt-2*, like *elt-7(-/-) end-1(-/-)* animals, exhibit striking caudal extension of the valve cell markers (Sommermann et al., 2010). We found that ELT-2 is expressed at wildtype levels in *elt-7(-/-) end-1(-/-)* larvae, owing to its positive autoregulation (Figure 2.5L). This suggests that the expansion of vpi gene expression in the intestine we observed in *elt-7(-/-) end-1(-/-)* animals is independent of ELT-2 function. It is currently unclear whether the

expression of vpi reporters in the intestine reflects *bona fide* transformation of gut cells into valve-like cells or aberrant development of vpi and mispositioning of excess valve cells. Regardless, our results demonstrate the important roles of intestinal GATA factors in the development of a cohesive digestive tract.

Discussion

The development of *C. elegans* endoderm provides a powerful system to study the regulatory logic underlying cell specification and differentiation. In this study, we reported four major findings: (1) the hierarchical organization and feedforward regulation of GATA factors promote robust and rapid lockdown of endodermal cell fate during *C. elegans* early embryogenesis. (2) END-1 participates in both specification and differentiation and mediates a smooth regulatory state transition. (3) ELT-2 and -7 repress the expression of *pha-4* in the mid-gut to establish regulatory state boundary between the pharynx and the intestine. (4) END-1, ELT-7 and ELT-2 repress the characteristics of pharyngeal valve cell fate at the anterior gut terminus, further define the spatial domains of the foregut and midgut. Our study therefore provides an important insight into the regulatory circuits that directs specification-to-differentiation transition and subsequent restriction and maintenance of differentiation pattern during development.

Architecture of the *C. elegans* Endoderm Regulatory Cascade

This study, together with findings reported in other publications, provided a comprehensive view of the core endoderm regulatory cascade, with six GATA factors acting through reiterated sequential feedforward loops (Figure 2.6). At the top of the cascade, maternally provided SKN-1 binds to and turns on the *meds* and the *ends*

(Maduro et al., 2001, 2005a). Although MED-1 and MED-2 protein sequences are nearly identical, we found distinguishable contributions between the two paralogs, with MED-2 acting upstream of MED-1. Indeed, embryos lacking MED-1 show a weaker loss-of-gut phenotype than those lacking MED-2, when SKN-1 function is debilitated (Maduro et al., 2007). Moreover, *med-2* is expressed slightly earlier than *med-1* (Maduro et al., 2007; Tintori et al., 2016), suggesting they are differentially regulated as we have observed in this study.

In the E blastomere, SKN-1 and the MEDs collaboratively activate END-3. MED-1/2 and END-3 in turn activate END-1. While the two endoderm-specifying factors, END-1 and -3, perform largely overlapping functions, our data suggest that END-3 alone is sufficient to direct endoderm specification and suppress inappropriate mesectodermal development, consistent with the lack of detectable phenotype of in *end-1(-)* single mutants. Interesting, we found that END-1, poising at the interface between specification and differentiation, works synergistically with ELT-2 and -7 to activate the endoderm differentiation program (Figure 2.6). Supporting our model, in vitro gel-shift assays demonstrate the binding of END-1, ELT-7, and ELT-2 to TGATAA sites which are highly enriched in the promotors of intestinal genes (Du et al., 2016; McGhee et al., 2009; Wiesenfahrt et al., 2016). Remarkably, END-1 is able to initiate endoderm differentiation in *Xenopus* embryos, demonstrating its role as a potent organ selector (Shoichet et al., 2000). Hence, it appears that specification and differentiation involve a *bona fide* handoff of regulatory events bound by END-1.

Regulatory Logic of Developmental GRN

We showed that the *C. elegans* endoderm GRN comprises a recursive series of feedforward steps, culminating with rapid terminal differentiation (Figure 2.6). Each GATA factor in the entire cascade receives redundant activating inputs acting through an “OR” logic gate. Consequently, any single mutation in the regulatory cascade is largely phenotypically silent, with the exception of *elt-2(-)*; however, even *elt-2(-)* animals contain what appears to be a well-differentiated intestine. Coherent feedforward motifs of the type we observe reiteratively in the endoderm GRN are ubiquitous in developmental GRNs. Such a network configuration appears to result in a rapid response to activating signal and a delayed response when the inputs are removed (termed sign-sensitive delay), thereby prolonging the effect of a transient activator (Mangan and Alon, 2003). Additionally, feedforward loops are effective at buffering the system against stochastic noise, ensuring developmental robustness (Chepyala et al., 2016; Gui et al., 2016; Maduro, 2015) This design principal appears to be crucial to ensure timely and robust activation of *elt-7* and *-2*, as we and others have shown (Boeck et al., 2011; Dineen et al., 2018; Maduro et al., 2015). Delayed onset of *elt-2* in early embryos has been shown to cause sustained metabolic defects in larvae despite the reattainment of wildtype ELT-2 levels (Maduro et al., 2015).

Our results suggest that END-1 mediates an all-or-none switch in the differentiation program in the absence of ELT-2 and -7. END-1 straddles both specification and differentiation, being buttressed by END-3 upstream and ELT-2/7 downstream. The only difference in these END-1 functions appears to be its timing of action and partnership with another regulatory factor. Regulatory nodes in early specification can indeed directly control morphogenetic events in various contexts

(Davidson, 2010; Zhu and Rosenfeld, 2004). Interestingly, although END-1 decays shortly after gastrulation, we observed a persistent reduction in *act-5* expression in postembryonic larvae lacking *end-1*. One possible explanation for this observation might be that END-1 targets an unidentified factor (X; Figure 2.6), which may direct differentiation in at least a subset of endodermal progenitors. Like ELT-2 and -7, the X factor would be expected to be maintained through a positive autoregulatory loop, propelling endoderm differentiation after the expression of END-1 has subsided (Figure 2.6) (Sommermann et al., 2010). Alternatively, END-1 may directly activate differentiation gene batteries in early embryos, and that regulatory state might be sustained through the propagation of epigenetic memory. This priming mechanism has recently been demonstrated in the specification of the ASE sensory neurons in *C. elegans* (Charest et al., 2020). Two transiently expressed T-box factors, TBX-37 and -38, lock their target, *lsy-6*, in a transcriptionally active state during early embryogenesis, priming it for activation in restricted neuronal lineage (Charest et al., 2020). In mammals, Pax-7 (paired-box-7) initiates myogenic specification and differentiation. Interestingly, many enhancers of its target genes retain epigenetic signatures and remain active even in the absence of the initial activator (Zhang et al., 2020).

We found that knocking down *elt-2* causes a slight, but significant, increase in *end-1* expression in early embryos; however, we did not observe obvious perdurance of END-1 when ELT-2 and ELT-7 are depleted, though we cannot rule out the possibility that the modest negative feedback we observed was not due to incomplete RNAi penetrance. Nevertheless, we propose that this modest feedback inhibition may

function to facilitate the transition of regulatory states and ensure that developmental process moves inexorably forward. For example, the repression of an early cardiac specification factor, Bmp2, by homeodomain factor Nkx2-5 is necessary for the proper morphological development of the heart in mice (Prall et al., 2007).

Such transcriptional repression is also frequently used to install spatial subdivision of regulatory states (Davidson, 2010). As we have shown above, ELT-2, ELT-7 and END-1 may repress alternate cell fates in the mid-gut and define the boundaries of the digestive tract. It is noteworthy that structurally similar regulatory circuits are repeatedly deployed in biological networks of different contexts while performing similar functions. Thus, the functional output of a GRN depends not only on the specificity of the transcription factors, but also the underlying circuit architecture (Davidson, 2010; Peter, 2020).

Rapid Rewiring of the Endoderm GRN in *Caenorhabditis*

How might a regulatory system of the type described here evolve? Effectors acting on terminal differentiation gene batteries, such as ELT-2 and PHA-4, are widely conserved across the animal kingdom, while the upstream inputs into GRNs appear to be recent innovations that arose during the radiation of the Elegans supergroup within the *Caenorhabditis* genus (Maduro, 2020). The *ends* and *meds* have been proposed to have arisen from the duplication of *elt-2*. Hence, gene duplication, coupled with *cis*-regulatory changes, may have led to the emergence of new circuitry and rewiring of the endoderm GRN in nematodes.

Intercalation of the MEDs and ENDs in the cascade may serve to buffer the system against environmental variation and developmental noise by freeing ELT-2

from the direct control of SKN-1, which has been shown to play pleiotropic roles in stress response and lifespan regulation, at least in *C. elegans* (Ewe et al., 2020a, 2021a). As we and others have shown, robust induction of *elt-2* is critical to ensure the viability and fitness of the animals (Maduro et al., 2015; Raj et al., 2010). Moreover, the deployment of MEDs and ENDs in sequential hierarchy may allow canalization of the endodermal lineage by rapidly establishing its regulatory state in the E blastomere (Peter and Davidson, 2011). Consequently, this may enable increased developmental speed and early specification of the founder cells in *Caenorhabditis* species (see also Evolution of the Endoderm GRN).

Material and Methods

C. elegans Cultivation and Genetics

Worm strains were cultured using standard procedure (Brenner, 1974) and all experiments were performed at room temperature (20-23^{o}C). All genetic manipulations were performed according to standard techniques (Fay, 2013). *him-5(-)* or *him-8(-)* was introduced into some strains to generate males and facilitate crosses. See Supplemental Table 2.1 for a complete list of strains used in this study.

Immunofluorescence Analysis

Antibody staining with methanol-acetone fixation was performed as previously described (Sommermann et al., 2010). Antibodies MH27 (AB_531819), MH33, and 455-2A4 (AB_2618114) were used to detect AJM-1, IFB-2, and ELT-2, respectively. Alexa Fluor® 488 goat anti-mouse secondary antibody was used at 1:1000 dilution.

RNAi

RNAi feeding clones were obtained from the Ahringer (Kamath et al., 2003) or the Vidal (Rual et al., 2004) library. The bacterial strain was inoculated overnight at 37ºC in LB containing 50 µg/ml ampicillin. The bacterial culture was then diluted 1:10 and incubated for an additional 4 h. Next, 1 mM of IPTG was added to the bacterial culture and 100 µL was seeded onto 35 mm NGM agar plates containing 1 mM IPTG and 25 µg/mL carbenicillin. For simultaneous knockdown of *elt-2* and *elt-7*, the two bacterial strains, each expressing dsRNA for one gene, were concentrated and resuspended in 1 mL of LB in 1:1 ratio before seeding the NGM plates. Seeded plates were allowed to dry for 48 h before use. Next, 10-20 L4 animals were placed on the RNAi plates. 24 h later, the animals were transferred to fresh RNAi plates to lay eggs. The progeny was then collected for analyses.

Imaging and Fluorescence Quantification

The animals were immobilized using 10 mM Levamisole and mounted on 4% agarose pads. Images were acquired, typically at 60X, using Nikon Eclipse Ti-E inverted microscope fitted with ORCA-Flash2.8 camera. For expression studies, maximum intensity Z-projection was generated on the Nikon NIS-Elements AR v4.13.05. Images were then analyzed using ImageJ or Imaris v9.7.2.

RT-qPCR

RNA was extracted from synchronized L1 animals using Monarch® Total RNA Miniprep Kit (#TS010S). cDNA synthesis was performed using SuperScript™ III First-Strand Synthesis SuperMix (Thermo Fisher Scientific, #18080400). Quantitative PCR was performed using BioRad CFX96 Real-Time System. Each 15 µL reaction contained cDNA, primers, and PowerUp™ SYBR™ Green Master Mix (Thermo Fisher

Scientific, #A25743). The data were analyzed using the standard $2^{-\Delta\Delta CT}$ method (Livak and Schmittgen, 2001).

Modeling Endoderm Gene Regulatory Circuits

The topology of the gene circuits with temporal information was written as a system of differential equations, with expression of each factor dependent on the concentration of its activators. The gene cascade is initiated by SKN-1, which was modelled as a square wave in the EMS blastomere. Similarly, the positive inputs of (phosphorylated) POP-1 into *end-3* and *end-1* were modelled as a square wave in the E blastomere (23 mins after the four-cell stage). Model runs were calculated as time-discretized Euler approximations (Hahn, 1991) with time steps of 0.01 s. An iterative least-squares algorithm following a modified Gauss-Newton method (Ruhe, 1979; Yip et al., 2010) was used to fit the model parameters to published transcriptomics data (Baugh et al., 2003; Tintori et al., 2016). The performance of the final model was then evaluated by comparing the predicted phenotypes of the single mutants with published results (Boeck et al., 2011; Dineen et al., 2018; Maduro et al., 2005b, 2015). Finally, predictions of *elt-2* activation (a readout for the commitment to E fate) in the mutant combinations were generated by holding the concentration of knockout genes at zero and otherwise running the model as described. The source code is available on https://github.com/RothmanLabCode/endoderm_GRN_model.

Statistics and Figure Preparation

Statistics were performed using R software v3.4.1 (https://www.r-project.org/). The specific statistical tests were reported in the figure legends. Plots were generated

using R package ggplot2 or Microsoft Excel. Figures were assembled in Inkscape v0.92.4 (https://inkscape.org/).

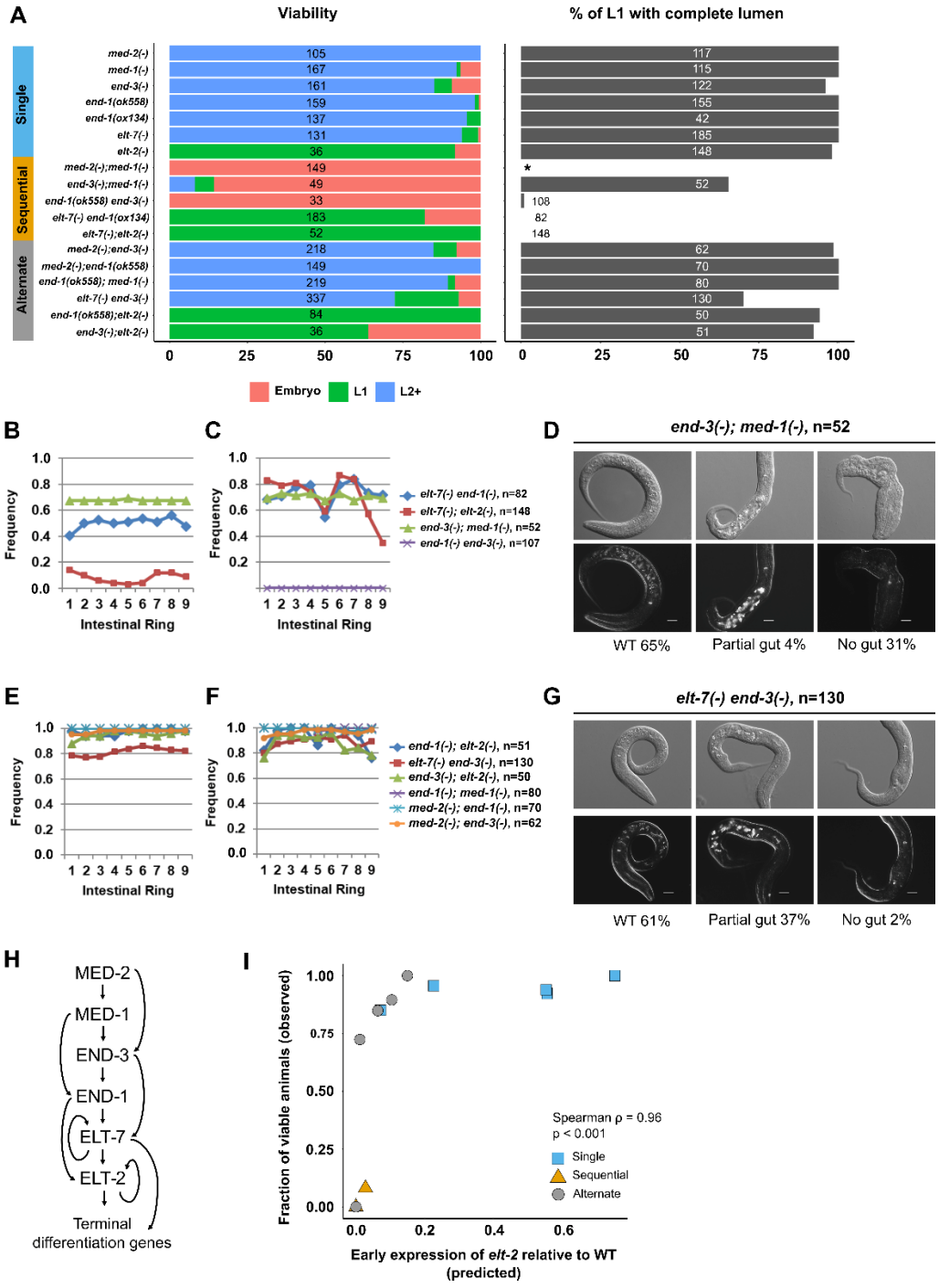

Figure 2.1: Evidence for recursive feedforward loops in the endoderm GRN.
A) Comparison of viability and gut lumen morphology in mutant combinations lacking one or two GATA factors in the endoderm regulatory cascade. Mutants missing sequential members of the endoderm cascade exhibit more penetrant developmental defects than mutants with alternate steps disrupted. We note the two loss-of-function alleles of *end-1*, *ox134* (14822 bp deletion; also removes the adjacent *ric-7* gene) and *ok558* (879 bp deletion), do not result in significant loss in viability (Fisher's exact test;

p = 0.31) or other discernible phenotypes. We used *ox134* in subsequent analyses unless stated otherwise (see Supplemental Table 2.1). The total number of animals scored for each genotype is indicated. No L1 animals were scored for *med-2(-); med-1(-)* (indicated by *) as all double mutants arrest as embryos owing to misspecification of MS (and E in majority but not all of the embryos). The frequencies of (B, E) visible lumen and (C, F) gut granules are dramatically reduced in double mutants missing (B, C) sequential GATA pairs compared to those lacking (E, F) alternate members of the endoderm cascade. (D, G) *end-3(-); med-1(-)* shows a more severe defect in intestinal differentiation than *elt-7(-) end-3(-)*. 31% of *end-3(-); med-1(-)* and 2% of *elt-7(-) end-3(-)* show no overt signs of endoderm differentiation. (G) Many *elt-7(-) end-3(-)* larvae contain a partial gut as observed by DIC microscopy and birefringent gut granules, presumably due to sub-threshold levels of END-1-dependent activation of *elt-2*. Scale bar = 10 μm. (H) The sequential redundancy model of the endoderm GRN. (I) Computed *elt-2* expression levels predict the phenotype severity of the mutant combinations. All *med-2(-); med-1(-)* mutants show severe embryonic lethality despite elt-2 activation owing to a fully penetrant MS→C misspecification. We excluded *med-2(-); med-1(-)* from this analysis.

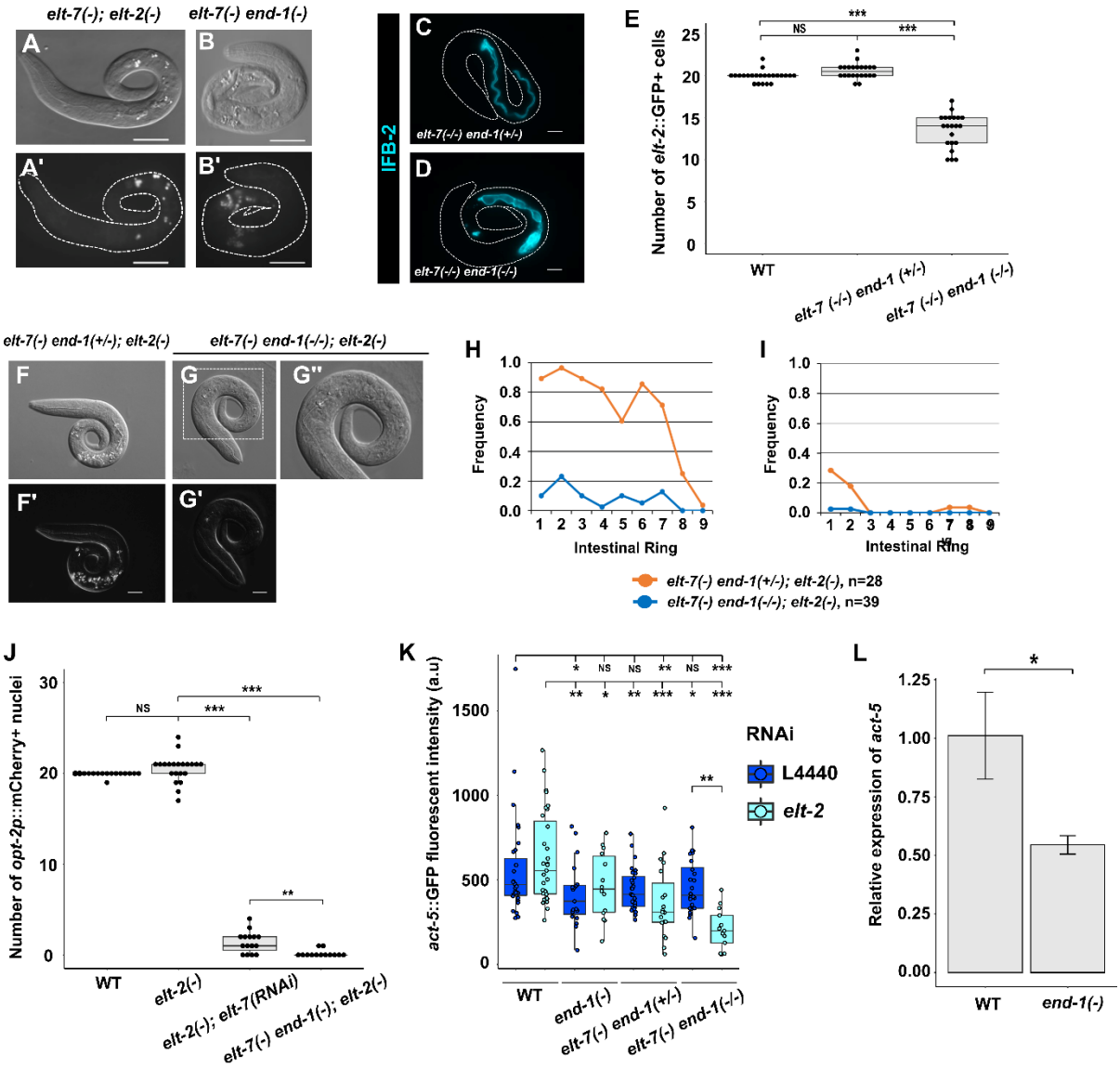

Figure 2.2: Synergistic actions of END-1, ELT-7 and ELT-2 mediate morphological differentiation of endoderm.

(A, B) *elt-7(-) end-1(-)* contains a grossly defective gut with sporadic patches of rhabditin granules interspersed with apparently undifferentiated regions, similar to that observed in *elt-7(-); elt-2(-)*. Scale bars = 20 µm. (C, D) Balanced *elt-7(-/-) end-1(-/+)* larva shows uniform expression of IFB-2 (*kcIs6* transgene) along the length of the animal, while *elt-7(-/-) end-1(-/-)* shows sporadic expression of the transgene. Scale bars = 10 µm. (E) Wildtype and *elt-7(-/-) end-1(-/+)* animals contain an average of 20 intestinal cells, marked by *elt-2::GFP* reporter. The number of differentiated gut cells is markedly reduced in *elt-7(-/-) end-1(-/-)* larvae (mean = 13.5 cells). (F, G) Representative micrographs of *elt-7(-) end-1(+/-); elt-2(-)* and *elt-7(-) end-1(-/-); elt-2(-)* triple mutants. (F, F') *elt-7(-) end-1(+/-); elt-2(-)* lacks a visible lumen and contains sporadic birefringent granules. (G, G') *elt-7(-) end-1(-/-); elt-2(-)* exhibits absolutely no signs of endoderm differentiation. (G") Magnified view of the animal present in (G).

Scale bars = 10 μm. (H, I) The average frequencies of (H) gut granule and (I) lumen are dramatically reduced in *elt-7(-) end-1(-/-); elt-2(-)* compared to *elt-7(-) end-1(+/-); elt-2(-)* animals. (J) Wildtype and *elt-2(-)* show similar number of differentiated intestinal cells, although the variance in *elt-2(-)* is significantly increased (F-test $p < 0.001$). The number of *opt-2p::mCherry* (*irSi24*) expressing cells is strongly reduced in *elt-2(-); elt-7(RNAi)*. No gut cells were detected in vast majority of *elt-7(-) end-1(-); elt-2(-)* triple mutants. (K) The expression of *act-5::GFP* translational reporter (*jyIs13*) in various mutant combinations. END-1, ELT-7, and ELT-2 appear to act together to regulate *act-5* expression in the intestine. (L) *act-5* is downregulated in *end-1(-)* compared to wildtype as detected by RT-qPCR. *act-1* was used as the internal reference. Three replicates were performed for each genotype. Error bars represent standard deviation. * $p \leq 0.05$ by two-tail t-test. For panels E and J, NS $p > 0.05$, ** $p \leq 0.01$, *** $p \leq 0.001$ by non-parametric Kruskal-Wallis test and pairwise Wilcoxon tests with Benjamini & Hochberg correction. For panel K, NS $p > 0.05$, * $p \leq 0.05$, ** $p \leq 0.01$, *** $p \leq 0.001$ by parametric one-way ANOVA followed by pairwise t-tests with Benjamini & Hochberg correction.

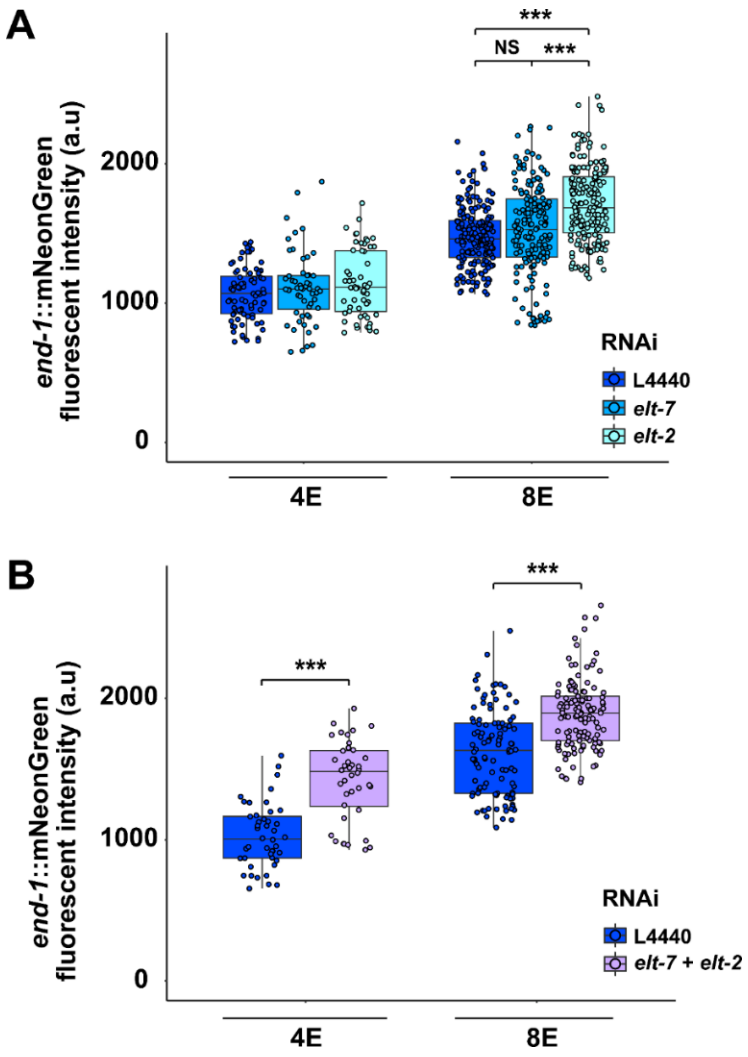

Figure 2.3: ELT-2 antagonizes *end-1* expression.
(A) Expression of endogenously tagged *end-1* increases in 8E embryos upon *elt-2* RNAi treatment. NS $p > 0.05$, *** $p \leq 0.001$ by Kruskal-Wallis test and pairwise Wilcoxon tests with Benjamini & Hochberg correction. (B) Knocking down both *elt-7* and *elt-2* further elevates END-1 expression in both 4E and 8E embryos. *** $p \leq 0.001$ by Wilcoxon tests.

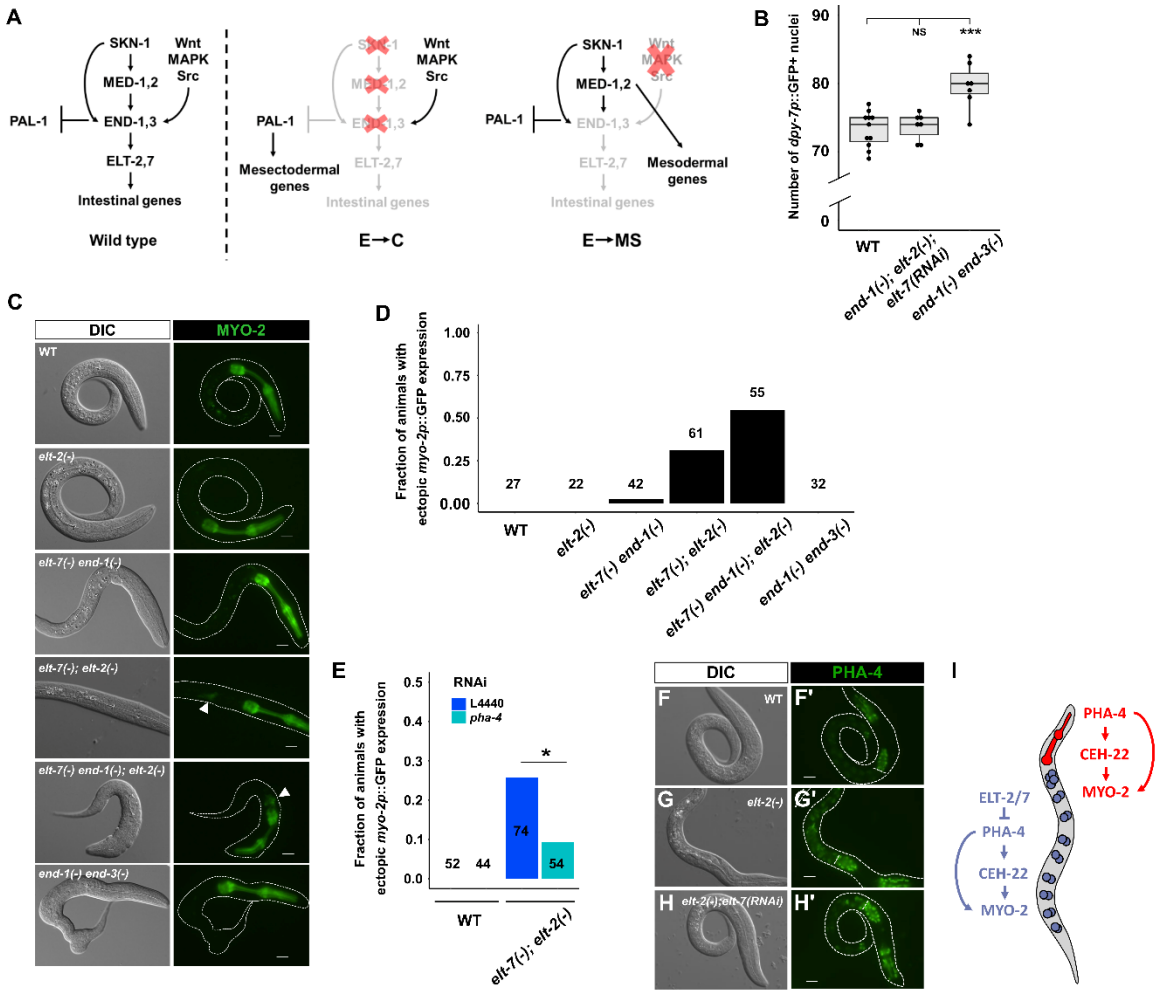

Figure 2.4: ELT-2 and ELT-7 repress pharyngeal fate in the intestine.
(A) E/C or E/MS binary fate choice during early embryogenesis. The Caudal homolog PAL-1 is required for the specification of mesectodermal C blastomere, which gives rise to epidermis and body wall muscles (Hunter and Kenyon, 1996). Maternally provided *pal-1* is specifically translated in the EMS and P_2 cells. In MS and E, PAL-1 activity is blocked by TBX-35 and END-1/3, respectively (Broitman-Maduro et al., 2006). Thus, depleting TBX-35, END-1/3, or their upstream activators, MED-1/2 and SKN-1, causes excess skin and muscle owing to the misspecification of MS and/or E as C, the somatic descendant of P_2 (Hunter and Kenyon, 1996). As EMS divides, Wnt, MAPK, and Src signaling from P_2 polarizes EMS, leading to the phosphorylation and nucleocytoplasmic redistribution of POP-1, and activation of *end-1/3* in E, but not MS. When the polarizing signal from P_2 is disrupted, POP-1 is unphosphorylated, and MED-1 and -2, instead, activate the development of mesoderm (MS), which gives rise to the posterior pharynx and body wall muscles (Maduro and Rothman, 2002; Maduro et al., 2002; Rocheleau et al., 1999; Shin et al., 1999). (B) Wildtype and *end-1(-); elt-2(-); elt-7(RNAi)* larvae contain ~73 epidermal cells, while *end-1(-) end-3(-)* larvae contain ~80 epidermal cells marked by *dpy-7p::GFP* expression. NS $p > 0.05$, *** $p \leqslant 0.001$ by parametric one-way ANOVA followed by pairwise t-tests with Benjamini &

Hochberg correction. (C) Representative DIC and fluorescent micrographs showing different mutation combinations expressing *myo-2p::GFP*. Ectopic expression *of myo-2* is evident in *elt-7(-); elt-2(-)* and el*t-7(-) end-1(-); elt-2(-)* mutants (arrowheads). (D) The frequency of animals showing mis-expression of *myo-2* as shown in (C). Number of animals scored for each genotype is indicated. (E) Knocking down *pha-4* partially rescues ectopic expression of *myo-2* in *elt-7(-); elt-2(-)* animals. * $p \leqslant 0.05$ by Fisher's exact test. (F-H) The expression of endogenously tagged *pha-4* reporter in (F, F') wildtype, (G, G') *elt-2(-)*, and (H, H') *elt-2(-); elt-7(RNAi)* worms. The white horizontal lines in (F'-H') mark the posterior end of the pharynx. Exposure time = 195 ms. All scale bars = 10 μm. (I) Model of spatial repression and fate exclusion in the digestive tract. ELT-2 and -7 repress *pha-4* and prevent the expression pharyngeal genes in the mid-gut.

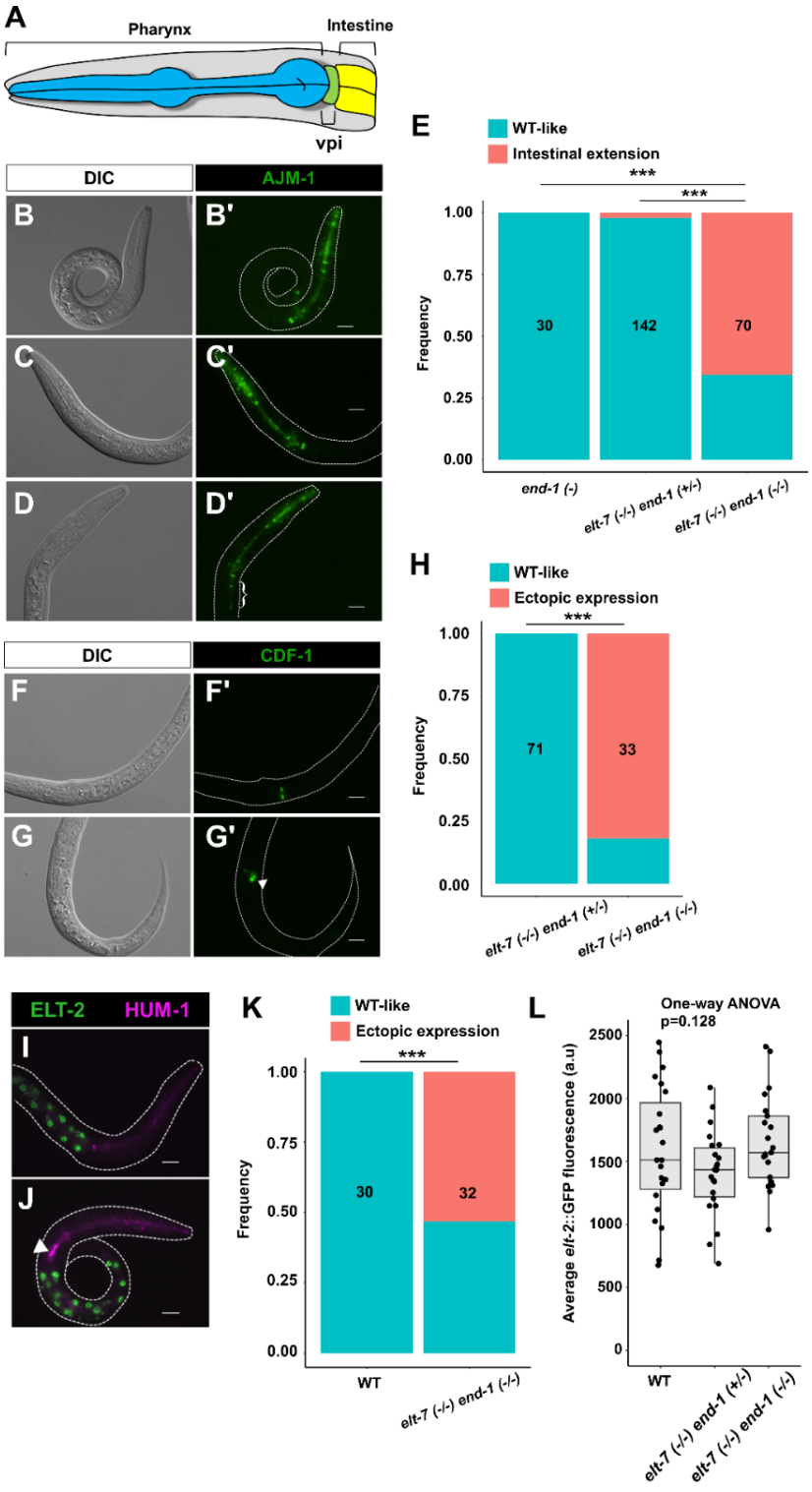

Figure 2.5: ELT-7 and END-1 function synergistically to repress ectopic expression of valve cell markers in the anterior gut.
(A) Drawing highlighting the anatomy of pharynx, vpi, and intestine. The expression of *jcIs1[ajm-1::GFP]* transgene appears wildtype in (B, B') *end-1(-)* and (C, C')

balanced *elt-7(-/-) end-1(+/-)* mutants. (D, D') *elt-7(-) end-1(-)* shows caudal expansion of *jcIs1* expression into the anterior gut (bracket). (E) The frequency of animals exhibiting intense *jcIs1* reporter expression in the anterior gut. (F, F') *cdf-1::GFP* expression is restricted to the vpi in *elt-7(-/-) end-1(+/-)*. (G, G') Ectopic expression of *cdf-1* reporter is observed in *elt-7(-/-) end-1(-/-)* animals (arrowhead). (H) The frequency of animals with ectopic *cdf-1::GFP* expression in the anterior gut. (I) HUM-1 is highly expressed in the vpi in wildtype animal as revealed by an endogenously tagged reporter. (J) Ectopic expression of *hum-1* is observed in *elt-7(-/-) end-1(-/-)* (arrowhead). The intestinal cells are marked by *elt-2::GFP*. (K) The frequency of animals with ectopic *hum-1::RFP* expression in the anterior gut. (L) The expression of ELT-2 is not altered in *elt-7(-/-) end-1(+/-)* and *elt-7(-/-) end-1(-/-)*, compared to wildtype L1 larvae. All scale bars = 10μm. For panels E, H, K, the number of animals scored is indicated in each graph. *** $p \leqslant 0.001$ by Fisher's exact test.

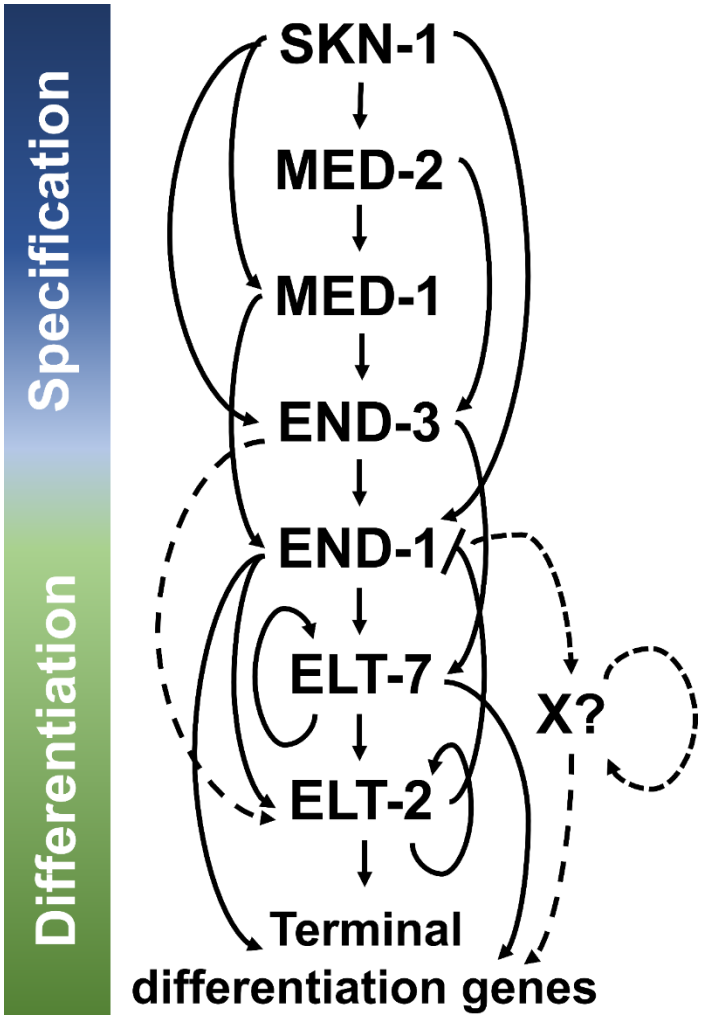

Figure 2.6: Current model for the *C. elegans* endoderm GRN.
Solid lines indicate known interactions identified biochemically or implied genetically, while dashed lines represent proposed interactions. Maternal factor SKN-1 initiates the endoderm cascade which consists of GATA transcription factors arranged in interlocking feedforward circuits. END-1 and -3 are also regulated by non-GATA transcriptional factors, including SPTF-3 (Sullivan-Brown et al., 2016), PAL-1 (Maduro et al., 2005a), PLP-1 (Witze et al., 2009), and POP-1 (Maduro et al., 2005a), which are omitted from this model for simplicity. The observation of residual gut differentiation in *elt-7(-) end-(-)* larvae suggests that END-3 may directly act on ELT-2 and initiate gut differentiation program in some, but not all, of the endodermal progenitors in the double mutants. END-1 may activate an unidentified transcription factor (X) which functions to promote gut differentiation after END-1 decays at ~16E embryonic stage (see text for details).

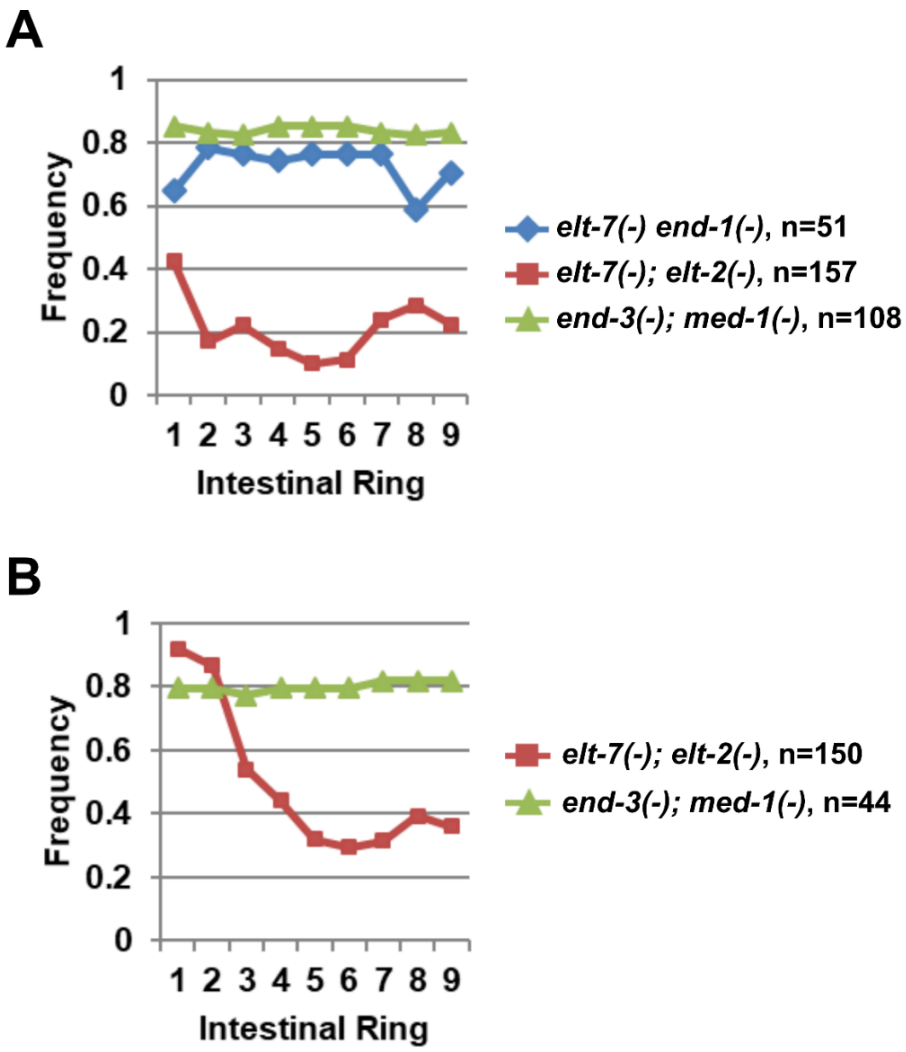

Supplemental Figure 2.1: Severe gut defects in mutants lacking sequential GATA pairs.
Eliminating sequential GATA pairs causes impaired gut differentiation and aberrant expression of immunoreactive (A) IFB-2 and (B) AJM-1.

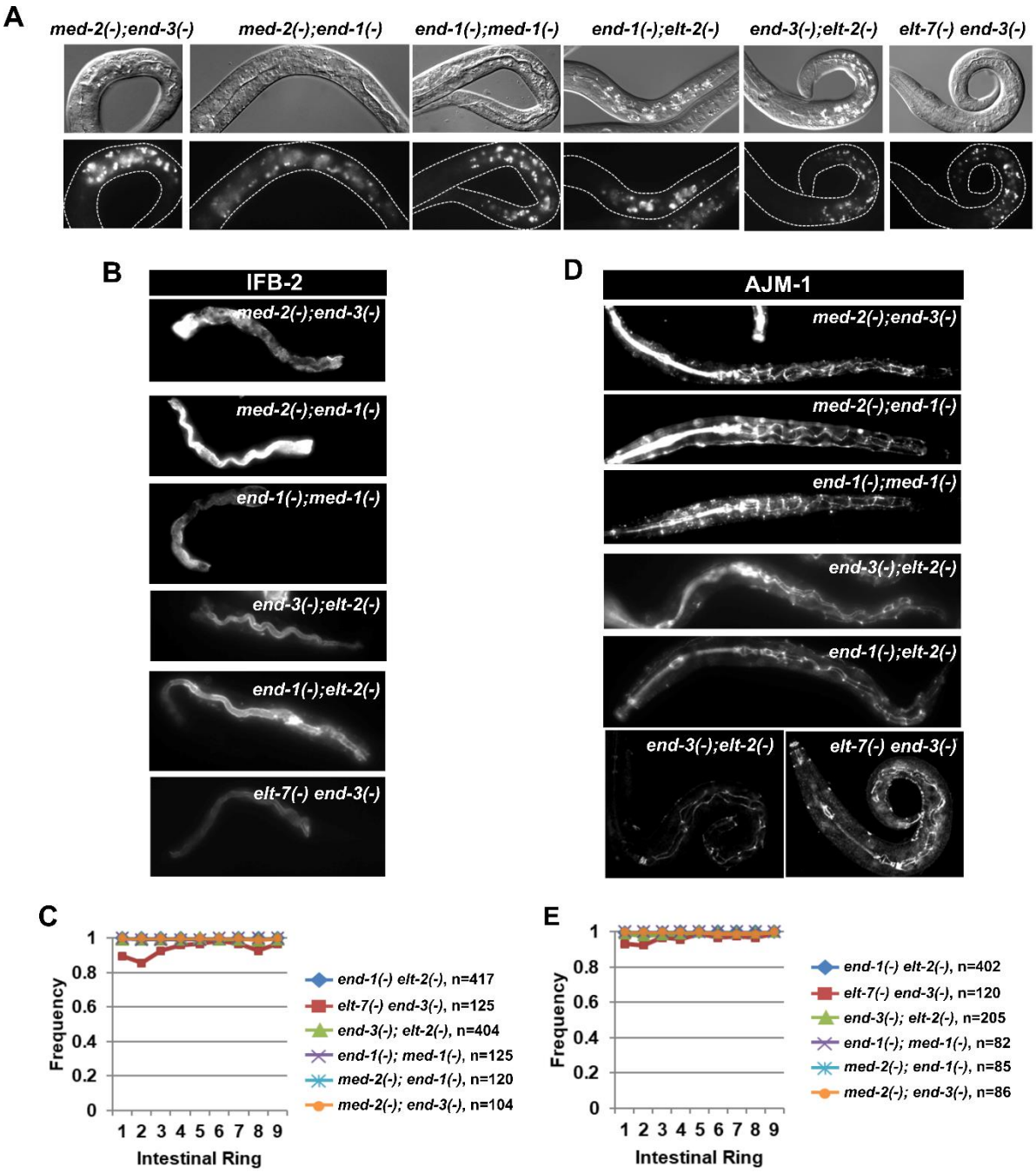

Supplemental Figure 2.2: Mutants lacking alternate GATA pairs do not show apparent gut defects.
(A) Mutants lacking alternate GATA pairs contain fully differentiated lumen (top row) and gut granules (bottom row) along the length of the animals. The same set of double mutants show wildtype expression of (B, C) immunoreactive IFB-2 and (D, E) AJM-1.

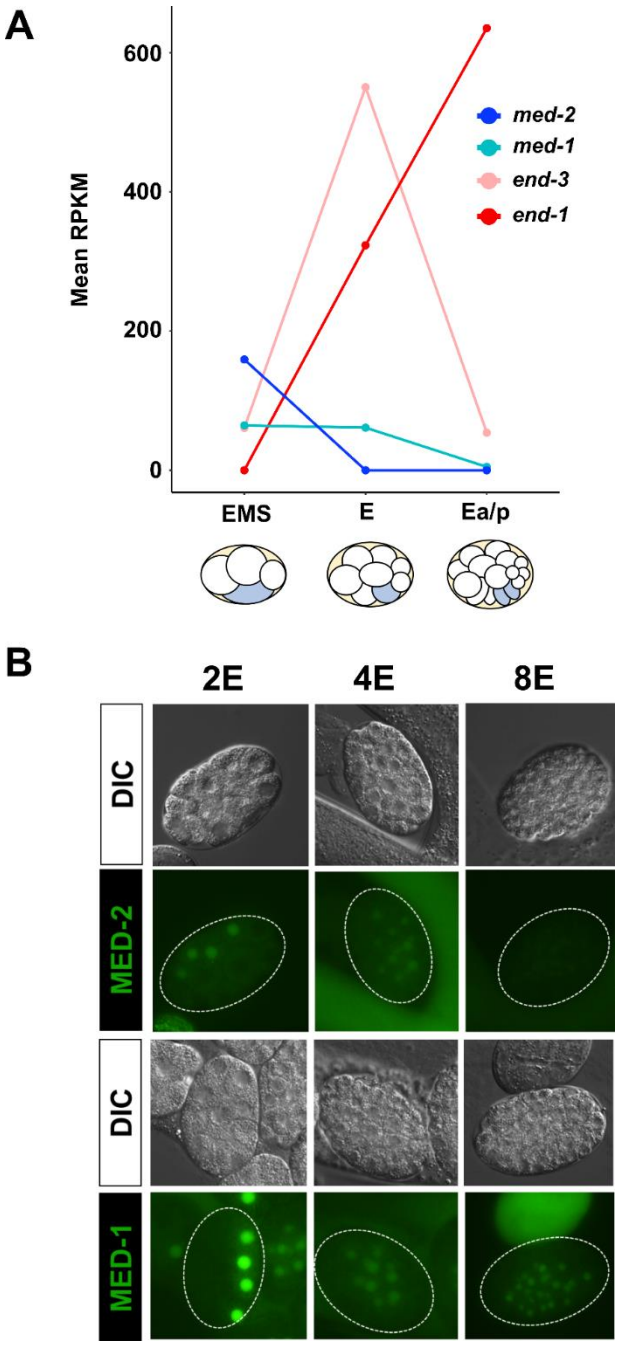

Supplemental Figure 2.3: The endoderm GATA factors are deployed in temporal order.
(A) Temporal expression of *med-2*, *med-1*, *end-3,* and *end-1* revealed by single-cell transcriptomic analysis (http://tintori.bio.unc.edu/) (Tintori et al., 2016). (B) Expression of MED-2 and MED-1 protein-fusion reporters in staged embryos.

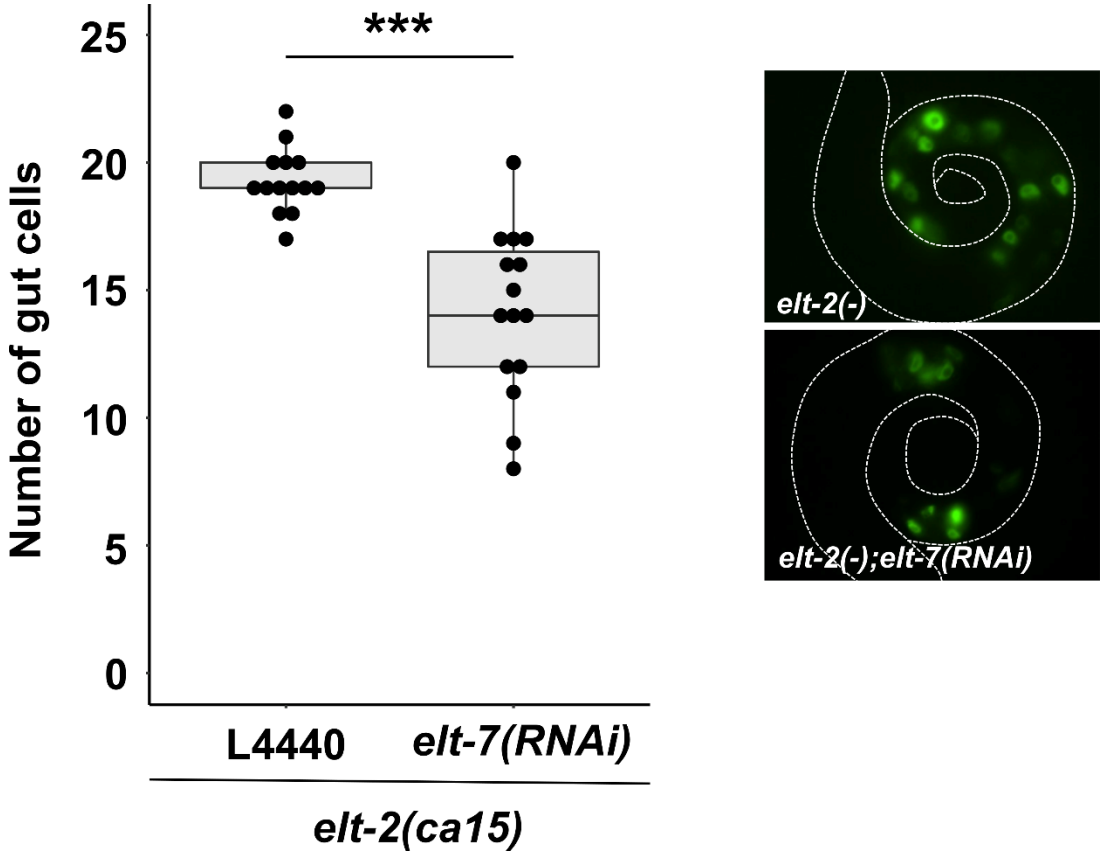

Supplemental Figure 2.4: Reduced number of differentiated intestinal cells in *elt-2(-); elt-7(RNAi)* animals.
On average, *elt-2(-)* animals contain 19.3 cells, while *elt-2(-); elt-7(RNAi)* animals contain 14.1 cells. The number of gut cells were scored by the expression of *elt-2p::GFP* transcriptional reporter *wIs84*. *** $p \leqslant 0.001$ by Wilcoxon tests.

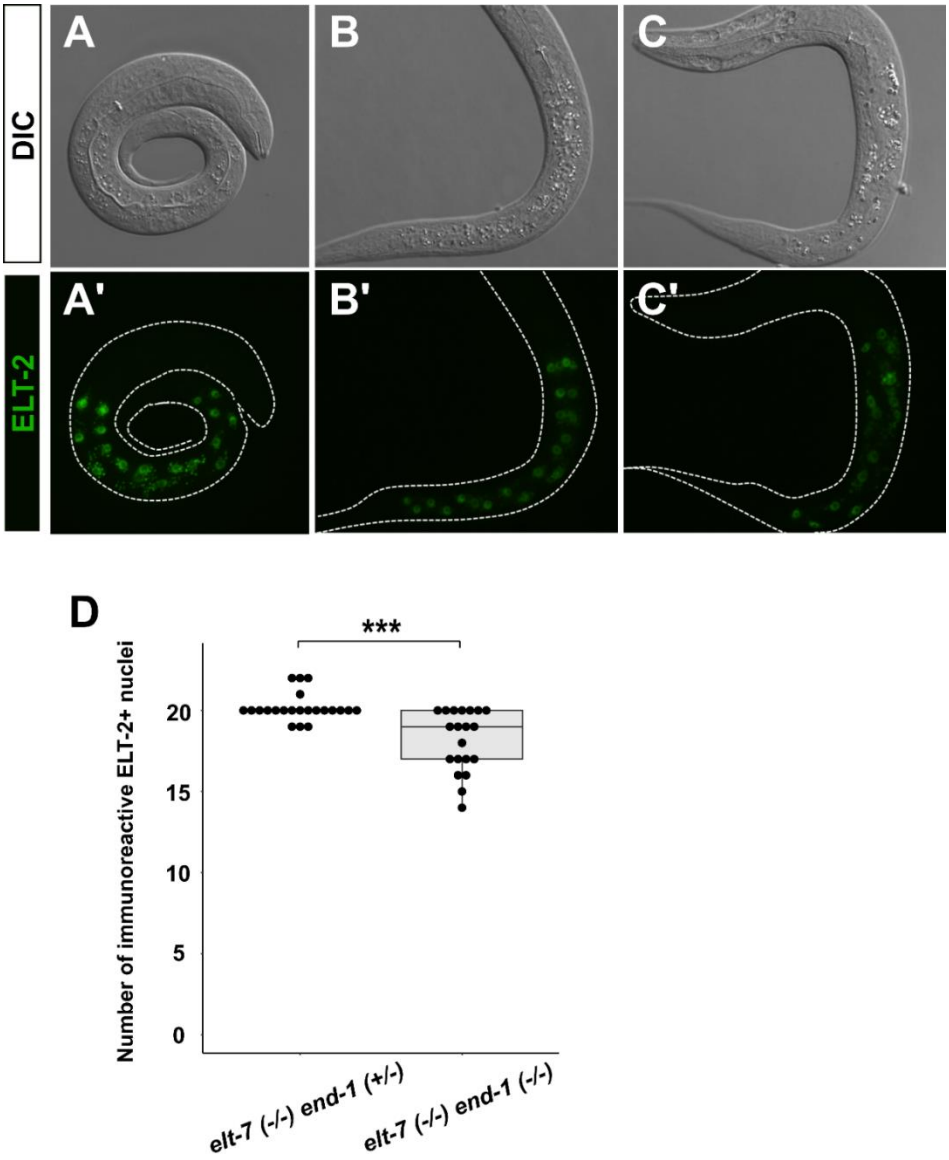

Supplemental Figure 2.5: Reduced number of differentiated intestinal cells in *elt-7(-) end-1(-)* animals.
(A-C) The expression of *elt-2::GFP* translational reporter in (A, A') wildtype, (B, B') *elt-7(-/-) end-1(+/-)*, and (C, C') *elt-7(-/-) end-1(-/-)* L1 larvae. (D) *elt-7(-/-) end-1(-/-)* double mutants contain fewer cells expressing immunoreactive ELT-2 than *elt-7(-/-) end-1(+/-)* animals. *** $p \leqslant 0.001$ by Wilcoxon tests.

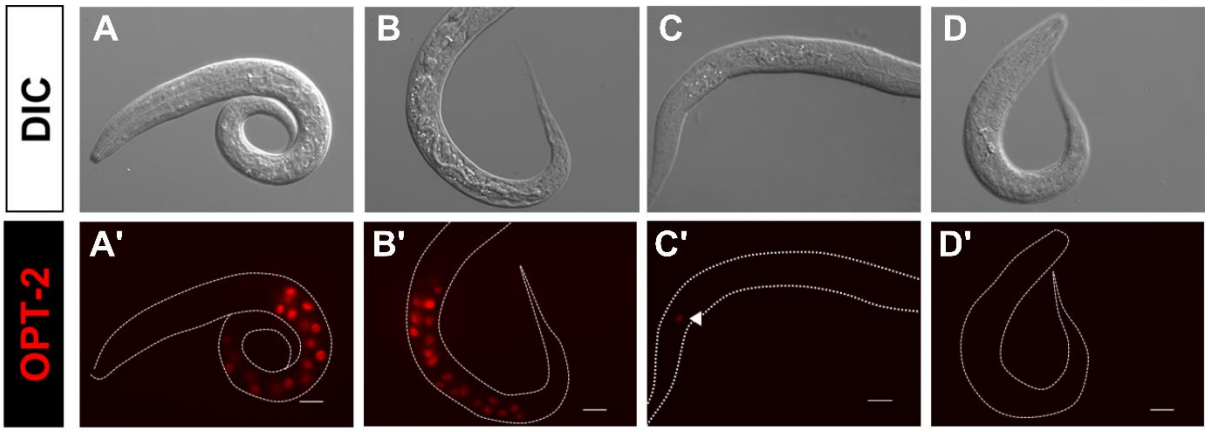

Supplemental Figure 2.6: Reduced number of differentiated gut cells in differentiation-defective mutants.
(A-D) DIC images of (A) wildtype, (B) *elt-2(-)*, (C) *elt-2(-); elt-7(RNAi),* and (D) *elt-7(-) end-1(-); elt-2(-)* animals. While wildtype and *elt-2(-)* worms contain a differentiated gut, *elt-2(-); elt-7(RNAi)* animals lack evident lumen and contains sporadic patches of gut granules. *elt-7(-) end-1(-); elt-2(-)* triple mutants show no apparent signs of differentiation. (A'-D') Fluorescent images of worms in (A-D) show expression of *opt-2p::mCherry*. The number of *opt-2*-expressing cells is markedly reduced in *elt-2(-); elt-7(RNAi)* (arrowhead)*. opt-2* expression is completely abolished in *elt-7(-) end-1(-); elt-2(-).* Scale bars = 10 μm.

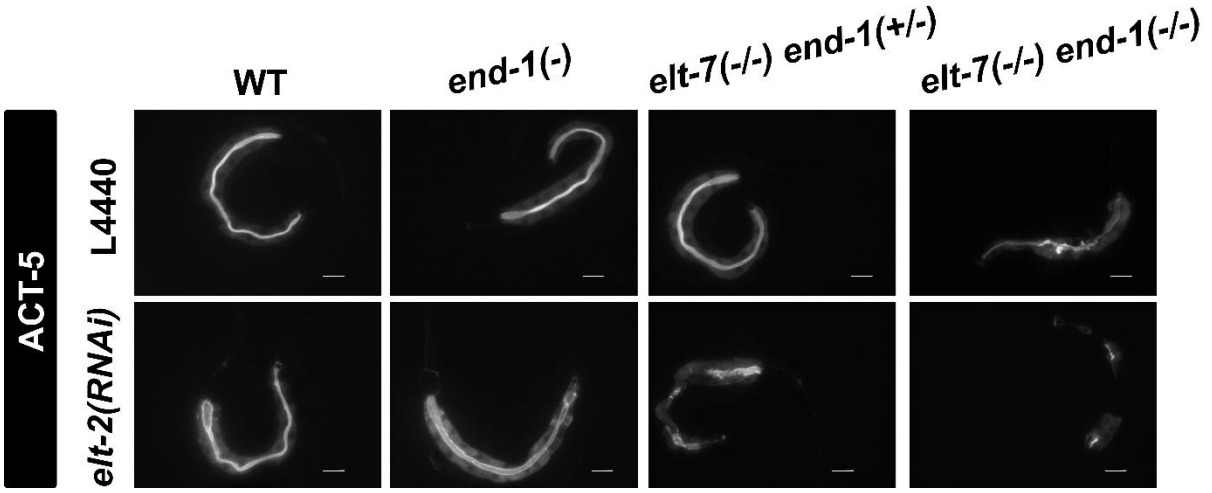

Supplemental Figure 2.7: END-1, ELT-7, and ELT-2 regulate *act-5* expression. *act-5* transgene (*jyIs13*) is expressed strongly in the intestine and weakly in the excretory canal cells. *act-5::GFP* signals appear sporadic in *elt-7(-/-) end-1(+/-); elt-2(RNAi)* and *elt-7(-/-) end-1(-/-)* animals, and are almost completely missing in *elt-7(-/-) end-1(-/-); elt-2(RNAi)* mutant. The residual *act-5* expression in *elt-7(-/-) end-1(-/-); elt-2(RNAi)* may be due to incomplete RNAi penetrance. Scale bars = 10 μm.

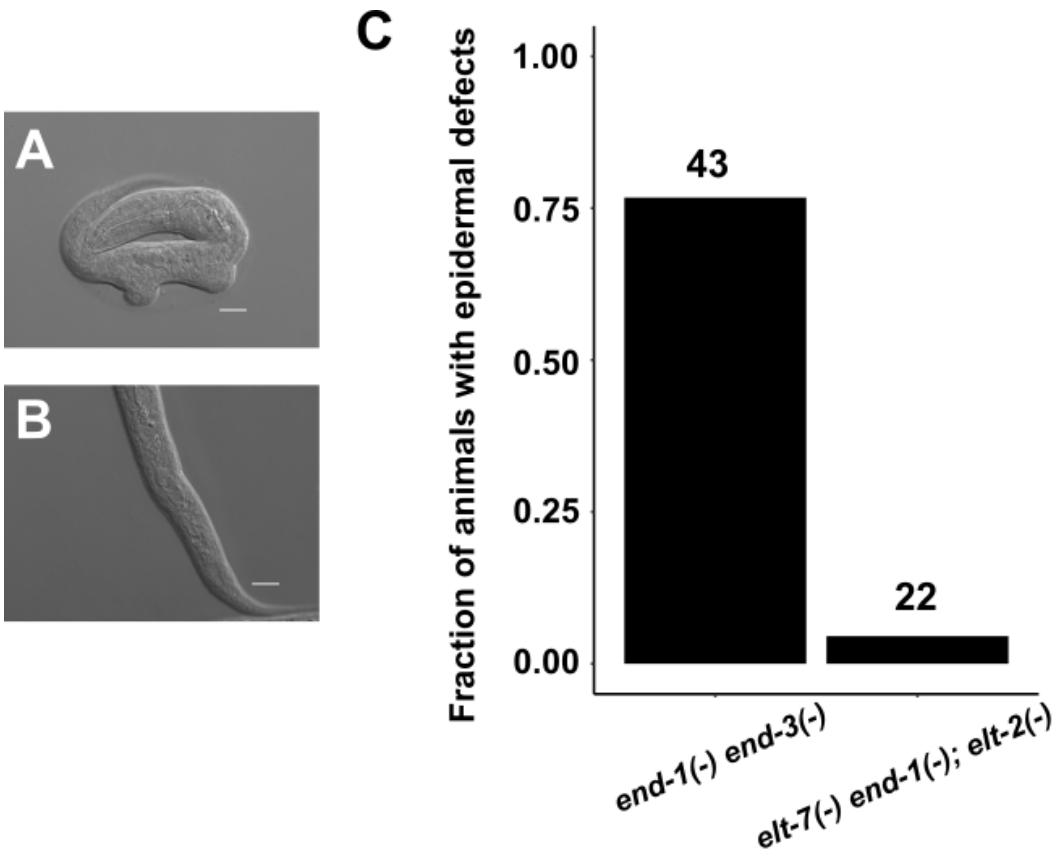

Supplemental Figure 2.8: Gross epidermal defects in GATA mutants.
(A) A representative *end-1(-) end-3(-)* arrested L1 shows gross epidermal defects due to E→C misspecification. (B) *elt-7(-) end-1(-); elt-2(-)* mutant does not show obvious epidermal defects, as observed by DIC microscopy. Scale bars = 10 μm. (C) A large fraction of *end-1(-) end-3(-)* mutants showed deformations of the epidermis, which was rarely observed in *elt-7(-) end-1(-); elt-2(-)* worms. Number of animals scored for each genotype is indicated.

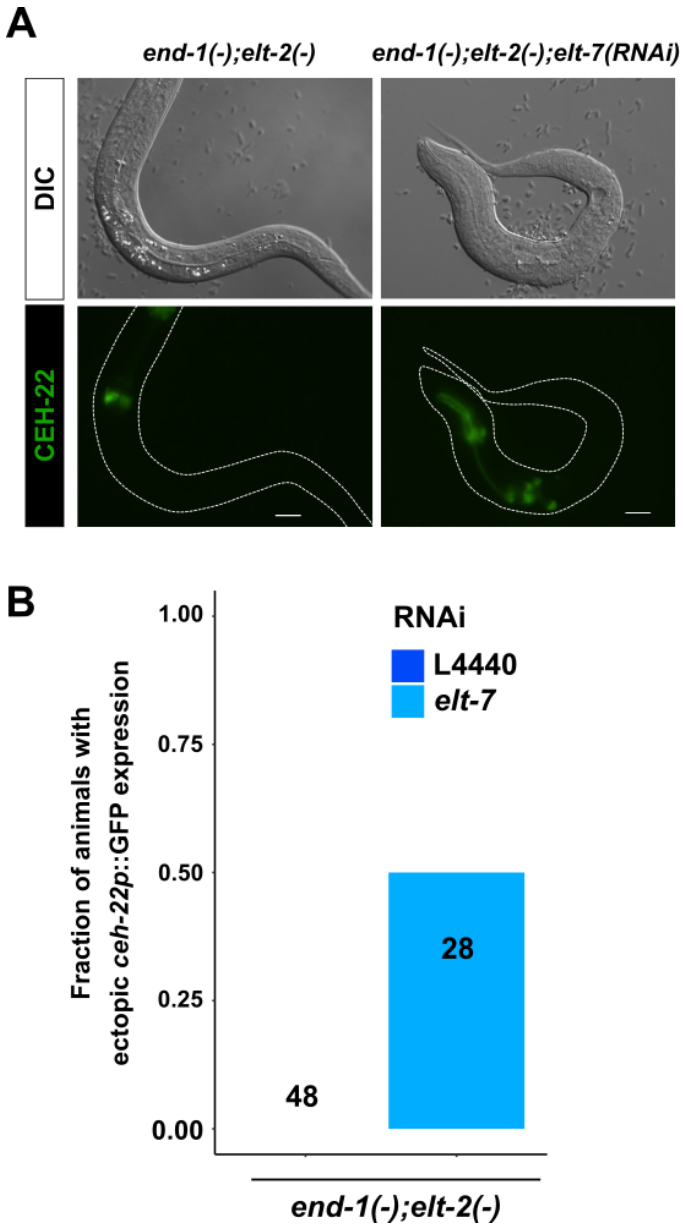

Supplemental Figure 2.9: Eliminating *end-1*, *elt-7* and *elt-2* causes ectopic expression of *ceh-22* reporter.

(A) A representative *end-1(-); elt-2(-)* worm contains a differentiated gut with defined lumen (top) and wildtype expression pattern of *ceh-22* that is restricted to the pharynx (bottom). On the other hand, *end-1(-); elt-2(-); elt-7(RNAi)* mutant shows no sign of gut differentiation as observed by DIC microscopy (top), and ectopic expression of *ceh-22p::GFP* reporter (bottom). Scale bars = 10 μm. (B) Knocking out *elt-7* in *end-1(-); elt-2(-)* worms causes ectopic expression of *ceh-22p::GFP* marker, as shown in (A). Number of animals scored for each genotype is indicated.

Supplemental Table 2.1: Worm strains used in this study.

Strain	Genotype	Source
MS1893	*unc-119(ed9?) III; irSi24[opt-2p::mCherry::H2B, Cb-unc-119(+)] IV*	(Choi et al., 2017)
IA105	*unc-76(e911)V; ijIs12[dpy-7p::GFP::lacZ, unc-76(+)]*	(Gilleard and McGhee, 2001)
SYS549	*ujIs113[pie-1p::mCherry::H2B; nhr-2p::mCherry::HIS-24-let858UTR;unc119(+)] II; end-1(dev162[end-1:: mNeonGreen]) V*	(Li et al., 2019)
JR1188	*wIs95[med-1p::GFP::MED-1+rol-6(su1006)]*	(Maduro et al., 2001)
MS1362	*med-2(cx9744) III; med-1(ok804) X; irEx581[T24D3, sur-5::dsRed]*	(Maduro et al., 2007)
MS386	*med-2(cx9744) III; dpy-11(e224) end-1(ok558) V*	(Maduro et al., 2007)
MS387	*dpy-11(e224) end-1(ok558) V; med-1(ok804) X*	(Maduro et al., 2007)
MS401	*end-3(ok1448) V; med-1(ok804) X*	(Maduro et al., 2007)
MS436	*med-2(cx9744) III; end-3(ok1448) V*	(Maduro et al., 2007)
MS1248	*end-1(ok558) end-3(ok1448) V; irEx568[K10F6, F58E10, pAS152(sur-5::dsRed)]*	(Owraghi et al., 2010)
JR3295	*elt-7(tm840) V; elt-2(ca15) X; irEx404[unc-119::CFP and elt-2(+)]*	(Sommermann et al., 2010)
MS851	*elt-2(ca15) X; irEx404[unc-119::CFP, elt-2(+)]*	(Sommermann et al., 2010)
RW10479	*unc-119(ed3) III; itIs37[pie-1p::mCherry::H2B::pie-1 3'UTR + unc-119(+)] IV; stIs10116[his-72(promoter)::his-24::mCherry::let-858 3'UTR + unc-119(+)]; stIs10426[med-2::TGF(6.2B3)::GFP::TY1::3xFLAG]*	CGC
AZ217	*unc-119(ed3) ruIs37 [myo-2p::GFP + unc-119(+)] III*	CGC
FX840	*elt-7(tm840) V*	CGC
MS123	*med-2(cx9744) II*	CGC
OP56	*unc-119(ed3) III; gaEx290[elt-2::TY1::EGFP::3xFLAG(92C12) + unc-119(+)]*	CGC
RB1331	*end-3(ok1448) V*	CGC
RB930	*med-1(ok804) X*	CGC
VC271	*end-1(ok558) V*	CGC
ERT60	*jyIs13 [act-5p::GFP::ACT-5 + rol-6(su1006)] II*	CGC

OH15876	*pha-4(ot946[pha-4::GFP]) V*	CGC
JR4405	*ruIs37 [myo-2p::GFP + unc-119(+)] III; him-5(e1490) V; elt-2(ca15) X; IrEx404[unc-119::CFP, elt-2(+)]*	This study
JR4384	*ruIs37 [myo-2p::GFP + unc-119(+)] III; elt-7(tm840) V; elt-2(ca15) X; IrEx404[unc-119::CFP, elt-2(+)]*	This study
JR4369	*hum-1(cv21[hum-1::RFP]) I; elt-7(tm840) end-1(ox134)/ elt-7(tm840) tmC12[egl-9(tmIs1197)] V; gaEx290[elt-2::TY1::EGFP::3xFLAG(92C12) + unc-119(+)]*	This study
JR4371	*hum-1(cv21[hum-1::RFP]) I; gaEx290[elt-2::TY1::EGFP::3xFLAG(92C12) + unc-119(+)]*	This study
JR4368	*ruIs37 [myo-2p::GFP + unc-119(+)] III; end-1(ok558) end-3(ok1448) V; irEx568[K10F6, F58E10, pAS152(sur-5::dsRed)]*	This study
JR2488	*him-8(e1489) IV; end-1(ox134) V*	This study
JR3341	*elt-7(tm840) end-1(ox134)/ dpy-11(e224) unc-76(e911) V*	This study
JR3342	*elt-7(tm840) end-3(ok1448) V*	This study
JR4037	*elt-2(ca15) X; ijIs12[dpy-7p::GFP::lacZ, unc-76(+)]; irEx404[unc-119::CFP, elt-2(+)]*	This study
JR4063	*him-8(e1489) irSi24[opt-2p::mCherry::H2B, Cb-unc-119(+)] IV; elt-2(ca15) X; irEx404[unc-119::CFP, elt-2(+)]*	This study
JR4097	*elt-7(tm840) end-1(ox134)/ elt-7(tm840) tmC12[egl-9(tmIs1197)] V*	This study
JR4194	*jcIs1[ajm-1p::AJM-1::GFP + unc-29(+) + rol-6(su1006)] IV; elt-7(tm840) end-1(ox134)/ elt-7(tm840) tmC12[egl-9(tmIs1197)] V*	This study
JR4195	*elt-7 (tm840) end-1(ox134)/ elt-7(tm840) tmC12[egl-9(tmIs1197)] V; elt-2(ca15) X; irEx404[unc-119::CFP, elt-2(+)]*	This study
JR4200	*him-8(e1489) irSi24 [opt-2p::mCherry::H2B, Cb-unc-119(+)] IV; elt-7(tm840) end-1(ox134)/ elt-7(tm840) tmC12[egl-9(tmIs1197)] V; elt-2(ca15) X; irEx404[unc-119::CFP, elt-2(+)]*	This study
JR4304	*elt-7 (tm840) end-1(ox134)/ elt-7(tm840) tmC12[egl-9(tmIs1197)] V; wEx1751[cdf-1p::CDF-1::GFP + rol-6(su1006)]*	This study
JR4313	*elt-7(tm840) end-1(ox134)/ elt-7(tm840) tmC12[egl-9(tmIs1197)] V; gaEx290[elt-2::TY1::EGFP::3xFLAG(92C12) + unc-119(+)]*	This study

JR4364	*ruIs37 [myo-2p::GFP + unc-119(+)] III; elt-7(tm840) end-1(ox134)/ elt-7(tm840) tmC12[egl-9(tmIs1197)] V; elt-2(ca15) X; irEx404[unc-119::CFP, elt-2(+)]*	This study
JR4367	*ruIs37 [myo-2p::GFP + unc-119(+)] III; elt-7(tm840) end-1(ox134)/ elt-7(tm840) tmC12[egl-9(tmIs1197)] V*	This study
MS880	*dpy-11(e224) end-1(ok558) V; elt-2(ca15) X; irEx404[unc-119::CFP, elt-2(+)]*	This study
JR4407	*jcIs1[ajm-1p::AJM-1::GFP + unc-29(+) + rol-6(su1006)] IV; end-1(ox134) V*	This study
MS900	*end-3(ok1448) V; elt-2(ca15) X; irEx404[unc-119::CFP, elt-2(+)]*	This study
JR4412	*jyIs13 [act-5p::GFP::ACT-5 + rol-6(su1006)] II; elt-7(tm840) end-1(ox134)/ elt-7(tm840) tmC12[egl-9(tmIs1197)] V*	This study
JR4413	*jyIs13 [act-5p::GFP::ACT-5 + rol-6(su1006)] II; end-1(ox134) V*	This study
JR4439	*him-8(e1489) IV; cuIs1[ceh-22p::GFP + rol-6(su1006] end-1(ox134) V; elt-2(ca15); irEx404[unc-119::CFP, elt-2(+)]*	This study
JR4446	*elt-7(tm840) end-1(ox134)/ elt-7(tm840) tmC12[egl-9(tmIs1197)] V; kcIs6[ifb-2p::IFB-2::CFP]*	This study
JR4198	*end-1(ok558) end-3(ok1448) V; ijIs12[dpy-7p::GFP::lacZ, unc-76(+)]; irEx568[K10F6, F58E10, pAS152(sur-5::dsRed)]*	This study
JR4452	*end-1(ox134) V; elt-2(ca15); ijIs12[dpy-7p::GFP::lacZ, unc-76(+)]; irEx404[unc-119::CFP, elt-2(+)]*	This study
JR3315	*elt-2(ca15) X; wIs84[elt-2p::GFP+ rol-6(su1006)]; irEx404[unc-119::CFP, elt-2(+)]*	This study
JR4463	*pha-4(ot946[pha-4::GFP]) V; elt-2(ca15) X; irEx404[unc-119::CFP, elt-2(+)]*	This study

Chapter 3 : Natural Cryptic Variation in Epigenetic Modulation of an Embryonic Gene Regulatory Network[5]

"The past is never dead. It's not even past" - William Faulkner

[5] This chapter has been published in Ewe et al., PNAS (2020) with slight modifications.

Summary

Gene regulatory networks (GRNs) that direct animal embryogenesis must respond to varying environmental and physiological conditions to ensure robust construction of organ systems. While GRNs are evolutionarily modified by natural genomic variation, the roles of epigenetic processes in shaping plasticity of GRN architecture are not well-understood. The endoderm GRN in *C. elegans* is initiated by the maternally supplied SKN-1/Nrf2 bZIP transcription factor; however, the requirement for SKN-1 in endoderm specification varies widely among distinct *C. elegans* wild isotypes owing to rapid developmental system drift driven by accumulation of cryptic genetic variants. We report here that heritable epigenetic factors that are stimulated by transient developmental diapause also underlie cryptic variation in the requirement for SKN-1 in endoderm development. This epigenetic memory is inherited from the maternal germline, apparently through a nuclear, rather than cytoplasmic, signal, resulting in a parent-of-origin effect (POE), in which the phenotype of the progeny resembles that of the maternal founder. The occurrence and persistence of POE varies between different parental pairs, perduring for at least ten generations in one pair. This long-perduring POE requires piwi-piRNA function and the germline nuclear RNAi pathway, as well as MET-2 and SET-32, which direct histone H3K9 trimethylation and drive heritable epigenetic modification. Such non-genetic cryptic variation may provide a resource of additional phenotypic diversity through which adaptation may facilitate evolutionary changes and shape developmental regulatory systems.

Introduction

The “Modern Synthesis” of the early 20th century articulated how biological traits shaped by Darwinian forces result from random mutations following the rules of Mendelian inheritance (Dobzhansky, 1949). Since that formulation, it has become clear that non-genetic heritable mechanisms can underlie substantial differences in traits between individuals (Perez and Lehner, 2019a). Extensive epigenetic reprogramming occurs in the germline and in gamete pronuclei after fertilization to maintain the totipotent state of the zygote. In mammals, disruption of this process often leads to lethal consequences (Kelly, 2014; Ladstätter and Tachibana, 2019). In *C. elegans*, aberrant reprogramming of epigenetic memory can result in transgenerational accumulation of inappropriate epigenetic marks and a progressive sterile mortal germline (Mrt) phenotype (Andersen and Horvitz, 2007; Katz et al., 2009). In many cases, the Mrt phenotype is exacerbated by heat stress, demonstrating that environmental factors may influence epigenetic reprogramming in the germline and that these epigenetic modifications may be passed to subsequent generations (Buckley et al., 2012; Spracklin et al., 2017). Interestingly, *C. elegans* wild isotypes, each carrying a unique haplotype, exhibit variation in the temperature-induced Mrt phenotype, suggesting differential stress response and distinct epigenetic landscapes in natural populations of the species (Frézal et al., 2018).

Many of the documented instances of epigenetic inheritance in mammals are parental or *intergenerational* effects (no more than three generations for female transmission and less than two generations for male transmission), which can be attributed to direct exposure of the developing embryos *in utero* to the triggers that

alter epigenetic states (Perez and Lehner, 2019a). Parental traumatic experience can trigger heritable behavioral changes, and nutritional status of the parents can cause metabolic remodeling in the offspring, which often lasts for one or two generations (Dias and Ressler, 2014; van Steenwyk et al., 2018). Epidemiological analyses on different human cohorts demonstrate that paternal grandfather's food access during pre-puberty period affects the mortality of the grandsons (Bygren et al., 2001; Kaati et al., 2002; Vågerö et al., 2018), revealing the potential for long-term *transgenerational* epigenetic inheritance (TEI) that is induced by environmental conditions.

Studies over the past decade on *C. elegans* have provided convincing evidence for TEI that persists for at least three generations. Small RNAs are prime candidates for mediators of epigenetic memory, as their expression undergoes only minimal reprogramming in the germline and embryos (Chen et al., 2016; Houri-Ze'evi and Rechavi, 2016). Primary siRNAs, processed from exogenous dsRNAs or endogenous small RNAs by DICER, are loaded onto the RNA-induced silencing complex (RISC) and mediate degradation of mRNA targets, thereby silencing gene expression. In addition, primary siRNAs, including PIWI-interacting RNA (piRNA – 21U) in the germline, can guide RNA-dependent RNA polymerases (RdRPs) to particular target mRNAs and then amplify silencing signals by producing an abundance of secondary 22G siRNAs. In the germline, HRDE-1 binds to these secondary siRNAs and localizes to the nucleus, where it recruits NRDE-1/2/4 to the nascent transcripts and genomic sites targeted by the small RNAs. This complex then inhibits RNA polymerase II elongation and directs deposition of repressive H3K9me3 marks on the corresponding genomic loci, mediated by histone methyltransferases MET-2 (H3K9me1/2), SET-23

(H3K9me1/2/3) and SET-32 (H3K9me3). Amplification of secondary siRNAs by RdRPs prevents loss of epigenetic memory over multiple generations and, therefore, may permit long-term heritable epigenetic responses (Houri-Zeevi and Rechavi, 2017; Rechavi and Lev, 2017).

We have uncovered natural epigenetic variation in the modulation of the gene regulatory network (GRN) that directs embryonic endoderm development in *C. elegans*. The maternal SKN-1/Nrf2 transcription factor activates the mesendoderm GRN in the EMS blastomere at the four-cell stage. EMS subsequently divides to produce the E founder cell, which gives rise exclusively to the intestine, and its anterior sister, the MS founder cell, which produces much of the mesoderm. A triply redundant (Wnt, MAP kinase, and Src) extracellular signal sent from the neighboring P_2 blastomere is received by EMS and acts in parallel with SKN-1 to activate the endoderm GRN in the E lineage. In the wildtype laboratory N2 strain, elimination of maternal SKN-1 function causes fully penetrant embryonic lethality and a partially penetrant loss of gut: while the majority of the E cells in embryos lacking SKN-1 adopt the mesoectodermal fate of the normal C founder cell, ~30% undergo normal gut differentiation as a result of this parallel signaling input (see Chapter 1).

We recently found that the requirement for the SKN-1 and Wnt inputs into the endoderm GRN, shows widespread natural variation across genetically distinct *C. elegans* wild isotypes. While removal of SKN-1 in some of the isotypes causes loss of intestine in virtually 100% of embryos, in other isotypes a majority of the embryos still differentiate endoderm. Interestingly, low SKN-1 requirement appears to be partially compensated by a higher MOM-2/Wnt requirement. Thus, the early stages in the

endoderm GRN has undergone rapid change during relatively short evolutionary periods in *C. elegans* (see Rapid Developmental System Drift among *C. elegans* Wild Isolates) (Ewe et al., 2020a; Torres Cleuren et al., 2019). In this study, we focus on variation in a single major input node, SKN-1.

We report here that, although much of the variation in SKN-1 requirement results from genetic differences between the wild isotypes (Torres Cleuren et al., 2019), it is also determined in part by cryptic, stably heritable epigenetic variation. This effect is uncovered from reciprocal crosses between wild isotypes with quantitatively different phenotypes. This parent-of-origin effect (POE) is transmitted exclusively through the maternal germline. When mothers experience dauer diapause, an alternative developmental stage in *C. elegans* that confers resistance to environmental insults and longevity, the POE appears to be transmitted through the maternal nucleus, rather than cytoplasmic factors, and can persist through many generations. We further show that this stress-induced POE requires factors that direct H3K9 methylation and the nuclear RNAi machinery. These findings reveal that heritable epigenetic states can underlie differences between natural wild isotypes and can influence developmental plasticity in early embryos. Such cryptic epigenetic variation provides a potential resource upon which natural selection might act, thus contributing to evolution of GRN architecture (Waddington, 1953).

Results

Transgenerational Parent-of-origin Effect Alters the SKN-1 Dependence of Endoderm Formation

The requirement for SKN-1 in endoderm specification varies dramatically across *C. elegans* isotypes (Torres Cleuren et al., 2019). Depending on the isotype tested, between 0.9% and 60% of arrested *skn-1(RNAi)* embryos undergo gut differentiation when maternal SKN-1 function is eliminated. The behavior of each isotype is quantitatively highly reproducible, showing low variability through many generations, when analyzed by different laboratories and researchers, and from independent lines established from different founder animals (Torres Cleuren et al., 2019).

While performing crosses between isotypes with quantitatively different SKN-1 requirements, we found that the outcomes differed depending on the sex of the parent in reciprocal crosses. We initially tested two isotypes in which we observed dramatically different *skn-1(RNAi)* phenotypes: the laboratory N2 strain (29 $\pm$ 0.4% sd with gut; n = 1320) and the wild isotype JU1491 (1.2 $\pm$ 0.4% sd; n = 1228) (Supplemental Figure 3.1, $p < 0.001$). These results agree well with our previous findings (Torres Cleuren et al., 2019). Consistent with variation at the level of maternal components, we found that in reciprocal crosses (i.e., male N2 x JU1491 hermaphrodite, and *vice-versa*), the quantitative requirement for SKN-1 reliably followed that of the maternal line (Figure 3.1B). Unexpectedly, however, we found that this non-reciprocality persisted in subsequent generations: the average phenotype of F2 and F3 embryos continued to follow more closely the behavior of their

grandmothers and great-grandmothers than their paternal ancestors (Figure 3.1C), despite the fact that, with the exception of the mitochondrial genome, the F1 progeny genotypes should be identical regardless of the sex of the founder P0. Thus, these two strains showed a strong parent-of-origin effect (POE) that persists through multiple generations.

Dauer Diapause Stimulates Long-term Transgenerational POE through the Maternal Line

As epigenetic inheritance can be environmentally triggered, it was conceivable that the POE we observed might be influenced by the experience of the parents. Indeed, we found that POE was seen only when the P0 parents had been starved and experienced an extended period (~2 weeks) of dauer diapause. In contrast, the progeny of P0's that were continuously well fed showed an intermediate average phenotype that was not significantly different between descendants of reciprocal crosses (Figure 3.1C), consistent with the known multigenic characteristic of the phenotype (Torres Cleuren et al., 2019).

We sought to determine whether this environmentally triggered POE extends to other wild isotypes. Isotypes MY16 (in which only 2.2 $\pm$ 1% sd (n = 1169) of *skn-1(-)* embryos make endoderm) and JU1172 (40 $\pm$ 3% sd; n = 1491) (Supplemental Figure 3.1, $p < 0.001$) show widely different quantitative phenotypes (Torres Cleuren et al., 2019). Consistent with our previous findings, in reciprocal crosses of MY16 and JU1172, we observed a strong maternal effect in the requirement for SKN-1: F1 embryos from mated *skn-1(RNAi)* mothers followed the maternal phenotype (Figure 3.1D). Once again, in control experiments with well-fed founder P0 worms, this

maternal effect quickly dissipated and was not detectable in F2 embryos (Figure 3.1D and E). However, when the parental worms experienced dauer diapause, the average *skn-1(RNAi)* phenotype of their descendants reliably followed that characteristic of the maternal line through at least ten generations (Figure 3.1D and E – the experiments shown in the two panels were performed using parents of different ages; see below), a strongly perduring effect.

While dauer development enhances POE, we found that it is not an absolute requirement in all cases. Specifically crosses of JU1491 and JU1172 revealed weak POE even without the diapause trigger, although the effect was enhanced by dauer development (Figure 3.2C). This observation suggests that cryptic epigenetic differences between some natural isotypes may exist even in the absence of an environmental or physiological trigger. Finally, we found that this effect does not appear to be general to all isotype pairs that show very different phenotypes: for example, diapause-induced POE was not detectable with N2 and MY16 (Supplemental Figure 3.2).

As expected for successful crosses, in all cases ~50% of the F1 offspring were males (Supplemental Figure 3.3A and D; one-sample t-test, $p > 0.05$). Further, cultures established from at least eight randomly selected F1s of successful crosses (with ~50% F1 males) all showed POE (Supplemental Figure 3.3C), thus ruling out the possibility that the maternal-line bias of the phenotype might result from frequent selfing.

To distinguish between the paternal and maternal contributions to the POE, we starved either the P0 male or hermaphrodite and traced the POE for five generations

following reciprocal crosses. These experiments demonstrated that the diapause-induced POE is inherited exclusively through the maternal germline (Figure 3.1F; % of F1 males - Supplemental Figure 3.3B). This stable non-reciprocality cannot be explained by long-perduring maternal factors in the cytoplasm: each animal produces ~250 progeny and after five generations, this would result in a dilution factor of ~10^{11}.

It is noteworthy that *skn-1(RNAi)* is highly penetrant in the isotypes used in this study, with 100% *skn-1(RNAi)*-induced lethality observed across all experiments. This suggests that POE reflects *bona fide* variation in the endoderm developmental input (Torres Cleuren et al., 2019), although we cannot rule out that RNAi sensitivity might play a minor role.

Heritability of POE is Associated with the Maternal Nucleus, not Heritable Mitochondrial or Cytoplasmic Factors

Dauer larvae and post-dauer adults exhibit a metabolic shift which may reflect changes in mitochondrial function. Further, starvation has been shown to impact mitochondrial structure and function (Burnell et al., 2005; Yuan et al., 2013). Thus, the observed maternally directed POE results might arise from differences between the mitochondrial genome sequences in the two strains or might be driven by other cytoplasmically inherited factors. Indeed, wild isotypes MY16 and JU1172 contain 13 polymorphisms in mitochondrial protein coding genes (Table 3.1), which could alter energy metabolism and stress responses. To test whether the POE we observed is attributable to maternal inheritance of mitochondria with particular genomic characteristics, we performed reciprocal crosses in which progeny were repeatedly backcrossed to the paternal strain to obtain lines with primarily the MY16 nuclear genome and mitochondria from the JU1172 line and *vice-versa* (Figure 3.2A). While

a strong POE was initially observed in F2 *skn-1(RNAi)* embryos, this effect was rapidly eliminated as more paternal nuclear DNA was introduced. By the F5 generation, the phenotype was indistinguishable from that of the respective paternal strain (Figure 3.2B), suggesting that POE is attributable to the nuclear, rather than mitochondrial, genome. Moreover, the transgenerational POE observed with JU1491 and JU1172 (Figure 3.2C) is unlikely to be the result of variation in mitochondrial DNA, as these two strains carry identical mitotypes. Collectively, our results suggest that the POE we observe is not likely to be caused by mitochondrial inheritance.

To further assess whether nuclear or cytoplasmic/mitochondrial factors underlie the observed POE, we took advantage of a genetic system that generates germlines containing nuclei derived fully from the paternal line with maternally derived cytoplasm (including mitochondria). In zygotes overexpressing GPR-1 ($N2^{GPR\text{-}1\ OE}$) (Artiles et al., 2019; Besseling and Bringmann, 2016), which is required to modulate microtubule-based pulling forces, excessive pulling forces cause the maternal and paternal pronuclei to be drawn to opposite poles before nuclear envelope breakdown. This effect generates mosaic embryos in which the anterior daughter (AB) inherits only the maternal chromosomes, while the posterior (P_1) receives only the paternal chromosomes. These non-Mendelian events can be scored with the appropriate fluorescent markers (Figure 3.2D; Supplemental Figure 3.4) (Artiles et al., 2019). We found that 72% (n = 230) of the viable F1 progeny from crosses of $N2^{GPR\text{-}1\ OE}$ hermaphrodites with JU1491 males contained an exclusively paternally derived P_1 lineage. If cytoplasmic maternal factors were responsible for the observed diapause-induced POE, the effect would be expected to follow the cytoplasm of the founder P0

worms in the F1 hybrids. In contrast, however, we found that the *skn-1(RNAi)* phenotypes of F2 and F3 descendants of F1 mosaic animals (those with an N2-derived AB and JU1491-derived P_1; Supplemental Figure 3.4; see Materials and Methods) were indistinguishable from that of the JU1491 strain, regardless of the feeding status of the parents (Figure 3.2E). This finding suggests that the diapause-induced POE is associated with heritable changes in the maternal haploid nucleus, not heritable cytoplasmic maternal factors, including the mitochondrial genome.

POE is not the Result of Competition in Fitness or Maternal Incompatibility

Parental age has been shown to affect progeny phenotypes in *C. elegans* and other organisms (Bock et al., 2019; Perez et al., 2017). To test the possibility that the POE is influenced by differences in maternal age, we collected embryos from day-one adults (Figure 3.1D) and day-two adults (Figure 3.1C, E and F; Figure 3.2C). We detected a strong POE in all cases. Moreover, despite large variation in the *skn-1(RNAi)* phenotype that arises from genetic variation, we observed POE in F5 populations that were established from very late broods (the last few progeny) produced by senescent F1 animals (Figure 3.3A). These findings indicate that parental age does not contribute substantially to the POE observed.

The differences in SKN-1 requirement seen as the result of the POE might reflect maternal incompatibility, which favors particular genetic regions as a result of lethality or slow growth (Ben-David et al., 2017; Seidel et al., 2008). If such regions included those known to influence the requirement for SKN-1 in the endoderm GRN (Torres Cleuren et al., 2019), there could be selection for the trait following recombination of the two parental genomes. We note that such a possibility would

also require that any such selection is triggered only after starvation and dauer development for the cases in which we observed such an essential requirement. Further, we observed strong diapause-induced POE in embryos from *skn-1* RNAi-treated F1 heterozygous mothers, whose genotypes would be identical in the two reciprocal crosses. Thus, the effect at this stage is not attributable to maternal incompatibility resulting in selection against particular allelic combinations that arise by recombination (Figure 3.1C-E).

To further investigate whether POE might be driven by genetic incompatibility that is environmentally triggered by starvation/dauer development, we also characterized lethality and fecundity of F2 progeny from the reciprocal crosses. Two mechanisms involving selfish genetic elements that result in maternal incompatibilities were previously described in *C. elegans*: the *peel-1/zeel-1* (Seidel et al., 2008) and *sup-35/pha-1* (Ben-David et al., 2017) toxin/antidote systems. The wild isotype JU1172 does not carry the paternal selfish *peel-1/zeel-1* element (Seidel et al., 2008). When mated, MY16 sperm deliver PEEL-1 toxin, causing F2 embryos that are homozygous for the JU1172 *zeel-1* haplotype (~25%) to arrest. We found that, indeed, crosses between JU1172 and MY16 are associated with embryonic lethality. However, although this lethality was slightly lower (~13-16%) when JU1172 was the paternal strain compared to the reciprocal crosses (20-26%; Figure 3.3B), the difference is insufficient to explain the strong POE we have observed. Furthermore, this effect does not change appreciably regardless of the experience of the P0 (fed or starved/dauer), which is not consistent with selection induced by this experience. As both MY16 and JU1172 harbor the active *sup-35/pha-1* maternal toxin/antidote element (Ben-David

et al., 2017), the lethality may reflect an unidentified maternal-effect toxin in the MY16 strain. In addition, the progeny of crosses between MY16 and JU1172 in either direction both showed somewhat reduced fecundity/viability, presumably owing to genomic incompatibility between the two strains (Figure 3.3C). However, the parental origin of the P0s did not influence the degree of larval lethality or sterility in the F2 animals (Figure 3.3C, Fisher's exact test $p > 0.05$). Together these results indicate that genetic incompatibility alone cannot account for the strong POE we observed. Rather, POE appears to result from perduring epigenetic inheritance reflecting the experience of the original founding parents of the cross.

Maintenance of POE Involves the Nuclear RNAi Pathway and Histone H3K9 Trimethylation

The findings noted above suggest that POE is mediated through nuclear signals. The nuclear RNAi pathway has been implicated in a number of examples of TEI (Buckley et al., 2012). To assess whether this pathway might be involved in transmitting the POE we have observed, we analyzed the F4 progeny of reciprocal crosses of post-dauer P0's in which *nrde-4* was knocked down by RNAi (strategy shown in Figure 3.4A). While a strong POE was observed in the control animals containing functional NRDE-4, *nrde-4(RNAi)* abrogated the POE in the F5 embryos (Figure 3.4B): i.e., the requirement for SKN-1 was not significantly different in the descendants of reciprocal crosses. It was conceivable that this effect might simply reflect a direct role for NRDE-4 in the requirement for SKN-1 *per se*. However, we found that the *skn-1(RNAi)* phenotypes of the MY16 and JU1172 isotypes previously subjected to *nrde-4* RNAi, were indistinguishable from those subjected to control RNAi

(Fisher's Exact test $p > 0.05$; Figure 3.4C). Thus, these findings implicate NRDE-4, and hence the nuclear RNAi pathway, in the POE process.

Gene silencing though the nuclear RNAi pathway that results in TEI is mediated through the Piwi-encoding homologue, *prg-1*, and piRNAs that trigger biosynthesis of secondary 22G RNAs (a second homologue, *prg-2*, is likely to be a pseudogene) (Ashe et al., 2012; Shirayama et al., 2012). We knocked down *prg-1/2* in F4 animals from MY16 and JU1172 reciprocal crosses and found that, in contrast to their siblings treated with control RNAi, POE was abrogated in the F5 embryos (Figure 3.4B). Control experiments demonstrated that *prg-1/2* RNAi does not affect *skn-1* RNAi efficacy in either parent line ($p > 0.05$; Figure 3.4C). Loss of nuclear RNAi factors lowers the efficacy of RNAi targeting of nuclear-localized RNAs (Burkhart et al., 2011; Guang et al., 2008, 2010); however, maternal *skn-1* mRNA in the early embryos is localized in the cytoplasm, and the silencing effect of *skn-1* RNAi would be expected to depend primarily on RISC in the cytoplasm (Seydoux and Fire, 1994).

NRDE-4 is required for the recruitment of NRDE-1 to the targeted loci and subsequent deposition of the repressive H3K9me3 mark, which results in gene silencing. Furthermore, H3K9me3 has been implicated in transgenerational silencing of transgenes or endogenous loci mediated by exogenous RNAi (Rechavi and Lev, 2017). These observations, and our findings that knockdown of *nrde-4* abolishes POE, led us to hypothesize that H3K9 methylation might function as a mediator of POE. Indeed, we found that treating F4 animals that showed POE with RNAi against *met-2* or *set-32*, in contrast to their control siblings, eliminated POE in the F5 embryos (Figure 3.4B). Although loss of MET-2 has been shown to enhance RNAi sensitivity

(Lev et al., 2017), we found that neither *met-2* RNAi nor *set-32* RNAi significantly modifies the *skn-1(RNAi)* phenotypes of MY16 and JU1172 wild isotypes ($p > 0.05$; Figure 3.4C). Thus, the loss of POE in the F5 generation with *met-2* or *set-32* RNAi is not attributable to modified RNAi response. We further found that a *set-32(-)* chromosomal mutation also eliminated TEI in N2/JU1491 crosses at the F2 generation, which implicates SET-32 not only in maintenance, but in initiation of this process. These results will be reported in greater depth elsewhere. Importantly, we found that POE persisted in F5 embryos when a control gene, *ced-4*, was knocked down in the F3 and F4 generations. CED-4/Apaf-1 is involved in germline programmed cell death and has no known role in endoderm development or TEI (Gumienny et al., 1999). This result suggests that elimination of POE is not the result of a non-specific RNAi response (Figure 3.4B and C, Supplemental Figure 3.5). Collectively, these results suggest that, in response to dauer diapause, piRNAs in the germline direct histone methylation through the nuclear RNAi pathway, thereby maintaining POE across generations (Figure 3.4D).

Discussion

While massive epigenetic reprogramming ensures totipotency of the germline during animal development, some epigenetic marks escape erasure, leading to stable epigenetic inheritance that can persist through many generations. Such long-term epigenetic inheritance has the potential to provide a source of cryptic variation upon which evolutionary processes might act; however, little is known about natural epigenetic variation within a species, how it is influenced by environmental conditions, and the degree to which it influences GRN plasticity. In this study, we report four major

findings that reveal cryptic natural epigenetic variation and its mechanistic action in modulating an embryonic GRN input in *C. elegans*: 1) dauer diapause can trigger POE that alters the SKN-1 requirement in endoderm development. 2) This effect is transmitted through the maternal germline across multiple generations apparently through nuclear signals. 3) Different combinations of wild isotypes exhibit variation in their capacity for establishing and maintaining these transgenerational epigenetic states. 4) This POE requires components of the piRNA-nuclear RNAi pathway and H3K9 trimethylation and does not appear to be eliminated by general RNAi response. These findings indicate that maintenance of an acquired epigenetic state in response to environmental stimulus can confer substantial plasticity to a core developmental program and may provide additional natural variation that may be subject to evolutionary selection.

Dauer Diapause Induces Persistent Epigenetic Inheritance

The perduring epigenetic effect that we have observed is triggered in parents that have experienced dauer diapause. Dauer entry and formation require extensive epigenetic remodeling and some of these changes are retained throughout the remainder of development: post-dauer adults contain distinct chromatin architecture and particular pools of small RNA that differ from animals that have not experienced dauer diapause (Hall et al., 2013). In addition, the progeny of starved animals show increased starvation resistance and lifespan (Rechavi et al., 2014; Webster et al., 2018). Consistent with the model that the effect of ancestral developmental history is carried across generations, we found that dauer diapause leads to TEI that modifies the quantitative SKN-1 input in endoderm development. While it is conceivable that

wild isotypes may exhibit natural variation in RNAi sensitivity and such difference can be epigenetically transmitted via maternal nuclei, we have previously shown that *skn-1* RNAi is highly effective across the wild isotypes, and we found fully penetrant *skn-1(RNAi)*-induced lethality in all experiments. In addition, all the strains we used in this study have been shown to be RNAi-competent (Paaby et al., 2015; Torres Cleuren et al., 2019). It is therefore likely that the POE we report here reflects variation in endoderm specification *per se*, although it is conceivable that epigenetic influences on RNAi sensitivity may play a minor role.

The TEI we have observed varies in its long-term perdurance, depending on the wild isotypes involved. In crosses between the laboratory strain N2 and wild isotype JU1491, dauer diapause-induced POE lasted for three generations, but was subsequently lost, similar to the transmission dynamics of the silencing effect induced by exogenous RNAi (Alcazar et al., 2008). This progressive transgenerational loss in the effect may result from passive dilution of regulatory small RNAs and active restoration of an epigenetic “ground state” over generations, although the detailed mechanisms for such a process are not well understood (Alcazar et al., 2008). In contrast, in crosses between the MY16 and JU1172 wild isotypes, we observed stable TEI that lasted for at least 10 generations and which conceivably persists longer. Consistent with a recent study that identified genetic determinants of efficient germline maintenance and epigenetic reprogramming among *C. elegans* wild isotypes (Frézal et al., 2018), our results showed that the generational duration of epigenetic inheritance may also be influenced by genetic background, suggesting an interplay

between genetics and epigenetics (see also MOdified Transgenerational Epigenetic Kinetics (MOTEK) genes in Rechavi and Lev, 2017)

The transmission of the silencing effects of exogenous RNAi in *C. elegans* has provided an excellent paradigm for revealing mechanisms of epigenetic inheritance. In those studies, animals were subjected to RNAi targeting a transgene (e.g. *gfp*) or endogenous gene (e.g., *oma-1*) and the heritable RNAi response monitored over generations (Lev et al., 2017, 2019; Spracklin et al., 2017). While inheritance of exogenous RNAi and physiological responses triggered by changing environment share overlapping machinery, our results reveal two key differences between the two processes: 1) we demonstrated that epigenetic memory triggered by dauer diapause is transmitted exclusively through the maternal germline. This contrasts with the inheritance of exogenous RNAi (Alcazar et al., 2008) and transgenes (Sha and Fire, 2005), which show paternal bias. 2) We found that PRG-1 is required for the *maintenance* of POE. In contrast, the piwi-piRNA pathway had previously been shown to be required for the *initiation*, but not *maintenance* of transgene silencing in the germline. Once established, this silencing state depends on the nuclear RNAi pathway, which promotes deposition of H3K9me3 marks on the transgene (Ashe et al., 2012; Shirayama et al., 2012). Supporting our findings, however, Simon *et al.* demonstrated that PRG-1 is important for maintaining germline mortality through a mechanism that is independent from its action in transgene silencing. Animals that lack PRG-1 exhibit dysregulation of gene expression and reactivation of transposons and tandem repeats, showing that piRNAs are required to maintain silencing of at least some endogenous loci (Simon et al., 2014; Weick et al., 2014).

Relationship of POE to Genomic Imprinting in *C. elegans*

Genomic imprinting is perhaps the best-studied example of epigenetic inheritance. Differential DNA methylation or histone modifications on the two parental chromosomes, established during gametogenesis or post-fertilization, escape epigenetic reprogramming, causing genes to be expressed in a parent-of-origin manner (Ferguson-Smith, 2011; Inoue et al., 2017). However, in the case of *C. elegans*, animals that inherit the entire paternal genome are fertile and viable, as we and others have shown (Artiles et al., 2019; Besseling and Bringmann, 2016). This observation reveals that genomic imprinting is not essential for normal development or survival in *C. elegans*, consistent with an early study in which animals containing individual chromosomes from only one parent were analyzed (Haack and Hodgkin, 1991). Nevertheless, the X chromosome of sperm, unlike that of oocytes, is devoid of H3K4me2 activation marks, a pattern that persists through several rounds of cell division cycles during early embryogenesis (Bean et al., 2004). In addition, the expression of sperm-derived autosomal transgenes is greater than that in oocytes, which may result from differential epigenetic remodeling in sperm and oocyte chromatin upon fertilization (Sha and Fire, 2005). While these findings demonstrate the imprinting capacity of *C. elegans*, endogenous imprinted genes have not yet been reported.

We propose that passage through dauer diapause may induce paternal-specific silencing through deposition of repressive H3K9me3 on paternal loci that affect the SKN-1 requirement (Torres Cleuren et al., 2019), leading to the POE we observed (Figure 3.4D). Although imprinting is not essential for viability in *C. elegans*, its effects may become significant in response to environmental stimuli. For example,

maternal dietary restriction elevates vitellogenin oocyte provisioning (Jordan et al., 2019). Both yolk-associated fatty acids and small RNAs, which have been proposed to be associated with yolk particles, promote epigenetic changes in the nucleus, and might thereby direct establishment of parent-of-origin epigenetic marks (Marré et al., 2016). Dauer-favoring conditions also reduce insulin/insulin-like growth factor signaling and enhance starvation stress resistance in the progeny (Jordan et al., 2019). With recent advances in techniques for examining transcriptional regulatory landscapes (Inoue et al., 2017), it will be of interest to identify loci that are responsive to environmental stimuli and that may be differentially imprinted across generations.

The Potential Role of Cryptic Epigenetic Variation in Accelerating Evolutionary Change

It is clear that in *C. elegans*, stress responses can be transmitted transgenerationally and influence physiology adaptively in the offspring (Rechavi et al., 2014; Webster et al., 2018). In *Arabidopsis*, it has been shown that experimentally induced, or naturally occurring epigenetic variations, once stabilized, can be subjected to artificial selection (Cortijo et al., 2014; Schmid et al., 2018), highlighting the potential capacity of TEI to facilitate adaptation and evolution. While TEI is prominent in worms and plants with a short life cycle, and hence environmental conditions may be relatively constant through multiple generations, there is evidence that TEI may also occur in mammals with much longer reproductive cycles (van Otterdijk and Michels, 2016). Epigenetic inheritance may be especially important in organisms with low genetic diversity, such as those, including *C. elegans* and *Arabidopsis*, that propagate by self-fertilization. Many *C. elegans* strains isolated from neighboring locations are near-identical and polymorphism rates are low even among genetically distinct

isotypes (Andersen et al., 2012). In such homogenous, genetically non-diverse populations, epigenetic variations may provide a particularly rich resource upon which natural selection may act.

Environmental factors can induce plastic phenotypic changes that are subjected to Darwinian selection. Over time, the phenotypic variants may become genetically fixed, a process known as “genetic assimilation” (Waddington, 1953). As the rate of genetic mutations is low in *C. elegans* (2.1×10^{-8} per nucleotide site per generation) (Denver et al., 2004), heritable epigenetic variants may act as a buffer to cope with rapid environmental change before adaptive mutations arise. Alterations in epigenetic states can also affect mutation rates and trait evolution (Makova and Hardison, 2015) and TEI might therefore accelerate the rate of evolution by facilitating genetic assimilation. We propose that epigenetic inheritance affecting SKN-1 dependence may contribute toward the rapid change in the modulation of the endoderm GRN that we previously observed among *C. elegans* wild isotypes (Torres Cleuren et al., 2019). We note that that the POE we observed likely reflects changes in epigenetic states that occur in response to a stressful environment (starvation and dauer formation) even in the absence of mating between wild isotypes (Webster et al., 2018). That is, we propose that crossing is not necessary for implementation of the effect; rather, crosses between strains with distinct *skn-1(-)* phenotypes primarily provides a readout that allows the underlying TEI to be revealed. SKN-1 acts pleiotropically, including its roles in mesendoderm specification, oxidative stress and unfolded protein responses, promoting longevity, and modulating metabolism during starvation (reviewed in Blackwell et al., 2015) (see also SKN-1/Nrf: a nexus in

development, homeostasis, and aging). It is conceivable that SKN-1 is particularly susceptible to plastic changes in its regulatory outputs as a means of adapting to frequently varying environmental conditions. It is possible that pleiotropically acting genes involved in stress response pathways, perhaps those that also modulate dauer development, may play a cryptic role in endoderm development. Hence, (heritable) change of function or expression of those genes in response to stress may subsequently alter the signaling during endoderm specification. In the wild, *C. elegans* experiences a boom-and-bust cycle and most worms isolated in the wild are present in the dauer stage (Schulenburg and Félix, 2017). As we have shown, dauer diapause is associated with strong heritable epigenetic effects (Webster et al., 2018) that may, therefore, influence developmental plasticity and adaptive evolution in response to the local environment. We believe that our findings may provide among the first example of environmentally-induced heritable epigenetic changes that modulate developmental input(s) into an embryonic GRN (see Chapter 4).

Materials and Methods

C. elegans Strains

N2 (Bristol, UK), MY16 (Mecklenbeck, Germany), JU1491 (Le Blanc, France), and JU1172 (Concepcion, Chile). JR3336*, (elt-2::GFP) X; (ifb-2::GFP) IV*. PD2227 (Artiles et al., 2019), *oxIs322 II; ccTi1594 III. oxIs322 contains [myo-2prom::mCherry::H2B + myo-3p::mCherry::H2B + Cbr-unc-119(+)] II. ccTi1594* contains *[mex-5prom::GFP::gpr-1::smu-1 3'UTR + Cbr-unc-119(+), III: 680195] III.* MD701, *bcIs39 [lim-7prom::ced-1::GFP + lin-15(+)] V*. JR3666, PD2227 and MD701 are N2-derived transgenic animals.

Worm Culture

Worm strains were maintained as described (Brenner, 1974) and all experiments were performed at 20ºC unless noted otherwise. To ensure no carry-over of a parental stress response, a fresh worm stock was obtained from -80ºC and maintained on 150 mm NGM plates seeded with *E. coli* OP50 for at least five generations prior to beginning experiments. To avoid genetic drift and lab domestication, a fresh worm stock was obtained every ~30 generations.

To obtain males for crosses, 20–30 L4 hermaphrodites were picked into 7% ethanol solution in microcentrifuge tubes and rotated for one hour (Lyons and Hecht, 1997). Worms were pelleted by centrifugation at 2000 rpm for 30 seconds. They were then transferred to NGM plates seeded with *E. coli* OP50. F1 male progeny were mated with sibling hermaphrodites to establish male stocks.

Dauer Induction and POE Assays

The animals were maintained on NGM plates seeded with OP50. Once the cultures became crowded and exhausted their food supply, they were incubated for an extra two weeks at 20ºC. The worms were then washed with M9 buffer and incubated in 1% sodium dodecyl sulfate (SDS) for 30-60 minutes with gentle agitation to select for dauer larvae (Cassada and Russell, 1975). Isolated dauer larvae were then washed with M9 to remove all SDS and allowed to recover overnight on 60 mm NGM plates seeded with OP50.

Reciprocal crosses were set up using L4s and the animals were allowed to mate overnight. Control experiments using well-fed animals were performed in parallel. Mated hermaphrodites, as indicated by the presence of copulatory plugs (except for

crosses involved N2 males which do not deposit plugs), were transferred to a fresh NGM plate to lay eggs for ~5-7 hours and the resulting early brood was discarded to avoid contamination of self-progeny. The hermaphrodites were then transferred to a fresh seeded NGM plate to lay eggs overnight. The hermaphrodite (P0) was then removed, leaving the F1s alone. Once the F1 worms reached early or mid-adulthood, they were treated with 15% alkaline hypochlorite solution to obtain F2 embryos which were allowed to hatch on food. This procedure was repeated until the F4 generation (F10 for the experiment shown in Figure 3.1D) was obtained. At each generation, L4 worms were used to analyze *skn-1* RNAi phenotype. As SKN-1 is maternally provided, the F2 phenotype, for example, is the result of *skn-1* RNAi treatment of F1 mothers. To examine the maternal effect, mating was performed on *skn-1* RNAi plates. The arrested F1 embryos from mated hermaphrodites were then collected for quantification of the number of animals containing gut granules (Figure 3.1A).

For crosses between PD2227 hermaphrodites and JU1491 males, the POE assay was performed as described above. F1 L4s were immobilized on a 5% agar pad with 5 mM levamisole diluted in M9 and observed using Nikon Eclipse Ti-E inverted microscope. Mosaic worms that expressed *myo-2*::mCherry, but not *myo-3*::mCherry and *mex-5*::GFP (i.e., PD2227-derived AB and JU1491-derived P1), were recovered on a seeded NGM plate in the presence of M9. 20 F2 animals were then randomly selected and observed to ensure no worms expressed fluorescent markers, i.e. JU1491 nuclear genotype (Figure 3.2D; Supplemental Figure 3.4).

Viability and Embryonic Lethality Scoring

To score viability, young hermaphrodites (F1 progeny of the reciprocal crosses) were allowed to lay eggs on an NGM plate seeded with OP50. The next day, newly hatched L1s (F2) were transferred to individual seeded plates. “Larval lethal” was defined as the percentage of worms that arrested as L1s. Worms that reached adulthood but failed to reproduce in five days were scored as sterile. To score embryonic lethality, individual young hermaphrodites (F1) were allowed to lay eggs on an NGM plate seeded with a small drop of OP50 for ~4-8 hours. The hermaphrodites were then removed, leaving the embryos. The fraction of unhatched embryos were counted and scored ~24 hours later. At least two independent broods were scored. We note that there were no obvious differences in brood sizes between the various crosses.

RNAi

Feeding-based RNAi experiments were performed as described (Torres Cleuren et al., 2019). RNAi clones were obtained from either the Vidal (Rual et al., 2004) or Ahringer (Kamath et al., 2003) libraries. RNAi bacterial strains were grown at 37^{o}C in LB containing 50 µg/ml ampicillin. The overnight culture was then diluted 1:10. After four hours of incubation at 37^{o}C, 1 mM IPTG was added and 60-100 µl was seeded onto 35 mm agar plates containing 1 mM IPTG. Seeded plates were allowed to dry and used within five days when kept at room temperature. For *skn-1* RNAi, five to 10 L4 animals were placed on each RNAi plate. 24 hours later, they were transferred to another RNAi plate to lay eggs for 12 hours. The adults were then removed, leaving the embryos to develop for an extra 5-7 hours. Embryos expressing birefringent gut granules were quantified and imaged on an agar pad using a Nikon

Ti-E inverted microscope under dark field with polarized light. We note that the *skn-1* sequence is highly conserved in the isotypes used in this study. It is therefore highly unlikely that variation in *skn-1(RNAi)* phenotypes is attributable to underlying *skn-1* polymorphisms.

For *met-2*, *set-32*, *nrde-4*, *prg-1/2* and *ced-4* RNAi, 15-30 F3 L4 animals showing POE were placed on plates of *E. coli* containing an empty control vector (L4440) or expressing double-stranded RNA. 24 hours later, they were transferred to another RNAi plate and allowed to lay eggs for another ~7 hours. The adults were then removed and the F4 animals were allowed to develop on RNAi feeder bacteria. F4 L4 larvae were used for the *skn-1* RNAi assay for POE as described above (Figure 3.4A).

Statistics and Figure Preparation

Statistics were performed using R software v3.4.1 (https://www.r-project.org/). Two-sample two-tailed t-tests were used to compare the *skn-1* RNAi phenotype between two groups, unless stated otherwise. Welch's t-tests were performed if the variances of the two groups being compared were not equal. Fisher's exact tests were used to determine the difference in proportions (Figure 3.3B, C; Figure 3.4C). Plots were generated using R package ggplot2. Figures were assembled in Inkscape v0.92.4 (https://inkscape.org/).

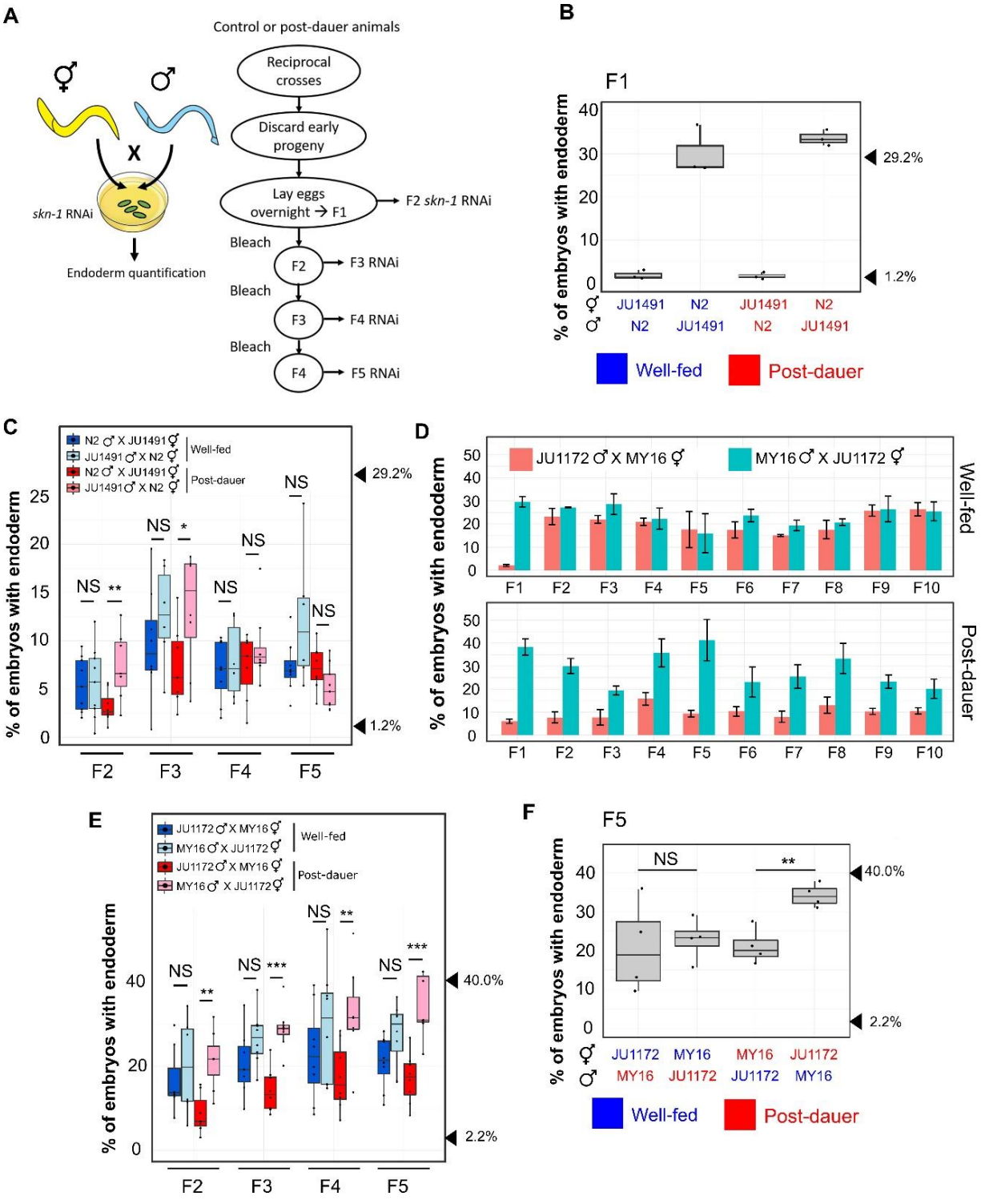

Figure 3.1: Dauer diapause-stimulated POE.
(A) Schematic of the POE assay strategy. (A, Left) To test for a maternal effect, reciprocal crosses using well-fed or post-dauer animals were performed on *skn-1* RNAi plates, and the fraction of arrested F1 embryos with differentiated gut was examined. Blue and yellow colors represent different wild isotypes. (A, Right) To study

the transgenerational phenotypes, reciprocal crosses were performed using different wild isotypes on NGM plates. Embryos were collected from mated hermaphrodites to establish the F1 population. Day 1 (D) or day 2 (C, E, and F and Figure 3.2C and Figure 3.4B and Supplemental Figure 3.2) gravid worms were treated with alkaline hypochlorite solution to obtain the next generation embryos. L4 hermaphrodites were isolated for *skn-1* RNAi assays at each generation (see Materials and Methods). (B) Strong maternal effect in F1 embryos from mated *skn-1(RNAi)* mothers in N2 × JU1491 crosses. At least three independent crosses were performed. Arrowheads indicate phenotypes of N2 (29.2%) and JU1491 (1.2%). The phenotypes of the F1 progeny are not significantly different from those of their respective mother in all crosses, regardless of feeding status. One-sample t test ($p > 0.05$). (C) POE in *skn-1(RNAi)* embryos from four generations: F2, F3, F4, and F5 derived from reciprocal N2 × JU1491 crosses. At least five independent crosses were performed for each treatment. Arrowheads indicate the phenotypes of N2 (29.2%) and JU1491 (1.2%). (D) Dauer diapause-induced POE persists for at least 10 generations in JU1172 × MY16 descendants. Three independent crosses were performed. Alkaline hypochlorite treatment was performed on day 1 gravid adults at each generation. Error bars represent ± SEM. Two-way ANOVA: $p = 0.08$ and 9.14×10^{-11} for the well-fed and pos-tdauer experiments (F2 to F10), respectively. (E) Robust POE in *skn-1(RNAi)* embryos over four generations: F2, F3, F4, and F5 derived from reciprocal JU1172 × MY16 crosses. At least five independent crosses were performed for each treatment. Alkaline hypochlorite treatment was performed on day 2 gravid adults at each generation. Arrowheads indicate the phenotypes of JU1172 (40.0%) and MY16 (2.2%). (F) POE seen in *skn-1(RNAi)* F5 embryos from reciprocal crosses between MY16 and JU1172. Data points represent independent crosses. Arrowheads indicate the phenotypes of JU1172 (40.0%) and MY16 (2.2%). For B and F, blue text represents experiments with well-fed animals, while red text is for experiments with post-dauer animals. Two-sample t test: not significant (NS), $p > 0.05$; *$p \leqslant 0.05$; **$p \leqslant 0.01$; ***$p \leqslant 0.001$. Boxplots represent medians, with range bars showing upper and lower quartiles.

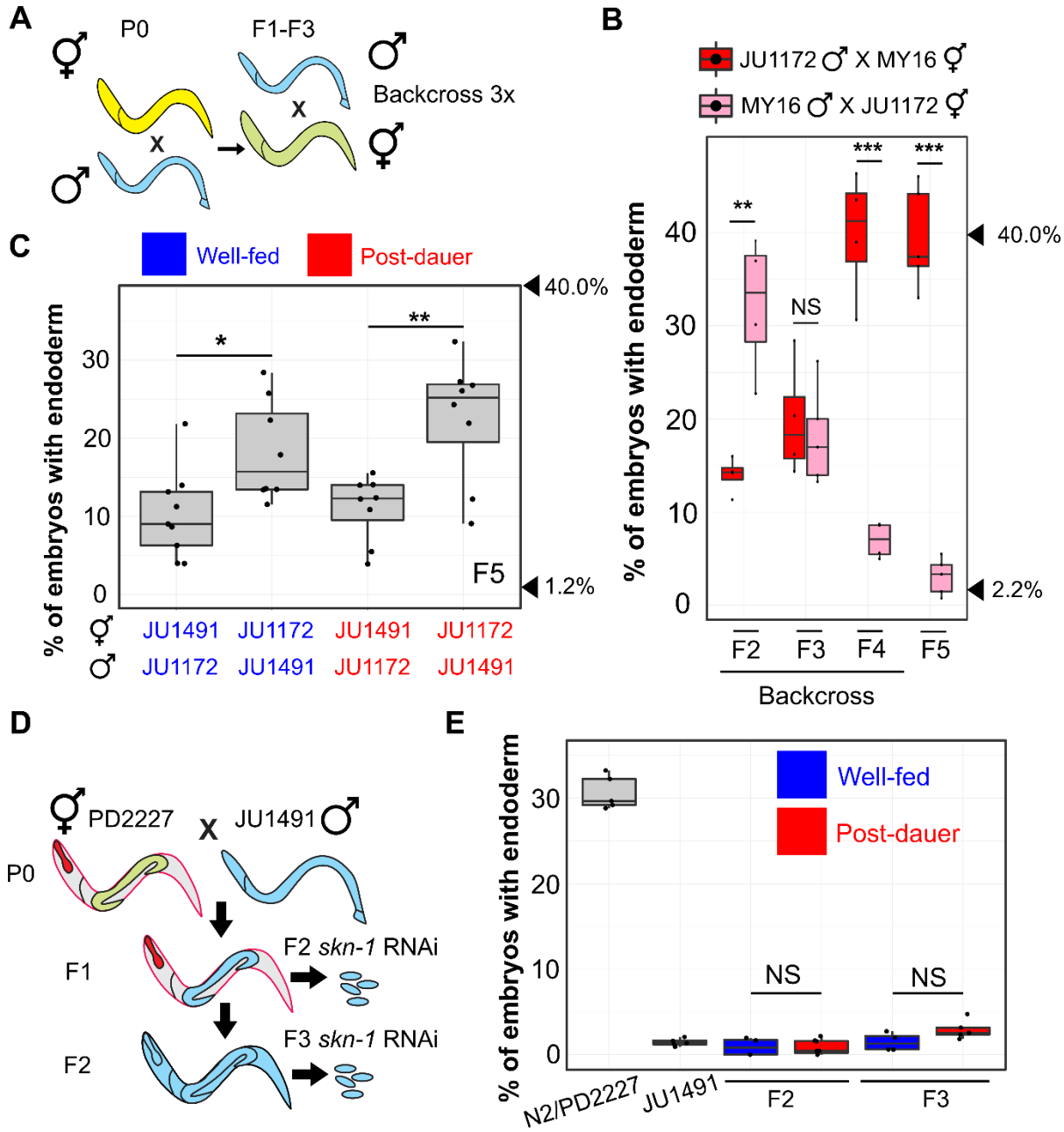

Figure 3.2: POE is not attributable to mitochondrial DNA or cytoplasmic inheritance.

(A) Schematic of mitochondrial transfer experiment. Blue and yellow represent different wild isotypes. Five to 10 hermaphrodites were used to backcross to the paternal strain at every generation for 3 generations. (B) POE in *skn-1(RNAi)* embryos. Data points represent replicates from a single reciprocal cross using post-dauer animals. Arrowheads indicate phenotypes of JU1172 (40.0%) and MY16 (2.2%). (C) POE shown by *skn-1(RNAi)* F5 embryos of reciprocal crosses performed between JU1491 and JU1172. Data points represent independent crosses. Arrowheads indicate phenotypes of original JU1172 (40.0%) and JU1491(1.2%)

strains. (D) When PD2227 ($N2^{GPR\text{-}1\ OE}$) hermaphrodites are mated to JU1491, non-Mendelian segregation of maternal and paternal chromosomes result in some F1 mosaic animals that express the maternally derived pharyngeal marker (*myo-2*::mCherry) but lose the body wall muscle (*myo-3*::mCherry) and germline (*mex-5*::GFP) markers. F2 self-progeny of the F1 mosaic animals contain only the JU1491 nuclear genome (Supplemental Figure 3.4). (E) *skn-1(RNAi)* phenotype of N2/PD2227, JU1491, and F2 and F3 embryos from the mosaic animals. For C and E, blue represents experiments performed using well-fed animals, while red represents experiments performed using post-dauer animals. Two-sample t test: not significant (NS), $p > 0.05$; *$p \leq 0.05$; **$p \leq 0.01$; ***$p \leq 0.001$. Boxplots represent medians, with range bars showing upper and lower quartiles.

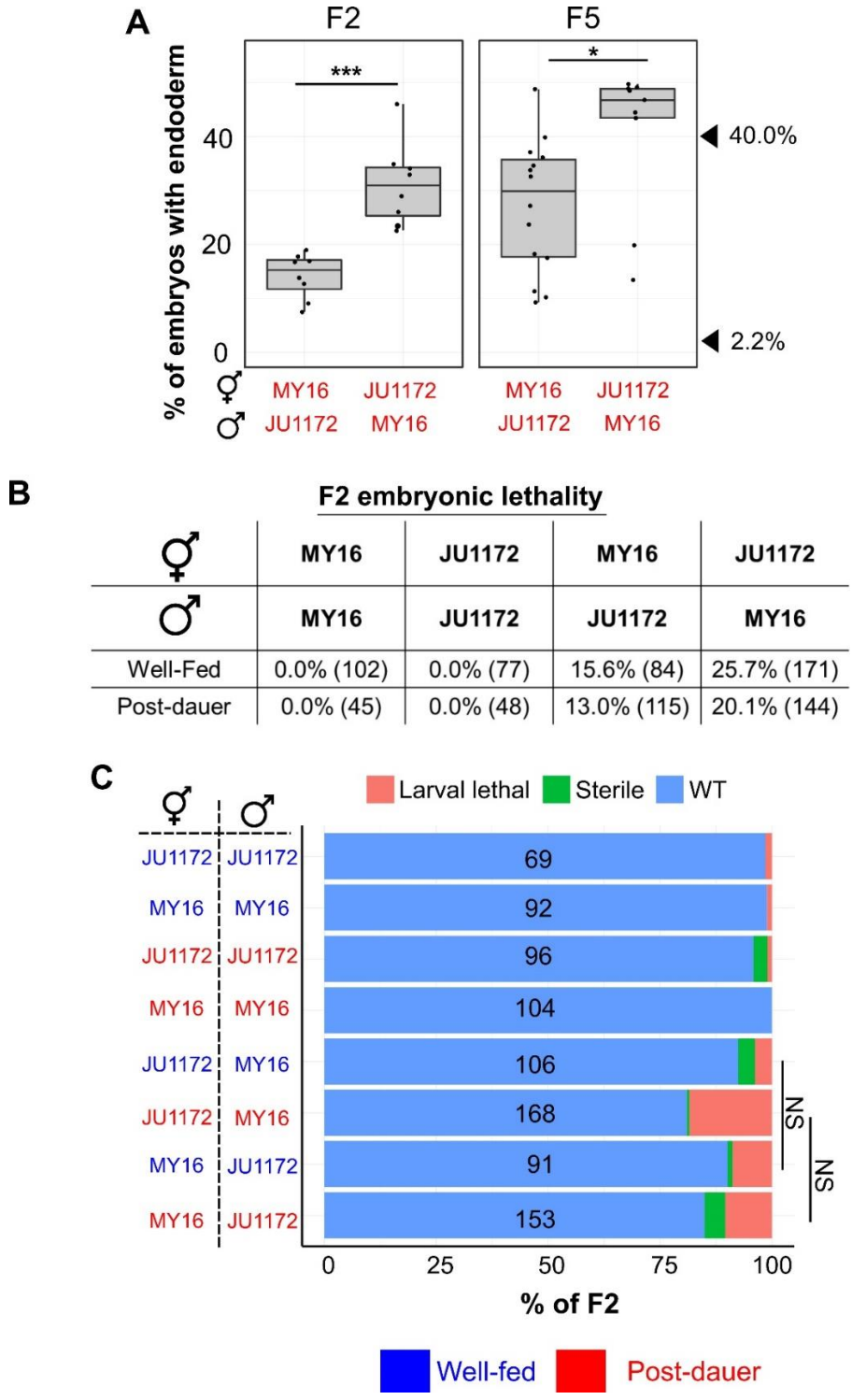

B

F2 embryonic lethality

♀	MY16	JU1172	MY16	JU1172
♂	MY16	JU1172	JU1172	MY16
Well-Fed	0.0% (102)	0.0% (77)	15.6% (84)	25.7% (171)
Post-dauer	0.0% (45)	0.0% (48)	13.0% (115)	20.1% (144)

Figure 3.3: POE is not attributable to competitive fitness or maternal incompatibility.

(A, Left) POE shown by skn-1(RNAi) F2 embryos of reciprocal crosses performed between MY16 and JU1172. (A, Right) Individual data points represent lines derived from late F2s of senescent F1 animals. Two independent crosses were performed for

each direction. Two-sample t test: not significant (NS), $p > 0.05$; *$p \leqslant 0.05$; **$p \leqslant 0.01$; ***$p \leqslant 0.001$. Boxplots represent medians, with range bars showing upper and lower quartiles. The arrowheads indicate the phenotypes of JU1172 (40.0%) and MY16 (2.2%). (B) Embryonic lethality in F2s. Two independent broods were examined. The total number of embryos scored is shown in brackets. (C, Right) Sterility and larval lethality of F2 progeny. (C, Left) Identity and the sex of the parents are indicated. The total number of animals scored is indicated. Fisher's exact test: NS, $p > 0.05$. WT, wildtype. For A and C, blue text represents experiments performed using well-fed animal, while red text represents experiments performed using post-dauer animals.

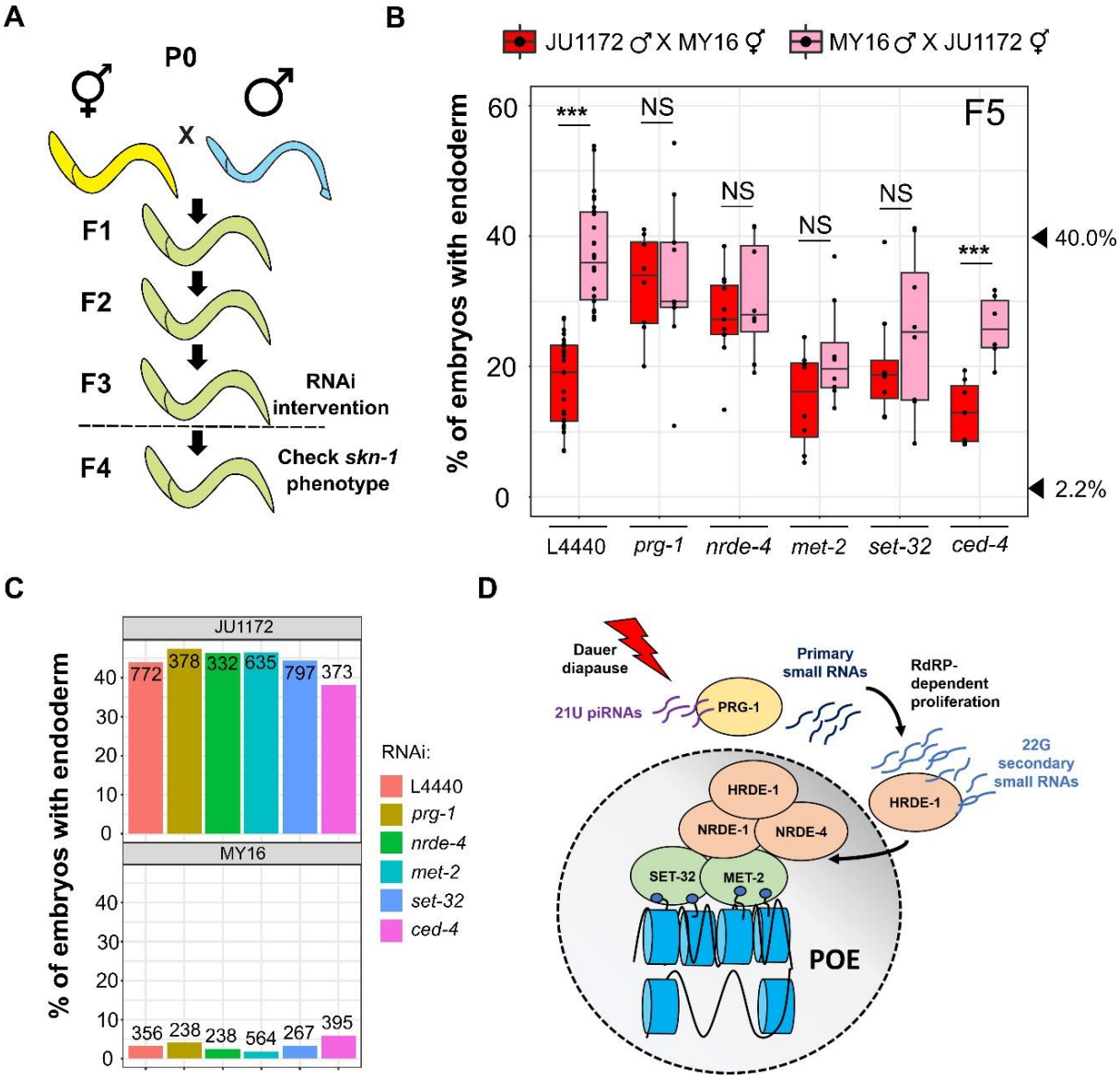

Figure 3.4: POE requires both the piRNA/nuclear RNAi pathway and factors required for H3K9me3 chromatin marks.

(A) Schematic of RNAi experiments that test requirement for epigenetic regulators in POE. F3 L4 animals were treated with the indicated RNAis, and F4 L4s were used for the *skn-1* RNAi assays. Animals in the control and treatment groups were siblings (see Materials and Methods). (B) Knocking down *prg-1*, *nrde-4*, *met-2*, and *set-32*, but not ced-4, eliminates POE. Data points are replicates from at least two independent crosses. Boxplots represent medians, with range bars showing upper and lower quartiles. Arrowheads indicate phenotypes of JU1172 (40.0%) and MY16 (2.2%). Two-sample t test: not significant (NS), $p > 0.05$; ***$p \leqslant 0.001$. (C) The effect of RNAi treatments on the *skn-1(RNAi)* phenotype. MY16 and JU1172 L4s were exposed to L4440 (control), *prg-1*, *nrde-4*, *met-2*, *set-32*, or *ced-4* RNAi feeder strains, and the *skn-1(RNAi)* phenotype of the F1 were quantified. No difference between different

RNAi treatments was detected (Fisher's exact test, $p > 0.05$). The total number of embryos scored is indicated. (D) Model for POE (see Maintenance of POE Involves the Nuclear RNAi Pathway and Histone H3K9 Trimethylation).

Table 3.1: Polymorphisms in the mitochondrial protein coding genes between MY16 and JU1172.

Genes	Position	MY16	JU1172	Modifications
nduo-6	112	T	G	Val4Leu
	227	G	A	Val39Ile
	382	A	T	Leu90Phe
nduo-1	2,476	A	T	Lys238Asn
atp-6	3,230	GTAATA	GA	Frameshift
nduo-2	3,614	G	T	Cys66Phe
	3,997	G	A	Gly194Ser
ctb-1	5,365	A	G	Ile288Val
	5,367	T	A	Ile288Met
ctc-1	9,242	T	A	Ile466Met
ctc-2	10,003	T	C	Leu119Met
nduo-5	12,714	G	A	Ala342Thr
	12,906	G	A	Val406Met

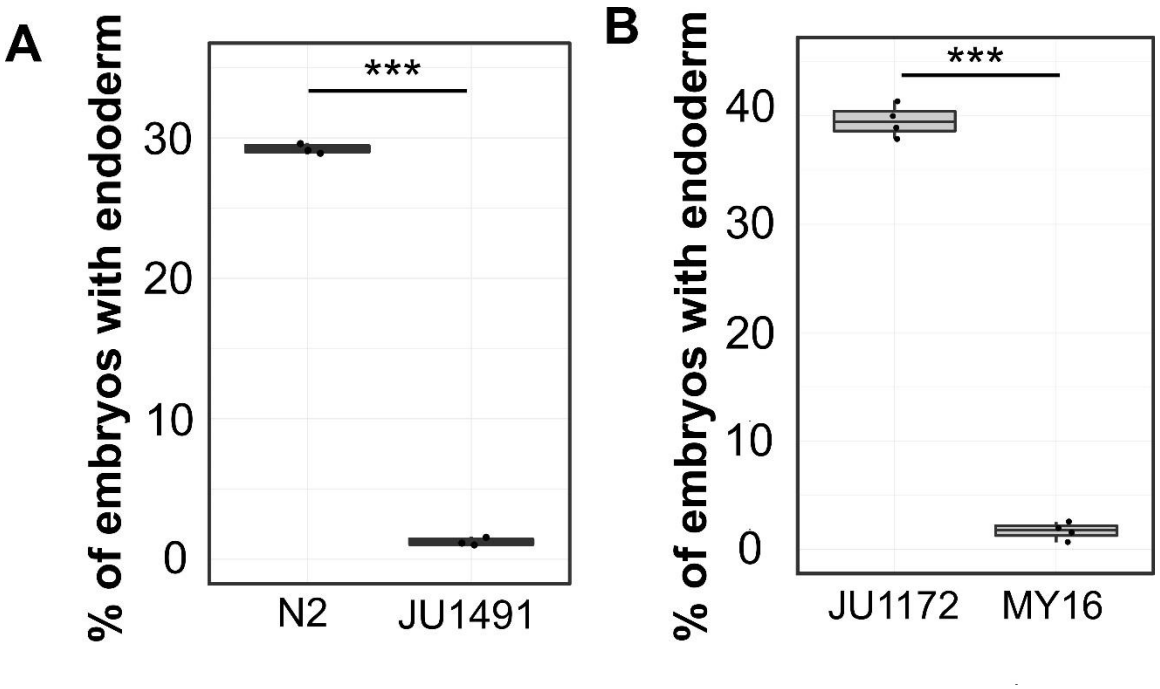

Supplemental Figure 3.1: Natural variation in SKN-1 requirement.
(A) *skn-1(RNAi)* phenotype of laboratory strain N2 and wild isotype JU1491. (B) *skn-1(RNAi)* phenotype of wild isotypes JU1172 and MY16. At least three replicates were performed for each strain, with >200 embryos per replicate. Two sample t-test: ***p ≤ 0.001.

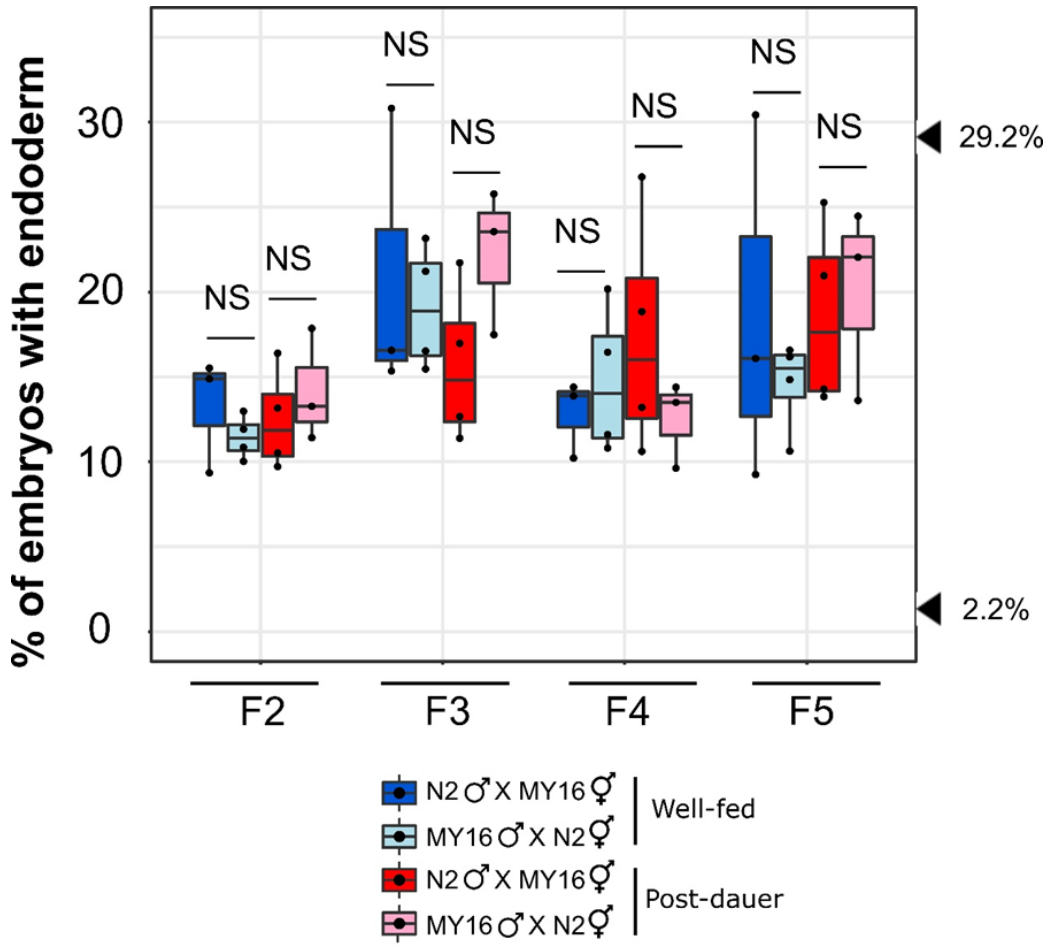

Supplemental Figure 3.2: Absence of POE in N2 x MY16.
No POE was observed in *skn-1(RNAi)* embryos from four generations: F2, F3, F4 and F5 derived from N2 x MY16 crosses. At least three independent crosses were performed for each treatment. Arrowheads indicate the phenotypes of JU1172 (40.0%) and MY16 (2.2%). Two sample t-test: not significant (NS), $p > 0.05$. Boxplot represents median with range bars showing upper and lower quartiles.

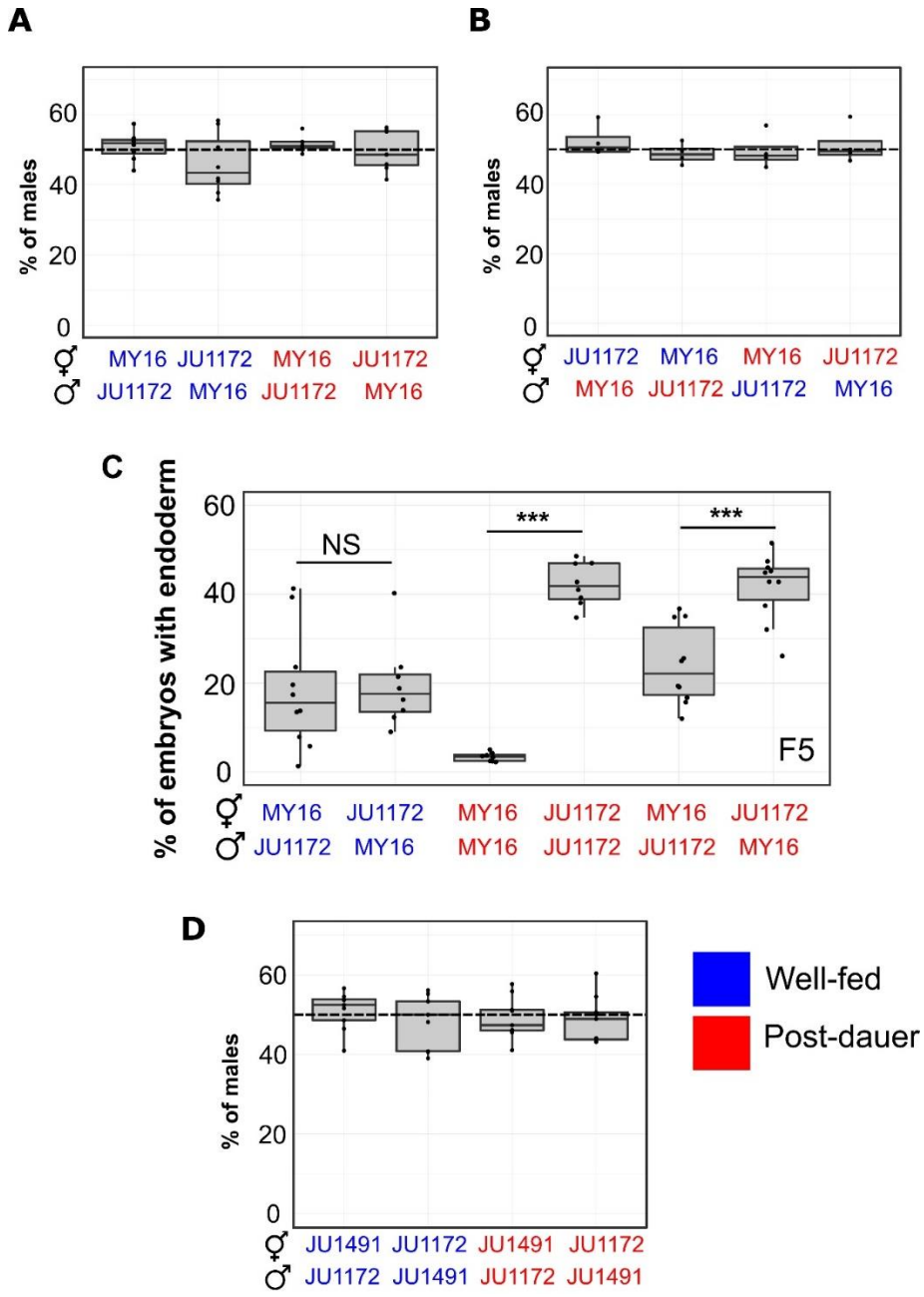

Supplemental Figure 3.3: POE is not the result of frequent selfing.
(A and B) Male frequency in the F1 offspring from reciprocal crosses between MY16 x JU1172 (related to Figure 3.1D and E). In all cases, ~50% of males were found (one-sample t-test, $p > 0.05$). (C) Individual data points represent *skn-1(RNAi)* F5 embryos of lines derived from isolated F1s. Two sample t-test: not significant (NS), $p > 0.05$, ***$p \leq 0.001$). (D) Male frequency in the F1 offspring from reciprocal crosses between JU1172 x JU1491 (related to Figure 3.2C). Boxplot represents median with range bars showing upper and lower quartiles. Blue text represents experiments performed using well-fed animals while red text represents experiments performed using post-dauer animals.

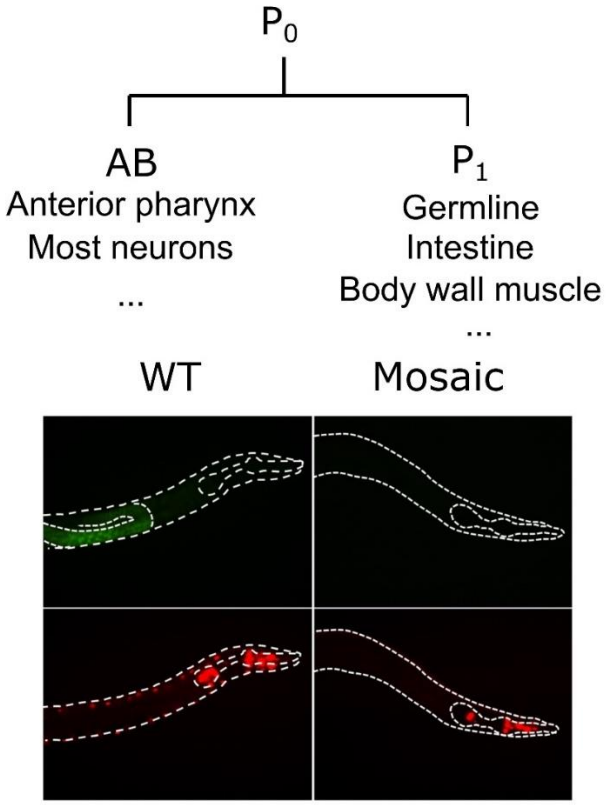

Supplemental Figure 3.4: Non-Mendelian chromosomal segregation in GPR-1 overexpression animals.
The two daughter cells, AB and P_1, arising from the first asymmetrical cell division develop into different cell lineages. When PD2227 ($N2^{GPR\text{-}1\ OE}$) hermaphrodites are mated to wildtype JU1491, unequal segregation of maternal and paternal chromosomes occurs, causing AB to contain only the maternal chromosomes and P_1 to contain only the paternal chromosomes. F1 mosaic animals express the maternally-derived pharyngeal marker (*myo-2*::mCherry) but not the body wall muscle (*myo-3*::mCherry) and germline (*mex-5*::GFP) markers.

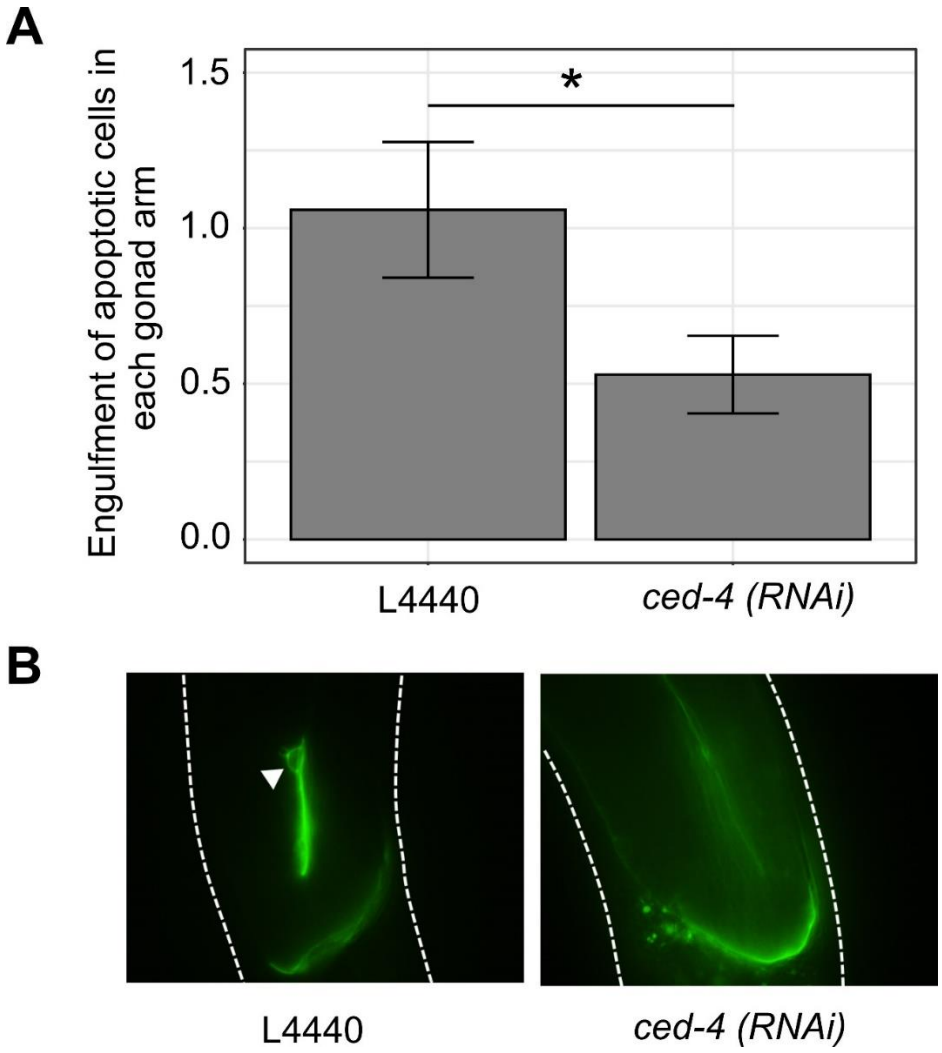

Supplemental Figure 3.5: *ced-4* RNAi suppresses apoptotic cell death of meiotic germ cells.
(A) Quantification of *bcIs39* engulfment of apoptotic cell corpses in MD701, which is an N2-derived strain. L4 animals were placed on plates of *E. coli* containing an empty control vector (L4440) or expressing double-stranded RNA. 24 hours later, they were transferred to another RNAi plate and allowed to lay eggs for ~7 hours. The adults were then removed and the F1 animals were allowed to develop on RNAi feeder bacteria. The number of apoptotic germ cells were scored in young adults (n=17 for each treatment). Error bars represent ± SEM. Two sample t-test: *p ≤ 0.05. B) Representative images of control and *ced-4(RNAi)* worms. *bcIs39 [CED-1::GFP]* clusters around apoptotic cell corpses are indicated by white arrowhead.

Chapter 4 : Conclusion Remarks – Regimes of Canalization[6]

"I seem to have been only like a boy playing on the seashore, and diverting myself in now and then finding a smoother pebble or a prettier shell than ordinary, whilst the great ocean of truth lay all undiscovered before me" - Isaac Newton

[6] This chapter has been published in Ewe et al., Dev Biol (2021) with minor modifications.

It has become clear in recent years that alteration of epigenetic states triggered by stressful experience can be transmitted across multiple generations, breaking the Weismann barrier. This effect appears to be most prominent in organisms with a relatively short life cycle, including nematodes, plants, and insects (Houri-Zeevi and Rechavi, 2017; Perez and Lehner, 2019a). In *C. elegans*, the progeny of starved animals, for example, show increased lifespan and stress resistance through the inheritance small RNAs (Rechavi et al., 2014; Webster et al., 2018). Intestine-germline communication appears to be important for epigenetic inheritance in *C. elegans* (Figure 4.1A). Ingested dsRNA is specifically imported into the intestinal cells by a transmembrane transporter, SID-2, and subsequently triggers a systemic RNA interference (RNAi) response (Fire et al., 1998; Timmons and Fire, 1998; Winston et al., 2007). RNAi-defective mutants show enhanced susceptibility to viral infection (Félix et al., 2011; Lu et al., 2005; Schott et al., 2005). Interestingly, small RNA response launched in response to viral infection can be transmitted transgenerationally (Rechavi et al., 2011), suggesting interactions between the defense mechanisms in the intestine and the transcriptional programs in the germline. Tissue-specific elimination from the intestine of ASH-2, a component of the COMPASS complex that mediates H3K4 trimethylation (H3K4me3), alters the epigenetic state of the germline, leading to a heritable stress response in a process that involves the IIS pathway mediated by DAF-16 in the intestine, as well as the germline nuclear RNAi pathway (Nono et al., 2020). Similarly, offspring from parents exposed to heavy metal stressors exhibit enhanced resistance to oxidative stress. This heritable hormesis effect also requires the function of DAF-16 in the soma and

involves H3K4me3 (Kishimoto et al., 2017). Germline cues, in turn, modulate metabolism and proteostasis in the soma, in some cases involving SKN-1 and PHA-4 (see Pleiotropy may Facilitate the Evolution of the Endoderm GRN; Figure 4.1A) (Lapierre et al., 2011; Libina et al., 2003; Lin et al., 2001; Ratnappan et al., 2014; Sala et al., 2020; Steinbaugh et al., 2015).

Vitellogenin, a family of high-density yolk proteins, is synthesized in the adult hermaphrodite intestine and loaded into oocytes via endocytosis mediated by a member of the low-density lipoprotein receptor superfamily, RME-2 (Perez and Lehner, 2019b). It was found that provision of yolk increases with maternal age, and this has profound consequences on the fitness of the progeny. Compared to the offspring from older mothers, early progeny are slow developing, exhibit signs of pre-mature aging, and are less resistant to stress, much like *rme-2* mutants (Perez et al., 2017). Progeny of starved animals inherit small RNAs that regulate vitellogenin genes (Rechavi et al., 2014). In addition, exposing the mothers to dietary restriction reduces IIS and increases yolk provision, enhancing starvation resistance by downregulating IIS in the progeny (Hibshman et al., 2016; Jordan et al., 2019). Interestingly, eliminating *daf-2* in the maternal soma, but not in the germline, is sufficient to trigger this heritable stress response (Figure 4.1A) (Hibshman et al., 2016). Bet-hedging occurs when phenotypic variation in a population increases to facilitate adaption to stressful conditions at the expense of lowered mean fitness. The synthesis of vitellogenins is metabolically costly (Ezcurra et al., 2018). Increasing yolk titers to allow progeny to adapt to changing environment is, therefore, an exemplar of maternal bet-hedging (Olofsson et al., 2009).

Systemic gene silencing induced by exogenous dsRNA can persists for many generations (Vastenhouw et al., 2006). Exo-siRNA is found to be deposited into the oocytes, along with vitellogenin proteins, in an RME-2-dependent manner, mediating transgenerational gene silencing (Marré et al., 2016). In the germline, exo-siRNAs (and endogenous small RNAs) engage RNA-dependent RNA polymerase to produce an abundance of secondary small RNAs using the mRNA target as a template. The secondary small RNAs subsequently guide Argonaute proteins to their genomic targets and mediate transcriptional repression by inhibiting RNA polymerase II elongation and promoting deposition of H3K9 methylation at their targeted loci through the nuclear RNAi pathway (Rechavi and Lev, 2017). Lipoproteins and extracellular vesicles (EVs) can act as vectors for small RNAs in mammals (Raposo and Stoorvogel, 2013; Tabet et al., 2014; Vickers et al., 2011). In one striking example, it was shown that epididymosomes secreted from the epididymis (a somatic tissue lying along the posterior surface of testis) provide diet-regulated tRNA fragments upon fusion with the sperm and regulate gene expression in the developing mouse embryos. Cell non-autonomous activity of endogenous small RNA in *C. elegans* is not well-documented. Hence, it is not clear how physiological response may influence heritable transcriptional activities in the germline; however, it has been shown that isolated extracellular vesicles abundant in small RNA, including piRNA (Russell et al., 2018), may serve as a vector of epigenetic memory. piRNAs have been implicated in transgenerational epigenetic inheritance (Ashe et al., 2012; Heestand et al., 2018; Moore et al., 2019; Shirayama et al., 2012; Simon et al., 2014). Furthermore, a recent

report demonstrated that microRNA *mir-83* released from the intestine of aged worms disrupts autophagy in a cell non-autonomous manner (Zhou et al., 2019).

SKN-1 has been found to play a role in mediating adaptive heritable stress response. Maternal dietary restriction promotes developmental success by promoting SKN-1 and DAF-16 activity in the progeny (Jordan et al., 2019). Animals that have experienced nutritional stress produce larger offspring. This effect requires the function of SKN-1 and PHA-4, which have been shown to increase progeny size independent of the IIS pathway (Hibshman et al., 2016). It is conceivable that, in response to nutritional stress, lipid biogenesis is upregulated in the intestine, initiated by PHA-4 and DAF-16 (Amrit et al., 2016; Perez and Van Gilst, 2008; Wu et al., 2018). SKN-1 subsequently coordinates increased maternal yolk provision, ensuring developmental success of the progeny (Jordan et al., 2019; Lynn et al., 2015). Indeed, DAF-16 and PHA-4 have been shown either directly or indirectly to regulate *vit-2* expression in the intestine (Goszczynski et al., 2016), and disrupting fatty acid metabolism inhibits the intergenerational effect (Hibshman et al., 2016). It is noteworthy that in a *skn-1* gain-of-function mutant, starvation and oxidative stress induce rapid transfer of lipids from the intestine to the maturing oocytes in aging worms. Accordingly, treating the animals with an antioxidant leads to excessive accumulation of lipids in intestine, but not in the germline (Lynn et al., 2015). How SKN-1 regulates reallocation of lipid stores from the intestine to the germline is not yet known, but it has been shown to require the functions of vitellogenin proteins (Lynn et al., 2015). Bioactive lipid molecules in the deposited yolk may further influence the epigenetic landscapes in oocytes and embryos (Papsdorf and Brunet, 2019).

SKN-1 is required for bacterial pathogen resistance (see SKN-1/Nrf: a nexus in development, homeostasis, and aging) (Papp et al., 2012). Intriguingly, a recent study reported a role of SKN-1 in mediating heritable adaptation to *Pseudomonas vranovensis* infection. Exposing the worms to *P. vranovensis* confers significant offspring resistance to the pathogen, and reducing SKN-1 function negatively impacts progeny adaptation (Burton et al., 2020). It is conceivable that SKN-1 activity is upregulated in the embryos in response to parental exposure to the pathogen. Indeed, various stressors (heavy metal, starvation and hyperosmosis) induce inheritance of this hormesis effect such that the progeny exhibit higher tolerance to oxidative stress, and requires proper SKN-1 signaling (Kishimoto et al., 2017). Heritable RNAi response is strengthened if the parents, but not the offspring, are exposed to stress. In contrast, the silencing effect is reduced, and the pool of small RNAs is reprogrammed if the F1 progeny are subjected to stress. Importantly, SKN-1 and MAP kinase pathways, as well as H3K9 methylation, are required for resetting the epigenetic memory, perhaps to cope with the mismatch between the parental and the offspring's environment (Houri-Zeevi et al., 2021).

C. elegans wild isotypes exhibit a broad variation in SKN-1 requirement in endoderm specification, in part due to accumulation of cryptic genetic variants, as discussed above (see Rapid Developmental System Drift among *C. elegans* Wild Isolates). Remarkably, dauer diapause triggers a heritable epigenetic state that modifies SKN-1 requirement such that the phenotypes of the progeny persistently follow that of the maternal founder for multiple generations when different isotypes are mated (Chapter 3) (Ewe et al., 2020b), suggesting altered SKN-1 expression and/or

function during early embryogenesis (Singh et al., 2016; Vu et al., 2015). In support of this notion, dauer diapause evokes differential expression of DAF-16 target genes that persists for several generations (Webster et al., 2018), which may in turn influence the regulation of SKN-1 (Jia et al., 2004; Robida-Stubbs et al., 2012; Schuster et al., 2010; Tullet et al., 2008).

As discussed, environmental stimuli may alter the regulation and/or quantitative maternal provision of SKN-1 that persist for many generations (Burton et al., 2020; Ewe et al., 2020b; Jordan et al., 2019; Kishimoto et al., 2017; Webster et al., 2018). This phenotypic plasticity provides substrates on which Darwinian forces may act, leading to the accumulation of new mutations that may impact both stress response and mesendoderm specification, perhaps through a process of “genetic assimilation” (Waddington, 1942). In the endoderm GRN, (conditionally) neutral mutations can rapidly accumulate owing to its robust architecture (Chapter 2) (Torres Cleuren et al., 2019). In Waddington’s framework, a ball rolls down an epigenetic landscape and into a “default” developmental trajectory in a typical environment. However, environmental perturbation may move the rolling ball into an alternate path which can be readily remodeled and eventually become canalized in the absence of the initial trigger (Figure 4.1) (Waddington, 1942). The early stages of the endoderm GRN in nematodes has undergone rapid rewiring (Ewe et al., 2020a; Lin et al., 2009; Torres Cleuren et al., 2019). We propose that this substantial plasticity maybe driven by both genetic and epigenetic mechanisms (Sommer, 2020).

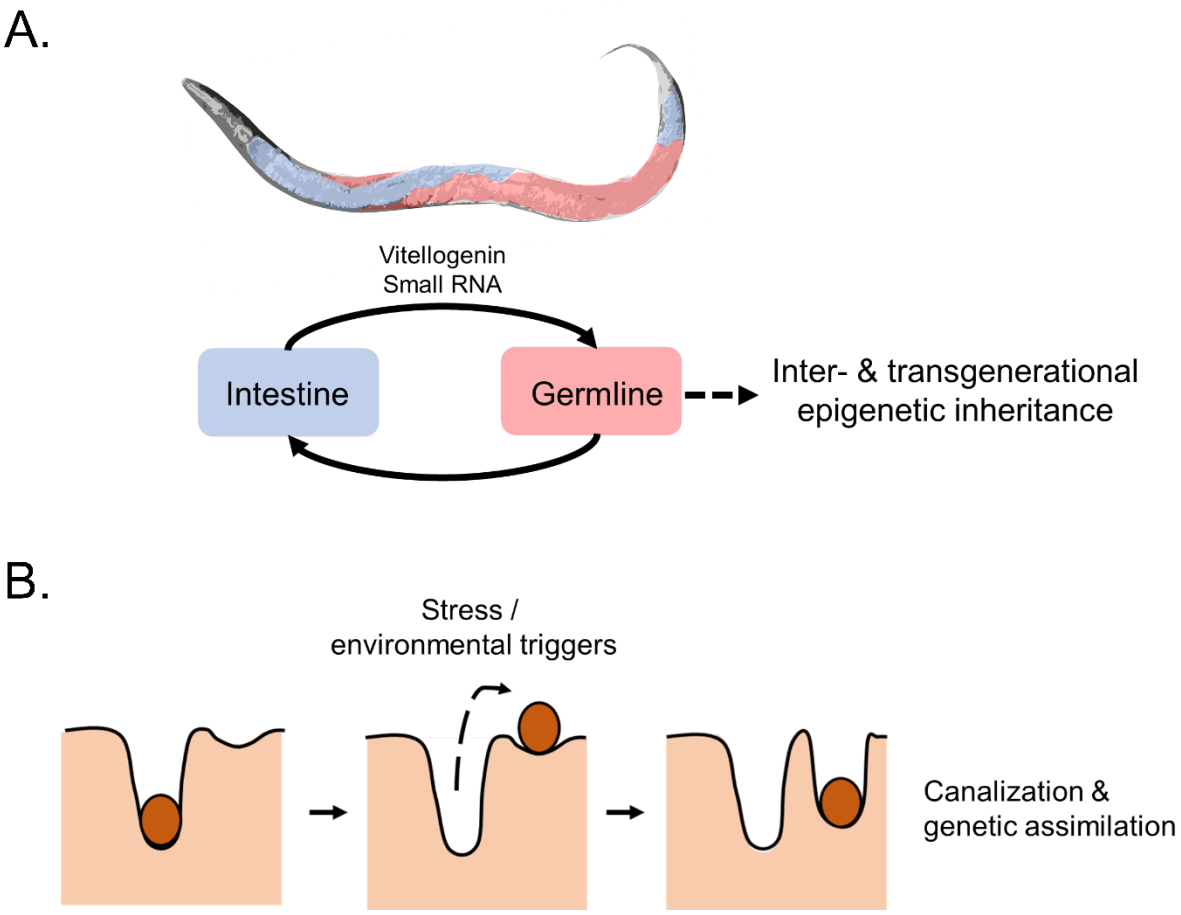

Figure 4.1: Epigenetic inheritance may facilitate evolution.
(A) Small RNAs and yolk from the intestine (blue) may influence transcriptional response in the germline (red) and the developmental outcome of the progeny, leading to epigenetic inheritance. In turn, germline cues may regulate metabolic activities in the intestine, although the molecular details are not well-understood. (B) Waddington's epigenetic landscape modeled as a ball rolling into a canalized pathway. Stress or environment can redirect the ball into a different path. Over time, genetic mutations accumulate, thereby heightening the ridges, in a process termed genetic assimilation (Waddington, 1942).

Chapter 5 : Appendix

"You have made your way from worm to man, and much within you is still worm" -
Friedrich Nietzsche

Appendix I: ICD-1/BTF3 Antagonizes SKN-1-mediated Endoderm Specification in *C. elegans*[7]

Basal transcription factor 3 (BTF3) facilitates transfer of nascent polypeptide chains into mitochondria and regulates transcription in plants and animals (Jamil et al., 2015). We previously found that the *C. elegans* BTF-3 orthologue, ICD-1, is required to prevent apoptosis: eliminating *icd-1* leads to increased cell death in embryos and larvae (Bloss et al., 2003). However, consistent with its potential function as a transcription factor, ICD-1 contains a putative nuclear localization signal in the N-terminus (Figure 5.1A) (Lange et al., 2007). Here, we report that ICD-1 performs a function in endoderm specification. We found that *icd-1* RNAi does not affect endoderm specification in a wildtype N2 background or the gut-less phenotype of *skn-1(-)* embryos. However, knockdown of *icd-1* strongly suppresses the absence of gut in *mom-2/Wnt(-)* embryos (*mom-2(or42)*: 26.0% ± sd 4.5% with gut *vs. mom-2(or42); icd-1(RNAi)*: 75.9% ± sd 2.6%). Similarly, depleting ICD-1 rescues the gut-less phenotype of *mom-4/Tak1(-)* embryos (*mom-4(or39)*: 67.9% ± sd 6.3% with gut *vs. mom-4(or39); icd-1(RNAi)*: 95.5% ± sd 1.2%) (Figure 5.1B). Our findings suggest a model in which ICD-1 antagonizes the SKN-1 input, perhaps by preventing SKN-1 from binding to the *end* promotors. This possibility is also consistent with the finding that competition between ICD-1 and SKN-1 is seen in the context of the unfolded protein response (UPR). SKN-1 binds to and activates *hsp-4*, which codes for an endoplasmic reticulum chaperone BiP (Glover-Cutter et al., 2013). Depleting ICD-1 results in upregulation of *hsp-4* and activation of the UPR (Arsenovic et al., 2012),

[7] This section has been published in Ewe et al., MicroPubl (2019).

suggesting that ICD-1 and SKN-1 perform opposing functions in other contexts. In this hypothesized model, ICD-1 may act to fine-tune developmental signals, thereby ensuring proper specification and differentiation of endoderm (Figure 5.1C).

Materials and Methods

C. elegans Strains

JJ185, *dpy-13(e184) skn-1(zu67) IV; mDp1 (IV;f)*. JR3936, *dpy-13(e184) skn-1(zu67) IV/nT1 [qIs51] (IV;V)*. EU384, *dpy-11(e1180) mom-2(or42) V/nT1 [let-?(m435)] (IV;V).* EU414, *unc-13(e1091) mom-4(or39)/hT2 I; +/hT2 [bli-4(e937) let-?(h661)] III.*

RNAi and Quantification of Endoderm Specification

E. coli HT115 expressing *icd-1* dsRNA was obtained from the Ahringer RNAi library (Kamath and Ahringer, 2003). RNAi experiments for embryonic endoderm specification were performed as described (Torres Cleuren et al., 2019). In brief, bacteria were grown at 37^{o}C in LB containing 50 µg/ml ampicillin. The overnight culture was then diluted 1:10. After 4 hours of incubation at 37^{o}C, 1 mM of IPTG was added and 60 µl was seeded onto 35 mm agar plates containing 1 mM IPTG and 25 µg/ml carbenicillin. Seeded plates were allowed to dry overnight before use. 20-30 L4 or young adults were placed on the seeded RNAi plate. 24 hours later, they were transferred to a fresh RNAi plate and allowed to lay eggs for four hours. The adults were then removed, leaving the embryos to develop for an extra 5-7 hours. Embryos expressing birefringent gut granules were quantified and imaged on an agar pad using a Nikon Ti-E inverted microscope under dark field with polarized light (Clokey and Jacobson, 1986; Hermann et al., 2005). All experiments were performed at 20^{o}C.

A

MDSKAIAERIKKLQAQQEHVRIGGKGT**PRRKKKV**IHKTAAADDKKLQSNLKKLSVTNIPGIEEVNMIKDDG
TVIHFNNPKVQTSVPANTFSVTGSADNKQITEMLPGILNQLGPESLTHLKKLANNVTKLGPDGKGEDEDVP
ELVGDFDAASKNETKADEQ

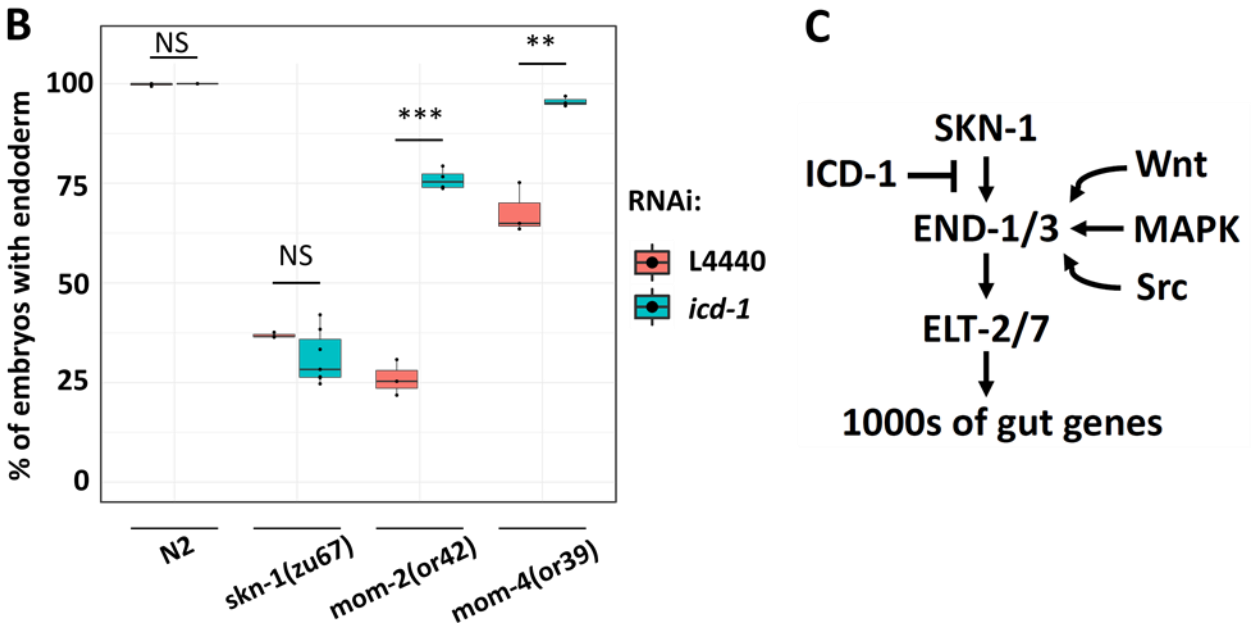

Figure 5.1: ICD-1 antagonizes SKN-1 input during endoderm specification.
(A) Amino acid sequence of ICD-1. The putative nuclear localization signal is highlighted in red. (B) The effects of *icd-1* RNAi on N2, *skn-1(zu67)*, *mom-2(or42)*, and *mom-4(or39)* absence-of-endoderm phenotype. At least three replicates were performed per experiment with >200 embryos scored per experiment. Student t-test: not significant (NS), $p > 0.05$, **$p \leqslant 0.01$, ***$p \leqslant 0.001$. (C) Hypothesized model of ICD-1 function in endoderm specification, positing that it antagonizes the SKN-1 input upstream of END-1/3.

Appendix II: Natural variation in the *plp-1/PURα* gene modifies SKN-1 requirement

Loss of maternal SKN-1 leads to a quantitatively reproducible bistable switch in fate. In N2, ~70% of *skn-1(-)* embryos make gut, while 70% of the arrested embryos undergo E→C transformation (Bowerman et al., 1992) (see Chapter 3 and Appendix I). We previously found that the requirements for SKN-1 in gut development varies dramatically across 97 genetically distinct isotypes (Torres Cleuren et al., 2019). In some isotypes, SKN-1 is absolutely required for endoderm development, in others, however, as many as 60% of embryos produce gut when *skn-1* is eliminated, suggesting that the early input into the GRN is highly plastic (Torres Cleuren et al., 2019). By applying genome-wide association study (GWAS), we identified a strongly significant peak associated with the variation in SKN-1 requirement on chromosome IV. Linkage mapping using N2 x MY16 recombinant inbred lines (RILs) similarly revealed a significant quantitative trait locus (QTL) in the same genomic region (Torres Cleuren et al., 2019). One of the genes in this QTL is *plp-1*, which encodes the *C. elegans* orthologue of Purα, a conserved nuclear DNA binding protein (Daniel and Johnson, 2018; Graebsch et al., 2009). It has previously been shown that PLP-1 functions downstream of the MAP kinase pathway and may induce *end-1* expression by binding to the Lef-1 site, overlapping with the regulatory site through which POP-1 activates *end-1* expression (Witze et al., 2009). In many wild isotypes, the *plp-1* gene contains a SNP (T>A at IV:7,634,038) that predicts to encode a valine-to-aspartate variant at residue 112 (V112D), adjacent to the PLP-1 DNA binding domain (Figure 5.2A and B). Note that all examined *Caenorhabditis* species, unlike N2, contain a

negatively charged residue in this position, suggesting its functional importance (Figure 5.3).

To investigate whether the polymorphism in PLP-1 may underlie the variation in SKN-1 requirement, we introduced the single nucleotide variant into N2 using CRISPR-Cas9 gene editing and found that V→D112 conversion in N2 indeed suppresses the requirement for SKN-1 (Figure 5.2C). Deleting *plp-1* leads to transgene desilencing and reduced RNAi response (Vishnupriya et al., 2020) (Table 5.1). While *par-1* RNAi results in a fully penetrant embryonic lethal phenotype in wildtype animals, we found that ~60% of *plp-1(-); par-1(RNAi)* embryos hatched as L1 (Table 5.1), consistent with a recent study (Vishnupriya et al., 2020). Crucially, 100% of PLP-1 V112D embryos undergo embryonic arrest when *par-1* is depleted by RNAi (Table 5.1), showing that PLP-1 V112D is competent for RNAi and its effect on suppressing *skn-1(RNAi)* phenotype reflects modification of endoderm specification pathway *per se*, rather than diminished RNAi efficacy.

We previously reported that loss of *plp-1* (by RNAi or chromosomal mutation) reciprocally suppresses loss-of-gut in *skn-1(-)* and enhances it in *mom-2(-)* embryos (Torres Cleuren et al., 2019). Here, we showed that PLP-1 V112D modestly but significantly synergizes with MOM-2 to induce endoderm formation (Figure 5.2D), suggesting that V112D is a hypomorphic/reduction-of-function allele. Given that PLP-1 may compete with POP-1 for the same regulatory binding site on *end-1* promotor (Witze et al., 2009) (Witze E., PhD dissertation, unpublished), we asked whether the ability of PLP-1 V112D to rescue *skn-1(RNAi)* phenotype requires the functions of POP-1. While *pop-1* RNAi causes excess gut as the MS cell misspecifies to produce

E, loss of both *skn-1* and *pop-1* leads to a severe loss of gut (Figure 5.2E) (Maduro et al., 2005a). Importantly, PLP V112D does not rescues the phenotype of *pop-1(-); skn-1(RNAi)* mutant (Figure 5.2E). Hence, we propose that in "WT" (N2-like) animals, PLP-1 occupies *end-1* promotor, dampening POP-1 gut-activating input; however, V112D variant may hinder DNA binding, allowing POP-1 to outcompete PLP-1 and activate *end-1* expression (Figure 5.2F). In sum, we have shown that the endoderm GRN is rapidly rewiring and PLP-1 is important node that can be modified to adjust GRN output. This study has provided key insights into the genetic basis of DSD in the endoderm GRN in *C. elegans*.

Materials and Methods

C. elegans Strains

N2 (wildtype reference strain); PHX3858, *plp-1(sys3858* [V112D]*) IV*; JR4451, *plp-1(sys3858* [V112D]*) IV* (5x backcross version of PHX3856), JR4465, *pop-1(zu189) dpy-5(e61)/ tmC20 [unc-14(tmIs1219) dpy-5(tm9715)] I; plp-1(sys3858* [V112D]*) IV*; JR4453, *pop-1(zu189) dpy-5(e61)/ tmC20 [unc-14(tmIs1219) dpy-5(tm9715)] I*; RB1711, *plp-1(ok2155)IV*; GR1373, *eri-1(mg366) IV*; JR4472, *eri-1(mg366) plp-1(sys3858* [V112D]*) IV*. The *tmC20* balancer was generated by the Mitani lab (Dejima et al., 2018).

RNAi and Quantification of Endoderm Specification

E. coli HT115 expressing dsRNA of the target gene was obtained from the Ahringer (Kamath and Ahringer, 2003) or the Vidal (Rual et al., 2004) RNAi library. RNAi experiments for quantifying embryonic endoderm specification were performed as described previously (Torres Cleuren et al., 2019) (see also Appendix I: ICD-1/BTF3

Antagonizes SKN-1-mediated Endoderm Specification in *C. elegans*). All experiments were performed at 20^{o}C.

Generation of *plp-1(syb3858* [V112D]*)* CRISPR allele

plp-1(syb3858 [V112D]*)* was generated by SunyBiotech. The following primers were used to amplify the region containing the mutation, which was detected using Sanger sequencing.

Forward primer: 5'-CTGGTGAACACGCTGTAAGTTGC-3'

Reversed primer: 5'-CGAGTGCGGACATTGGAACG-3'

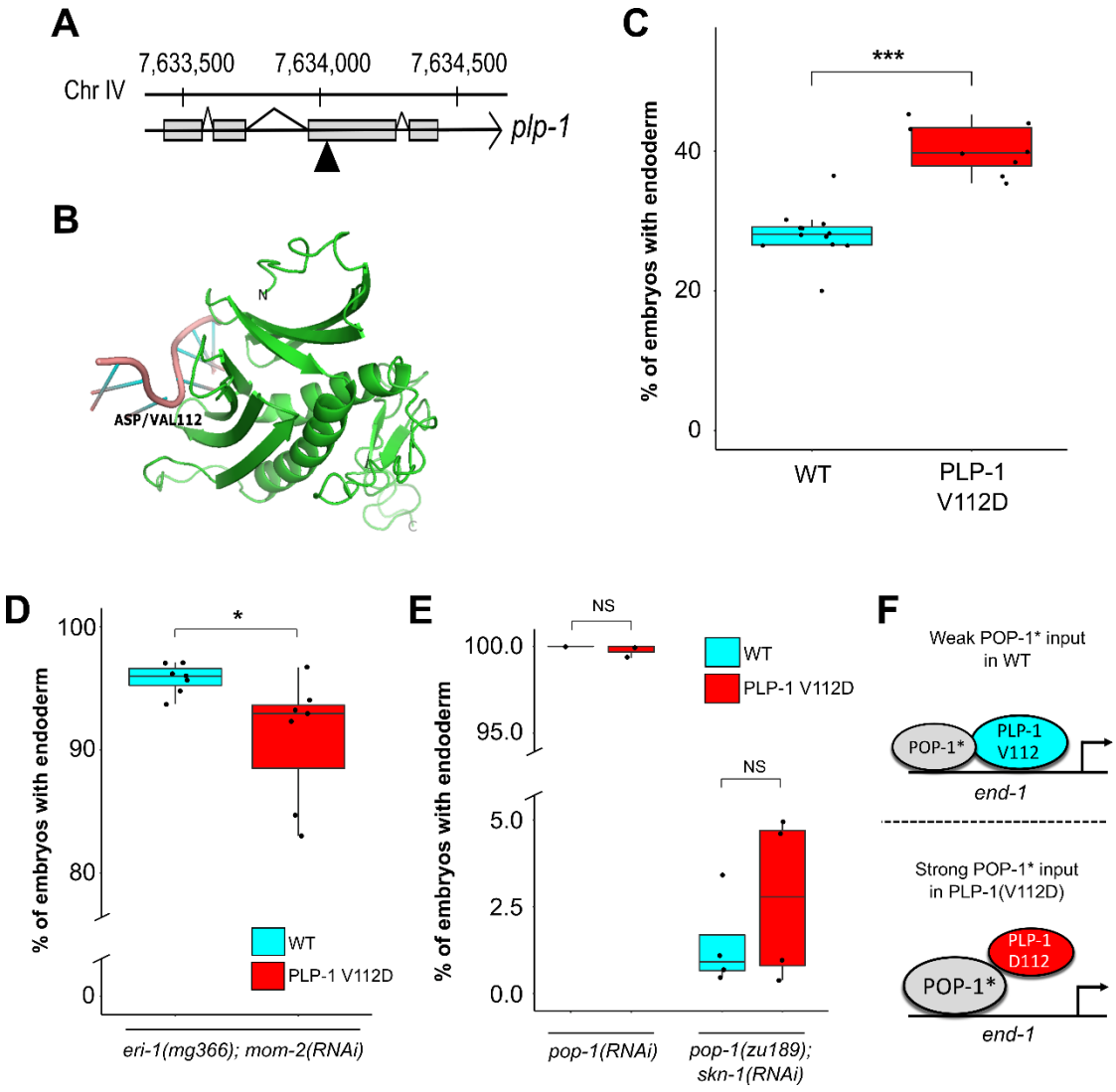

Figure 5.2: Variation in PLP-1 modulates SKN-1 requirement in endoderm development.

(A) *plp-1* contains a missense mutation (T>A at IV:7,634,038; indicated by the arrowhead) in many wild isotypes. (B) This SNP is predicted to encode a valine-to-aspartate variant at position 112 (V112D). The protein structure was predicted using the I-TASSER program (Zhang, 2008) (https://zhanggroup.org/I-TASSER/). (C) PLP-1(V112D) variant suppresses the gut-less phenotype of *skn-1(RNAi)* embryos in N2 genetic background. At least seven replicates were performed per experiment with >200 embryos scored per experiment. ***p $\leqslant$ 0.001 by two-sample t-test. (D) PLP-1(V112D) variant enhances *mom-2(RNAi)*-induced loss-of-endoderm phenotype. *eri-1(mg366)* was introduced to enhance RNAi efficacy. *p $\leqslant$ 0.05 by Wilcox test. (E) PLP-1(V112D) does not rescue the loss-of-gut phenotype of *skn-1(RNAi)* embryos in the absence of POP-1. NS p > 0.05 by two-sample t-test. (F) Hypothesized model of POP-1 and PLP-1 interactions to regulate *end-1* expression.

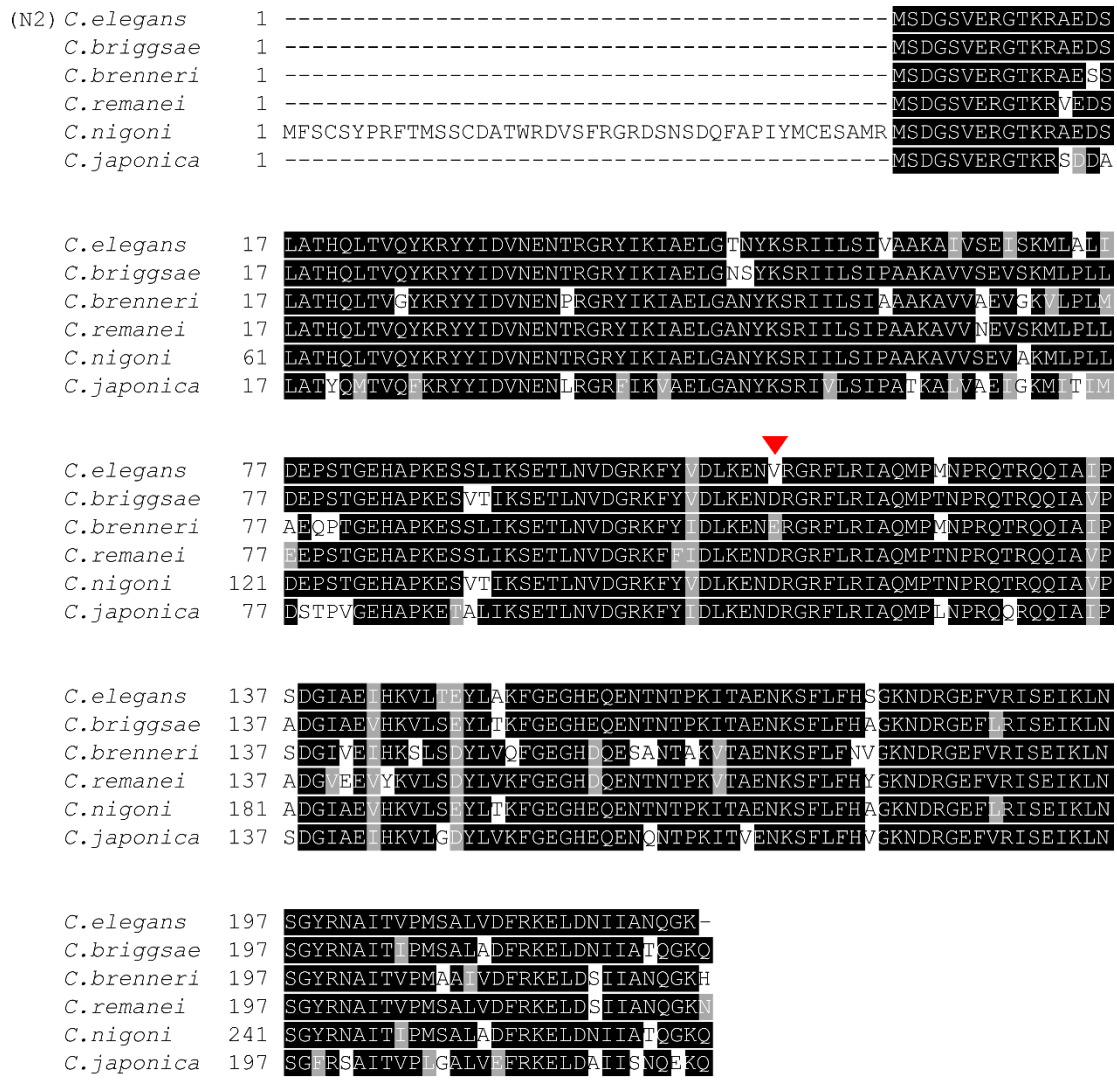

Figure 5.3: Sequence alignment of PLP-1 from different *Caenorhabditis* species. White text on a black background indicates identities among four or more proteins, while gray background denotes conservative substitutions. Red arrowhead highlights Valine 112 in *C. elegans* N2 strain. The alignment was performed using the program T-coffee (Notredame et al., 2000) (http://tcoffee.crg.cat/).

Table 5.1: *plp-1(sys3858* [V112D]*) is germline RNAi-competent.*

	% *par-1(RNAi)*-induced embryonic lethality	
	Non-diluted	2-fold diluted
WT	100 (332)	100 (304)
plp-1(sys3858)	100 (284)	100 (300)
plp-1(ok2155)	43 (100)	38 (137)

Appendix III: Quantitative trait loci for SKN-1 requirement on Chromosome V

Understanding genotype-to-phenotype relationships and accurately predicting disease risks and drug responses from genetic features represent the major goals in personalized medicine (Ho et al., 2019). The natural genetic variation in *C. elegans* wild isotype provides a powerful paradigm for quantitative genetics. GWAS have been instrumental in identifying QTLs underlying trait variation. However, multigenic complex traits are influenced by many SNPs of small effect sizes, which are often undetected by GWA mapping due to reduced statistical power (Andersen and Rockman, 2022; Widmayer et al., 2021). Alternatively, linkage mapping may be performed using RILs derived from wild isotypes with distinct phenotypes; however, the identification of causal variant(s) is limited by number of recombination events for a high-resolution map. Isolation of recombinant inbred advanced intercrossed lines (RIALs) that provide enhanced mapping resolution is an effective method for identifying causal variants (e.g., Andersen et al., 2015) but it is a labor-intensive approach and cannot be generalized to a variety of parental isotype pairs. To circumvent these challenges, Drs. Melissa R. Alcorn and Yamila N. Torres Cleuren (two former PhD students in Rothman lab) have developed a powerful machine learning (ML) approach based on Elastic Net regression to predict the genetic architecture of complex traits in natural population.

In this proof-of-concept study, we applied the Elastic Net algorithm from scikit-learn (Pedregosa et al., 2011) to facilitate the identification of the causal genetic loci modulating SKN-1 regulatory input during endoderm specification. This ML method identified all the cryptic genetic variants previously detected by GWAS and linkage

mapping (Torres Cleuren et al., 2019), as well as novel QTLs on chromosome V and X (Figure 5.4) (the details of computational methods are described in the PhD dissertation of Alcorn. M.R.). To validate the QTLs on chromosome V (16,887,320-17,011,168 bp and 18,907,824-19,042,487 bp) in vivo, we generated near-isogenic lines (NILs) that carry segments of chromosome V from N2 introgressed into JU440 and JU1172, which exhibit polymorphism at the most significant markers. We found that JU440 lines carrying the N2 chromosome V segment near 19.10 Mb (linked to *oxTi875*; see Materials and Methods) showed an enhanced *skn-1(RNAi)* phenotype (JU440: 55.0% ± sd 3.5% with gut *vs.* N2 > JU440 NILs: 37.5% ± sd 5.0%) (Figure 5.5A). Similarly, the introgressed N2 segment surrounding *oxTi875* (see Materials and Methods) enhances SKN-1 requirement in JU1172 (JU1172: 40.4% ± sd 3.5% with gut *vs.* N2 > JU1172 NILs: 26.1% ± sd 7.0%) (Figure 5.5B). Together, these results demonstrate the robustness and the sensitivity of the ML approach.

Next, we performed a small-scale RNAi screen to identify candidate genes in the chromosome V QTL that may modulate SKN-1 input. We targeted 15 genes with known genetic variation and found that knocking down *mrps-28*, which encodes the ortholog of human mitochondrial ribosomal protein S28, strongly suppresses the loss-of-gut phenotype of *skn-1(-)* embryos (Figure 5.6; Figure 5.7A). We further showed that the function of MRPS-28 appears to be restricted to the E lineage as knocking down *mrps-28* in *skn-1(-)* mutant rescues endoderm, but not mesoderm, development (Figure 5.7B). Importantly, depleting two other mitochondrial ribosomal proteins, MRPS-5 and MRPL-2, similarly rescues endoderm development in *skn-1(-)* (Figure 5.7C), suggesting that mitochondrial translation antagonizes gut induction. Our study

provides strong evidence for the novel role of mitochondrial translation in endodermal cell fate specification, perhaps by modulating Wnt input (Costa et al., 2019; Wen et al., 2019); however, it is currently unclear whether *mrps-28* is the causal quantitative trait gene that underlie variation in SKN-1 requirement in wild isotypes.

Materials and Methods

C. elegans Strains and Maintenance

The worm strains used in this study are listed in Table 5.2. The animals were cultured using standard procedure (Brenner, 1974) and all experiments were performed at 20^{o}C.

Introgression

oxTi401 [eft-3p::tdTomato::H2B::unc-54 3'UTR + Cbr-unc-119(+)] (chromosome V: 15,894,022 bp) and *oxTi875 [vha-6p::GFP::tbb-2 3'UTR + Cbr-unc-119(+)]* (chromosome V: 19,102,373 bp) were introduced from JR4315 (N2 background) into the different wild isolate genetic backgrounds through repeated outcrossing. We first crossed JR4315 males into a wild isotype hermaphrodite (so the resulting isogenic strains would contain wild isotype mitotype). We then selected an F2 line homozygous for the two fluorescent markers and crossed it with wild isotype males. This scheme was repeated to yield at least five outcrosses. During the last cross, we allowed the markers to segregate and created three isogenic lines for each genotype of interest.

RNAi and Quantification of Endoderm Specification

E. coli HT115 expressing dsRNA of the target gene was obtained from the Ahringer (Kamath and Ahringer, 2003) or the Vidal (Rual et al., 2004) RNAi library. RNAi experiments for quantifying embryonic endoderm specification were performed as

described previously (Torres Cleuren et al., 2019) (see also Appendix I: ICD-1/BTF3 Antagonizes SKN-1-mediated Endoderm Specification in *C. elegans*). Some RNAi experiments (Figure 5.7A and C) were performed blind with the assistance of Cricket Wood. All experiments were performed at 20^{o}C.

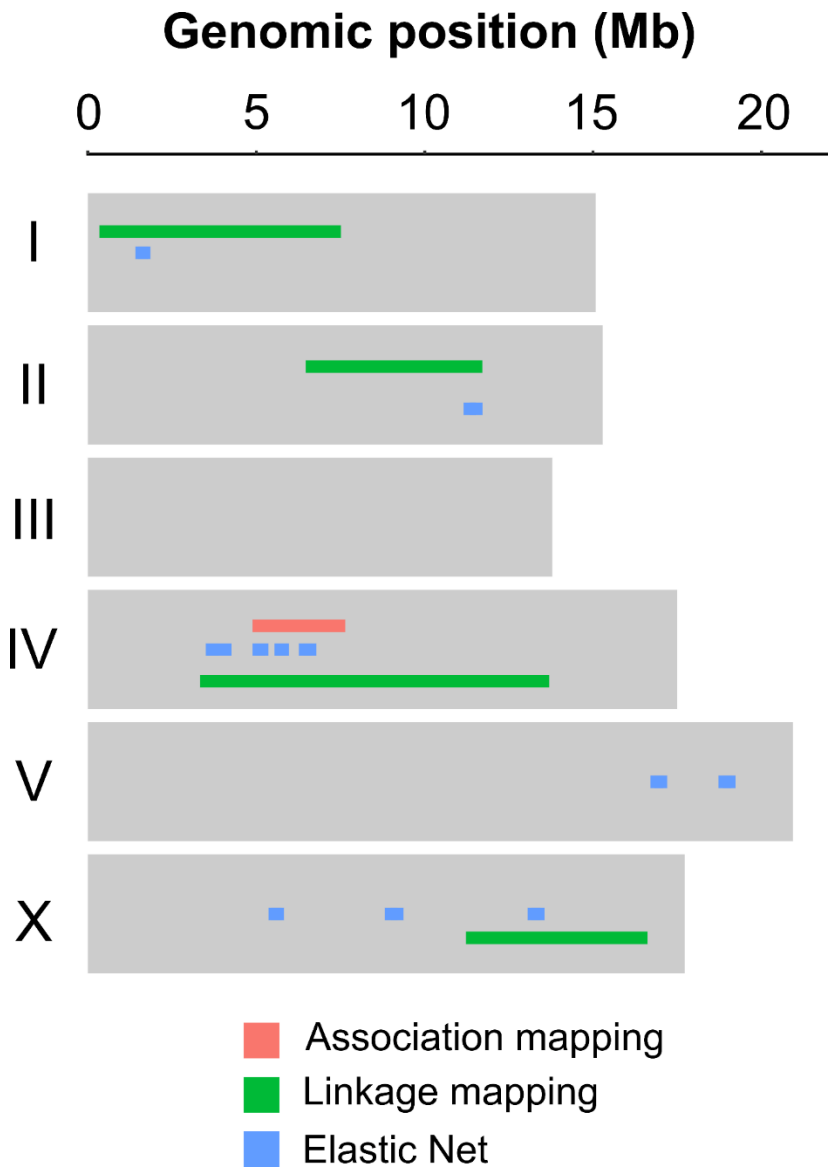

Figure 5.4: QTLs of SKN-1 requirement.
Association mapping (GWAS with EMMA) identified a significant peak on chromosome IV, while linkage mapping (multi-QTL model) using N2 x MY16 RILs identified QTLs on chromosome I, II, IV, and X (Torres Cleuren Y.N., PhD dissertation, unpublished) (Torres Cleuren et al., 2019). Elastic Net detected all known QTLs and four additional loci on chromosome IV and X that may underlie the variation in SKN-1 requirement (credit: Alcorn. M.R.).

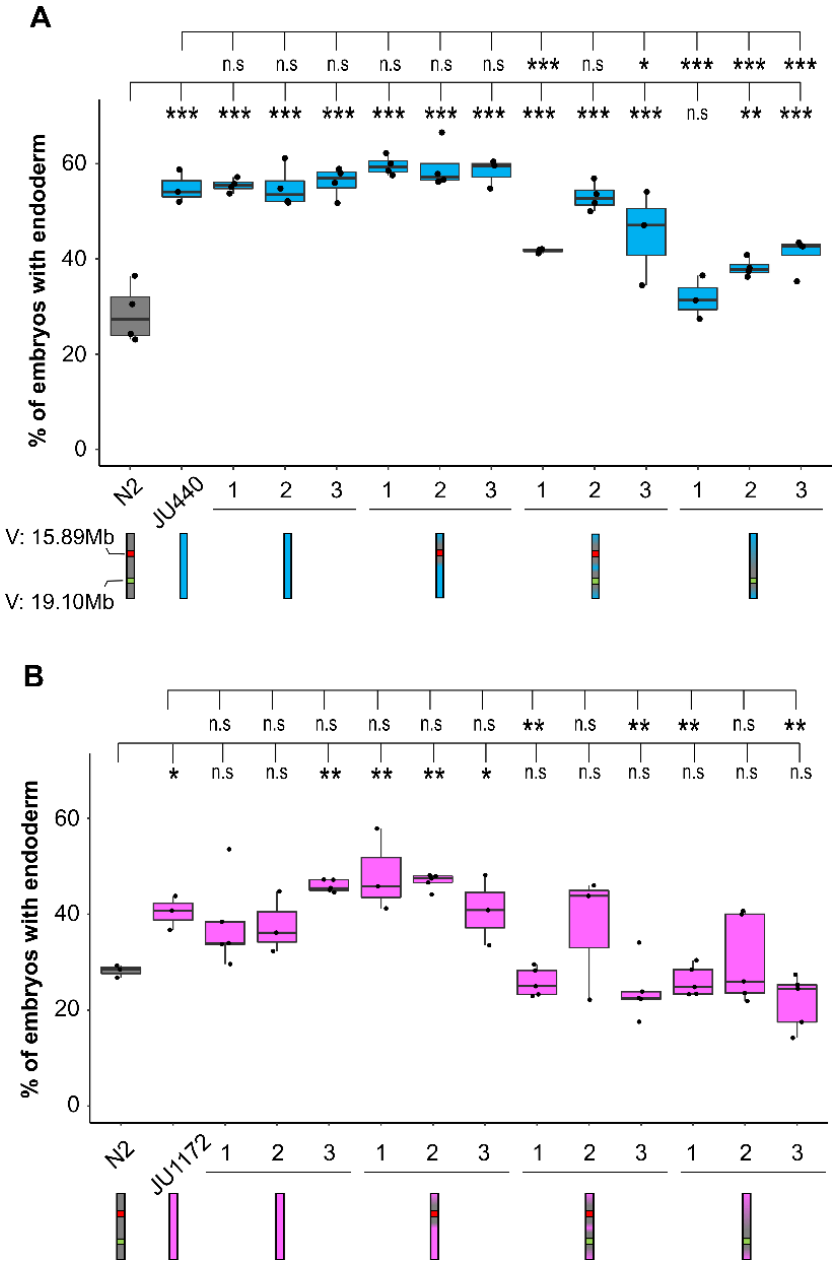

Figure 5.5: *skn-1(RNAi)* phenotypes of introgression lines on chromosome V. Near isogenic lines (NILs) of (A) N2 x JU440 and (B) N2 x JU1172. The N2 parental strain carries *oxTi401* (*eft-3p::tdTomato* at 15.89 Mb) and *oxTi875* (*vha-6p::GFP* at 19.10 Mb) that facilitate marker-directed selection of the genomic region(s) of interest during outcrossing (see Materials and Methods). In general, JU440 and JU1172 carrying N2 chromosome V segment linked to *oxTi875* showed an enhanced *skn-1(RNAi)*-induced loss-of-endoderm phenotype. NS $p > 0.05$, * $p \leqslant 0.05$, ** $p \leqslant 0.01$, *** $p \leqslant 0.001$ by parametric one-way ANOVA followed by pairwise t-tests with Benjamini & Hochberg correction.

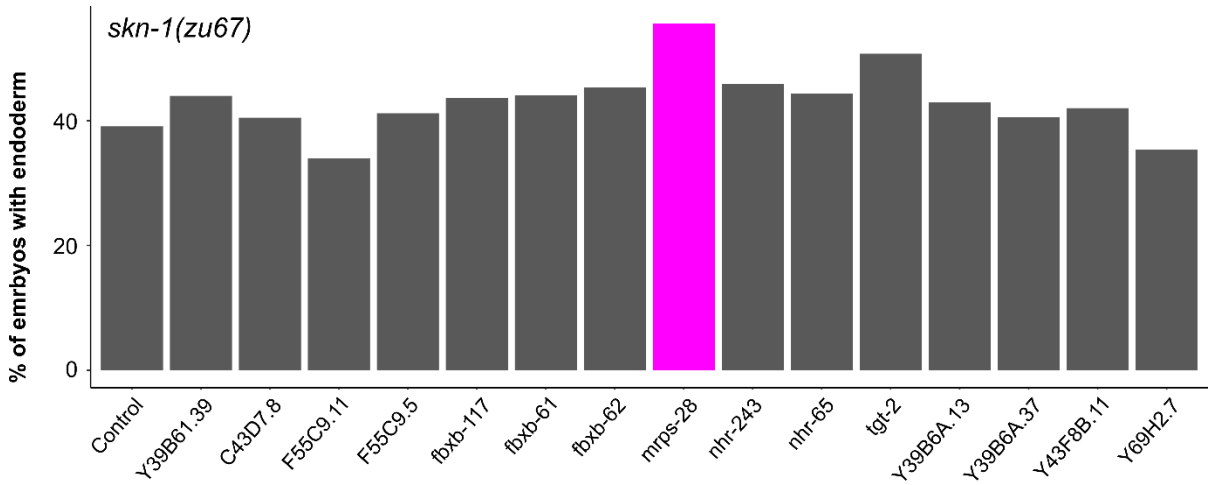

Figure 5.6 RNAi screen to identify candidate genes in QTL of chromosome V. Candidate genes with known genetic variation in the QTL region were knocked down in *skn-1(zu67)* mutant. Eliminating *mrps-28* (highlighted in magenta) significantly suppresses the loss of gut in *skn-1(zu67)* embryos. At least 200 embryos were scored for each candidate.

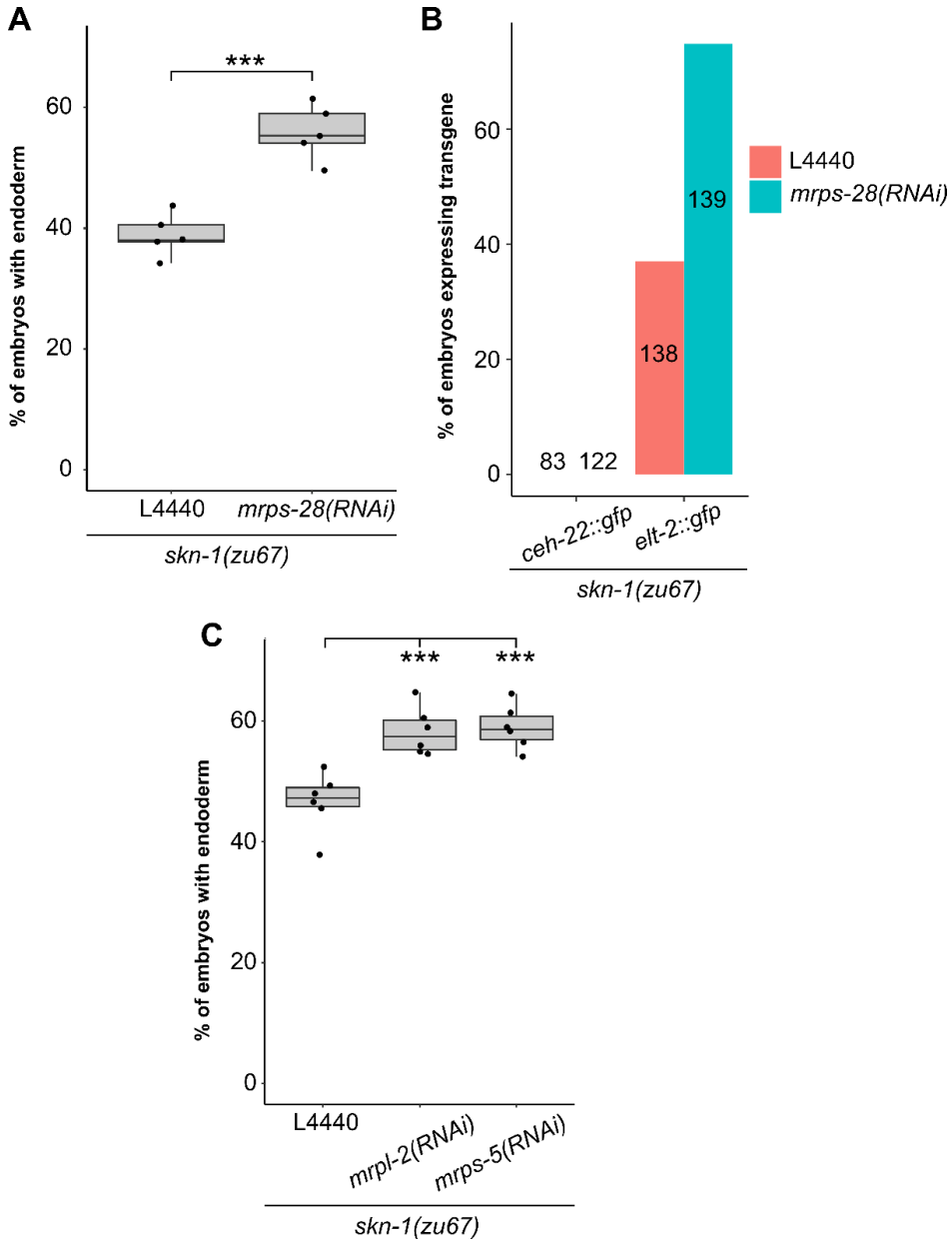

Figure 5.7: Reducing mitochondrial translation rescues gut-less phenotype of *skn-1(-).*

(A) Knocking down *mrps-28* suppresses the absence of endoderm in *skn-1(-)*. *** p ⩽ 0.001 by two-sample t-test. (B) Loss of *mrps-28* rescues endoderm, but not mesoderm, development. *cuIs1[ceh-22::GFP]* and *wIs84[elt-2::NLS::GFP]* were used as the reporters for mesoderm and endoderm differentiation, respectively. The number of embryos examined for each experiment is indicated. (C) Knocking down *mrpl-2* or *mrps-5* rescues *skn-1(-)* phenotype. *** p ⩽ 0.001 by parametric one-way ANOVA followed by pairwise t-tests with Benjamini & Hochberg correction.

Table 5.2: Worm strains used in this study.

Strain	Genotype	Source
N2	Lab reference strain	CGC
JU1172	Wild isotype	CGC
JU440	Wild isotype	CGC
JR4315	*unc-119(ed3) III; oxTi401 [eft-3p::tdTomato::H2B::unc-54 3'UTR + Cbr-unc-119(+)] oxTi875 [vha-6p::GFP::tbb-2 3'UTR + Cbr-unc-119(+)] V*	This study
JR4393	N2>JU1172 control line 1	This study
JR4394	N2>JU1172 control line 2	This study
JR4395	N2>JU1172 control line 3	This study
JR4396	*wIR3 [V:~15,849,022, N2>JU1172] V. Line 1*	This study
JR4397	*wIR3 [V:~15,849,022, N2>JU1172] V*. Line 2	This study
JR4398	*wIR3 [V:~15,849,022, N2>JU1172] V*. Line 3	This study
JR4399	*wIR3 [V:~15.849.022, N2>JU1172] wIR4 [V:~19,102,373, N2>JU1172] V.* Line 1	This study
JR4400	*wIR3 [V:~15.849.022, N2>JU1172] wIR4 [V:~19,102,373, N2>JU1172] V.* Line 2	This study
JR4401	*wIR3 [V:~15.849.022, N2>JU1172] wIR4 [V:~19,102,373, N2>JU1172] V.* Line 3	This study
JR4402	*wIR4 [V:~19,102,373, N2>JU1172] V.* Line 1	This study
JR4403	*wIR4 [V:~19,102,373, N2>JU1172] V.* Line 2	This study
JR4404	*wIR4 [V:~19,102,373, N2>JU1172] V.* Line 3	This study
JR4372	N2>JU440 control line 1	This study
JR4373	N2>JU440 control line 2	This study
JR4374	N2>JU440 control line 3	This study
JR4375	*wIR1 [V:~15.849.022, N2>JU440] V.* Line 1	This study
JR4376	*wIR1 [V:~15.849.022, N2>JU440] V.* Line 2	This study
JR4377	*wIR1 [V:~15.849.022, N2>JU440] V.* Line 3	This study
JR4378	*wIR1 [V:~15.849.022, N2>JU440] wIR2 [V:~19,102,373, N2>JU440] V*. Line 1	This study
JR4379	*wIR1 [V:~15.849.022, N2>JU440] wIR2 [V:~19,102,373, N2>JU440] V*. Line 2	This study
JR4380	*wIR1 [V:~15.849.022, N2>JU440] wIR2 [V:~19,102,373, N2>JU440] V*. Line 3	This study
JR4381	*wIR2 [V:~19,102,373, N2>JU440] V*. Line 1	This study
JR4382	*wIR2 [V:~19,102,373, N2>JU440] V*. Line 2	This study
JR4383	*wIR2 [V:~19,102,373, N2>JU440] V*. Line 3	This study
JR3936	*dpy-13(e184) skn-1(zu67) IV/ nT1[qIs51] (IV:V)*	(Ewe et al., 2019)
ENH400	*skn-1(zu67)/nT1[unc-?(n754);let-?] (IV:V); wIs84[elt-2::GFP]*	(Dresen et al., 2015)
ENH281	*skn-1(zu67)/nT1[qIs51] (IV:V); cuIs1[ceh-22::GFP]*	(Dresen et al., 2015)

Appendix IV: Natural Variation in the Requirement for LIT-1/Nemo in Endoderm Development

We previously found extensive plasticity in *C. elegans* endoderm GRN as evident by widespread variation in SKN-1 and MOM-2 requirement in gut development (Appendix II and III) (Torres Cleuren et al., 2019). Although MOM-2/Wnt signal is mediated through POP-1 (Figure 1.1), we did not observe quantitative variation in POP-1 requirement in the wild isotypes: like N2, 100% of the *pop-1(RNAi)* arrested embryos develop a gut across all examined strains (Torres Cleuren et al., 2019). In the absence of POP-1, MS is misspecified to produce E, giving rise to excess gut (Lin et al., 1995, 1998). The endoderm-repressive role of POP-1 in MS may therefore mask its activating function in E (Maduro et al., 2005a). As we have scored only for presence or absence of birefringent gut granules, it is conceivable that the E lineage is not properly specified in some strains, a possibility that cannot be ruled out without higher resolution lineage analysis.

During endoderm development, Wnt ligand MOM-2 binds to Frizzled receptor MOM-5 at EMS posterior cell cortex, leading to asymmetrical retention of WRM-1/β-catenin (Kaletta et al., 1997), which binds to and activates LIT-1. LIT-1/WRM-1 complex in turn phosphorylates POP-1, modifying its nucleocytoplasmic distribution (high nuclear level in anterior MS and low nuclear level in posterior E) (Yang et al., 2015). Consequently, LIT-1 is fully essential for gut induction. LIT-1/WRM-1/POP-1 function is not limited to endoderm: remarkably, they are pivotal regulators acting in a reiterative system that promotes asymmetric cell divisions throughout most of *C. elegans* development (Kaletta et al., 1997; Lin et al., 1998). In N2, all embryos lacking

LIT-1 fail to establish asymmetry of cell fate and show extensive posterior-to-anterior transformation (Kaletta et al., 1997). Given its important role in embryonic development, we were startled to discover extensive variation in LIT-1 requirement in endoderm development among 74 genetically distinct wild isotypes: while knocking down *lit-1* in some isotypes causes loss of intestine in 100% of embryos (like N2), in other strain, as few as 14.6% of embryos lack gut (Figure 5.8).

A major potential pitfall is that the variation in the phenotype might result from the variation in RNAi efficacy rather than in the GRN. To address this caveat, we introgressed the heat-sensitive *lit-1(or131)* chromosomal mutation into MY16, JU256, and JU847, whose phenotypes spanned the spectrum observed (Table 5.3). In all cases, however, we found that introgression of the allele through five rounds of backcrosses failed to recapitulate the RNAi effects and resulted in a fully penetrant loss-of-gut phenotype, similar to N2. While on its face these results might suggest the variation in LIT-1 requirement is the results of variable RNAi efficacy, we cannot rule out the possibility that the quantitative trait gene is tightly linked to *lit-1(or131)*, and as the result, N2 chromosomal segment containing the modifier(s) might be carried with the *lit-1* mutation through the introgression crosses. Additionally, repeated selection of lines showing 100% embryonic lethality at non-permissive temperature during backcrossing (see Materials and Methods) may have unwittingly imposed a strong selection for unwanted genetic background in the “near isogenic lines” and further complicate interpretation of the results.

To investigate the genetic basis of *lit-1(RNAi)* variation, we performed NemaScan, an open-source pipeline for GWAS in *C. elegans* (Widmayer et al., 2021)

(https://www.elegansvariation.org/); however, we did not find any significant QTL associated with the phenotype. These results suggest that *lit-1(RNAi)* variation may have a complex genetic architecture that is driven by many SNPs of small effect sizes and therefore reduced statistical power of GWAS. Future studies using increased sample size will improve the detection power of GWAS for this complex trait (Widmayer et al., 2021). Alternatively, linkage mapping using RILs generated from isotypes with distinct *lit-1(-)* phenotypes (e.g., N2 x AB1 (Duveau and Félix, 2012)) will greatly facilitate the identification of the causal quantitative trait gene(s).

Our preliminary findings of widespread variation in LIT-1 requirement suggest other kinases may adopt its function in symmetry breaking in some isotypes. One such attractive candidate is PIG-1/MELK which has been shown to function downstream of the Src signaling to orient the asymmetric cell division of EMS blastomere and promote endoderm specification (Liro et al., 2018). It will be interesting to investigate LIT-1 and PIG-1 requirement in other reiterative asymmetric cell divisions (e.g., in the ectodermal AB lineage), as well as POP-1 behavior in strains with relaxed LIT-1 requirement.

Materials and Methods

C. elegans Strains

EU603, *lit-1(or131) III; him-8(e1489) IV* (N2 background); JR4078, *MY16; lit-1(or131) III*; JR4084, *JU258; lit-1(or131)*; JR4085, *JU847; lit-1(or131) III*. See Table 5.3 for wild isotypes used in this study.

RNAi and Quantification of Endoderm Specification

E. coli HT115 expressing *lit-1* dsRNA was obtained from the Ahringer RNAi library (Kamath and Ahringer, 2003). RNAi experiments for embryonic endoderm specification were performed as described (Torres Cleuren et al., 2019) (see also Appendix I: ICD-1/BTF3 Antagonizes SKN-1-mediated Endoderm Specification in *C. elegans*). Note that the efficiency of *lit-1* RNAi is temperature-dependent. At 20^{o}C, *lit-1* RNAi causes a partial penetrant embryonic lethality and gut-less phenotype (40.7% ± sd. 5.7% with gut; n = 1208), whereas at 25^{o}C, all *lit-1(RNAi)* embryos fail to hatch and lack gut (0.5% ± sd. 0.4% with gut; n = 1611), resembling the phenotype of *lit-1(-)* genetic mutant. Hence, all experiments reported in this study were performed at 25^{o}C.

Introgression

To introgress *lit-1(or131)* into the different wild isotype genetic backgrounds, we crossed EU603 males into a wild isotype hermaphrodite at permissive temperature 15^{o}C. We then selected an F2 line that showed 100% lethality at non-permissive temperatures 25^{o}C (homozygous for *or131*) and crossed the mutant hermaphrodites with wild isotype males. This scheme was repeated to yield at least five outcrosses.

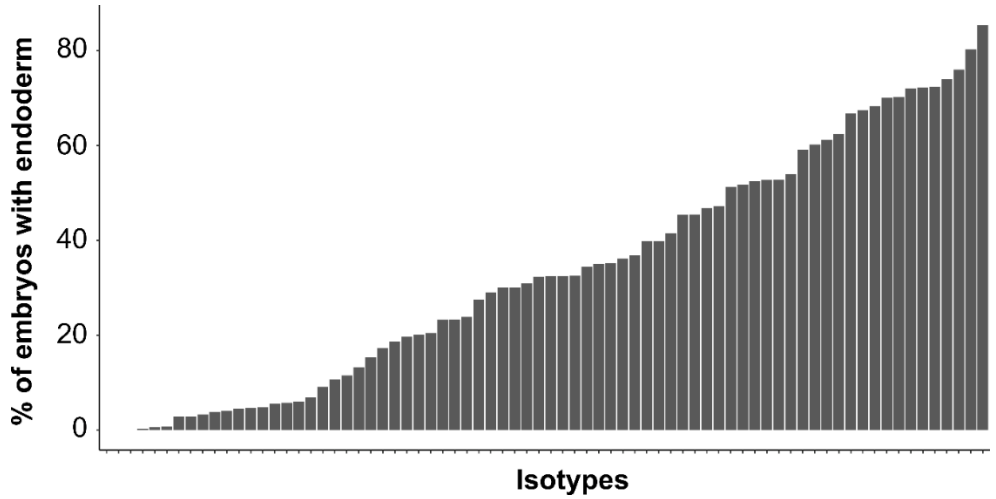

Figure 5.8: Widespread natural variation in *lit-1(RNAi)* phenotype
The mean % of *lit-1(RNAi)* embryos with endoderm in 74 wild isotypes (see Table 5.3).

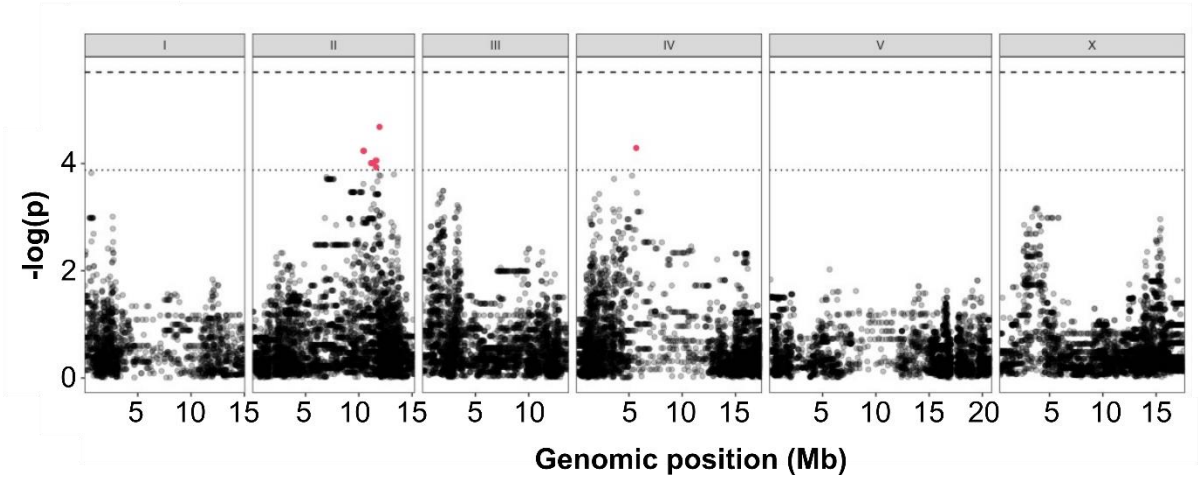

Figure 5.9: Manhattan plot from GWAS for the variation in *lit-1(RNAi)* phenotype
The genomic position in Mb, separated by chromosome, is plotted on the x-axis and the -log(p) for each SNP is plotted on the y-axis. Genome-wide Bonferroni-corrected significance threshold is denoted by the dashed black horizontal line. SNPs are colored pink if they pass the genome-wide Eigen-decomposition significance threshold, which is denoted by the dotted gray horizontal line. No significant QTL is detected.

Table 5.3: The mean % of embryos develop endoderm upon *lit-1* depletion in 74 isotypes.

Strain	Mean % of embryos with endoderm
LSJ1	0
JU1213	0
MY18	0
EG4347	0.27027
MY14	0.595238
MY16	0.684932
CB4852	2.854812
JU1172	2.857143
JU1896	3.202847
ED3012	3.773585
ED3077	4.039921
JU345	4.470121
CX11271	4.573805
AB4	4.797048
JU1568	5.494505
ED3017	5.728593
JU1200	5.986235
JU1652	6.818182
JU440	9.05704
PX179	10.60137
JU1395	11.46497
JU1088	13.166
JU1581	15.32847
CX11307	17.30104
JU367	18.59296
JU1530	19.67213
ED3073	20.05622
JU1586	20.45455
JU792	23.21068
PX174	23.24723
CX11314	23.80952
PB303	27.47281
CB4857	29.00552
CX11285	30.03195
MY10	30.04515
JU1440	30.88685
JU1580	32.27273
JU774	32.48408
JU775	32.5

JU642	32.52776
ED3046	34.39106
JU394	35.04873
ED3005	35.20408
JU310	36.13079
JU1491	36.84
MY1	39.83402
JU406	39.85954
AB1	41.45516
EG4349	45.34895
JU782	45.44427
JU1212	46.8
ED3048	47.23127
ED3011	51.29189
JU778	51.6776
JU1246	52.42863
EG4725	52.70044
CX11264	52.73076
JU258	54.00429
ED3049	59.06053
JU397	60.19841
CX11315	61.17454
EG4724	62.43655
JU1409	66.75258
JU323	67.43085
ED3040	68.32113
JU346	70.10462
JU830	70.24355
ED3052	72.00709
JU561	72.23729
JU360	72.37961
JU847	73.96216
KR314	76
EG4946	80.23952
JU393	85.36074

Appendix V: ELT-7 and END-1 Synergistically Repress Endodermal Cell Fate Cell Non-autonomously

In the course of studying the architecture of the endoderm GRN, we discovered an unexpected role of END-1 and ELT-7 in repressing endoderm cell fate in an unidentified cell in the head region. In wildtype animals, birefringent gut granules and *ifb-2::CFP* (*kcIs6* transgene), a multi-copy reporter for a gut-specific intermediate filament protein, were never found outside of the intestine. On the other hand, roughly 6% of *elt-7 end-1* double mutants showed ectopic expression of the two gut markers just anterior to the terminal bulb of the pharynx (Figure 5.10A). We confirmed this finding with an *elt-2* reporter expressed from its endogenous locus (Figure 5.10B), ruling out potential artifacts that may be caused by the modified genetic background in the animals carrying the *kcIs6* transgenic array. END-1 and ELT-7 do not express outside of the E lineage at any developmental stage (Sommermann et al., 2010; Zhu et al., 1997); hence, it appears that the two GATA factors function synergistically to repress endodermal cell fate cell non-autonomously, likely in an excretory or a glial cell based on the position of the ectopic gut cell. Future studies on this potential misspecification or transdifferentiation event will unveil the novel cell non-autonomous mechanism of cell fate control by the GATA factors and provide important insights into the molecular basis of developmental reprogramming.

Materials and Methods

C. elegans Strains and Maintenance

JR3596, *him-5(e1490) V; kcIs6[ifb-2p::IFB-2::CFP]*; JR4446, *elt-7(tm840) end-1(ox134)/ elt-7(tm840) tmC12[egl-9(tmIs1197)] V; kcIs6[ifb-2p::IFB-2::CFP]*; JR4263,

elt-7(tm840) end-1(ox134)/ elt-7(tm840) tmC12[egl-9(tmIs1197)] V; elt-2(dev99([mNeonGreen::elt-2]) X. All genetic crosses and experiments were performed at room temperature (20^{o}C-23^{o}C).

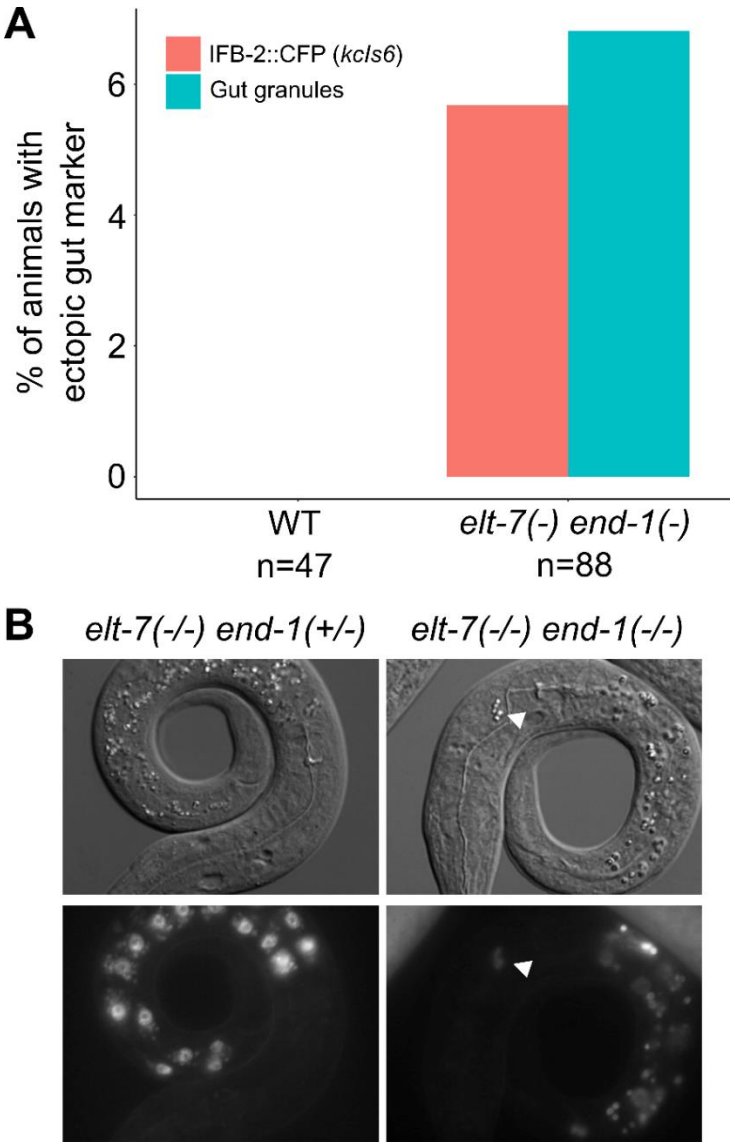

Figure 5.10: Ectopic gut-like cells in the head of *elt-7(-) end-1(-)* double mutants (A) The frequency of animals showing mis-expression of *ifb::CFP* (*kcIs6* transgene) or gut granule-like material in the head region. Number of animals scored for each genotype is indicated. (B) Representative DIC and fluorescent micrographs of animals expressing an endogenously tagged *elt-2* reporter. Roughly 6% of *elt-7(-) end-1(-)* double mutants contain ectopic gut-like cells (arrowhead).

Appendix X: The Genetic Basis of a Novel Migratory Behavior in Nematodes

When encounter unfavorable environmental conditions, such as heat, starvation and high population density, *C. elegans* larvae undergo developmental arrest and form stress-resistant, long-lived dauers. In the wild, *C. elegans* undergoes a boom-and-bust lifecycle, and the dispersal dauer stage is important for shaping the population dynamics (Félix and Duveau, 2012; Frézal and Félix, 2015). Dauer larvae exhibit a unique behavior called nictation where they lift and wave their bodies in the air, presumably to hickhike passing invertebrate species to find new food source and habitat (Lee et al., 2011).

While it is well-known that *C. elegans* undergoes phoretic dispersal by associating with mobile hosts, in this study, we found that dauers could migrate over long distance on a dry surface independent of a carrier animal. This behavior is subject to variation: while wild isotype CB4856 migrates very actively, the lab reference strain N2 is incapable of doing so (Figure 5.11A and B). We note that this migratory behavior is sensitive to various environmental variables, including humidity and atmospheric pressure. Therefore, unless stated otherwise, all experiments reported here were performed at ~100% humidity in an enclosed chamber at elevated pressure of 105kPa (Figure 5.11A) (see Migration Assay). However, despite our best effort to control for the environment variation, the number of worms migrated was highly variable across experiments, especially during rainy days and Winter due to unknown reasons.

To investigate the genetic basis of migratory behavior, we phenotyped 55 N2 x CB4856 RIAILs (Andersen et al., 2015) and found that 40% (22/55) of the RIAILs were migrators. Linkage mapping subsequently revealed a significant QTL (spanning

5,033,476 - 8,751,562 bp) on chromosome X that explains 26.6% of the phenotypic variation among the RIAILs (Figure 5.11C and D). N2 is known to have accumulated random mutations in the laboratory before cytogenic preservation in 1969 – roughly 18 years after its isolation in Bristol (Sterken et al., 2015). One such laboratory-derived allele occurs in *nrp-1*, a gene encoding for a neuropeptide receptor, located on chromosome X. This variation in *npr-1* causes N2 to exhibit many distinct behaviors, such as lower crawling speed and stronger CO_2 avoidance, compared to wild isotypes (Sterken et al., 2015). While it is conceivable that the inability of N2 to migrate is the result of lab domestication, the following argue strongly against this: 1) LSJ1, a sister strain of N2 that contains wildtype NPR-1 (McGrath et al., 2009), like N2, is a non-migrator. 2) NIL (CX11400) that contains N2 version of *nrp-1* introgressed into CB4856 can actively migrate. 3) All the RIAILs used in this study have the wildtype allele of *npr-1* and, therefore, the QTL we detected must be outside of this gene. 4) Finally, we observed natural variation of the migratory behavior among 17 divergent *C. elegans* wild isotypes (Figure 5.12A). By examining weather and climate information at the isolation location of the wild isotypes (Evans et al., 2017), we found that migrators tend to be isolated at lower relative humidity compared to non-migrators (Figure 5.12B), suggesting that the variation in migratory behavior is the result of niche specification.

In summary, our study has uncovered natural variation in a novel migratory behavior in *C. elegans* wild isotypes. We believe this active locomotion allows the larvae to disperse in the absence of carrier animals and may shape the boom-and-bust population dynamics in the animals' wild habitats. Perhaps unsurprisingly, we

found that migratory behavior is highly sensitive to environmental variation, suggesting that dauers integrate multiple sensory cues to generate dispersal decision important for survival. Future study will focus on narrowing the mapped interval on chromosome X using NILs and identifying a genetic variant that regulates migratory behavior and mediates environmental adaptations.

Materials and Methods

Worm Culture

All worm strains were maintained at room temperature (20-23^{o}C) using standard procedure (Brenner, 1974). The worm plates were parafilmed to avoid cross-contamination. See Table 5.4 for the complete list of strains used in this study.

Migration Assay

The animals were grown on thick seeded NGM plates supplied with uracil to obtain a large population. The worms were then treated with alkaline hypochlorite solution (5% sodium hypochlorite + KOH) and the embryos were plated densely on a fresh thick NGM plate (100mm) where they hatched and developed. Once the worm plate was freshly starved (~4-5 days post-bleaching), it was placed at the center of a large plastic plate (150mm), which was then moved to a pressure chamber that was modified from an air pressure paint tank by Dr. David Bothman, Mechanical Engineering, UCSB (Figure 5.11A). The starved worms were incubated at 105kPa at saturation humidity for 4 days and the number of dauers migrated out of the NGM plate onto the plastic surface was quantified. CB4856 and N2 were used as positive and negative controls, respectively, in all experiments. A worm strain that contained >100 dauers outside of the NGM plate in at least two trials was considered a migrator.

QTL Analysis

A total of 55 RIALs (Andersen et al., 2015) (gift from E. Andersen, Northwestern University) were phenotyped (migrator = 1, non-migrator = 0). Single QTL analysis was performed with R/qtl (Broman et al., 2003). The mapping was performed using the function `scanone` coupled with the argument model = “binary”. Genome-wide significance thresholds were calculated by permuting the phenotype data and mapping 1,000 times. 95% Bayes credible interval of the QTL was calculated using the function `bayesint`.

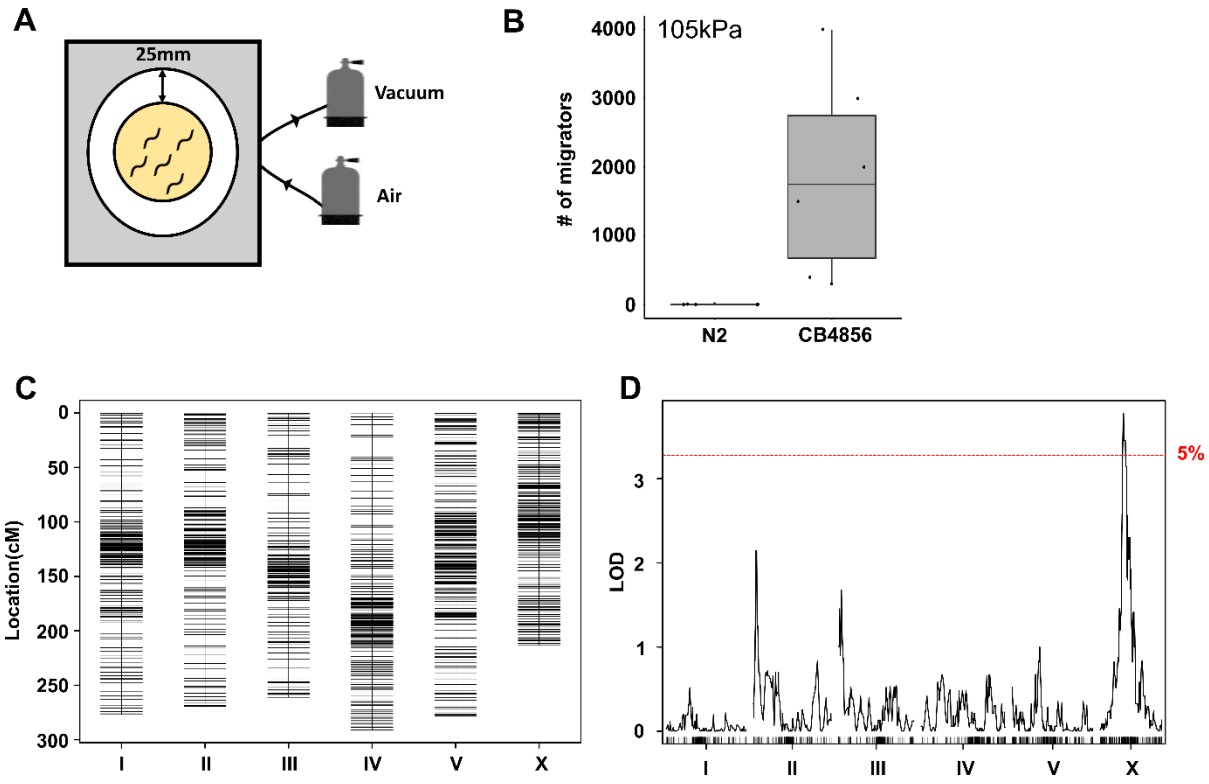

Figure 5.11: Migratory behavior of N2 *vs*. CB4956 and QTL analysis of N2 x CB4856 RIALs.

(A) The experimental scheme of the migration assay (see Materials and Methods). (B) Difference in migratory behavior between lab strain N2 and wild isotype CB4856. The experiments were performed at 105kPa at 100% humidity. (C) Genetic map of 55 RIALs with a total of 1454 markers. (D) Linkage mapping of migratory behavior detects a single QTL on chromosome X spanning 3.5 Mb. Genomic position is indicated on the x-axis and logarithm of odds (LOD) score is on the y-axis. The dotted red line indicates the LOD threshold for 5% false discovery rate (FDR) obtained by 1000X permutation. This QTL explains 26.6% of the phenotypic variation.

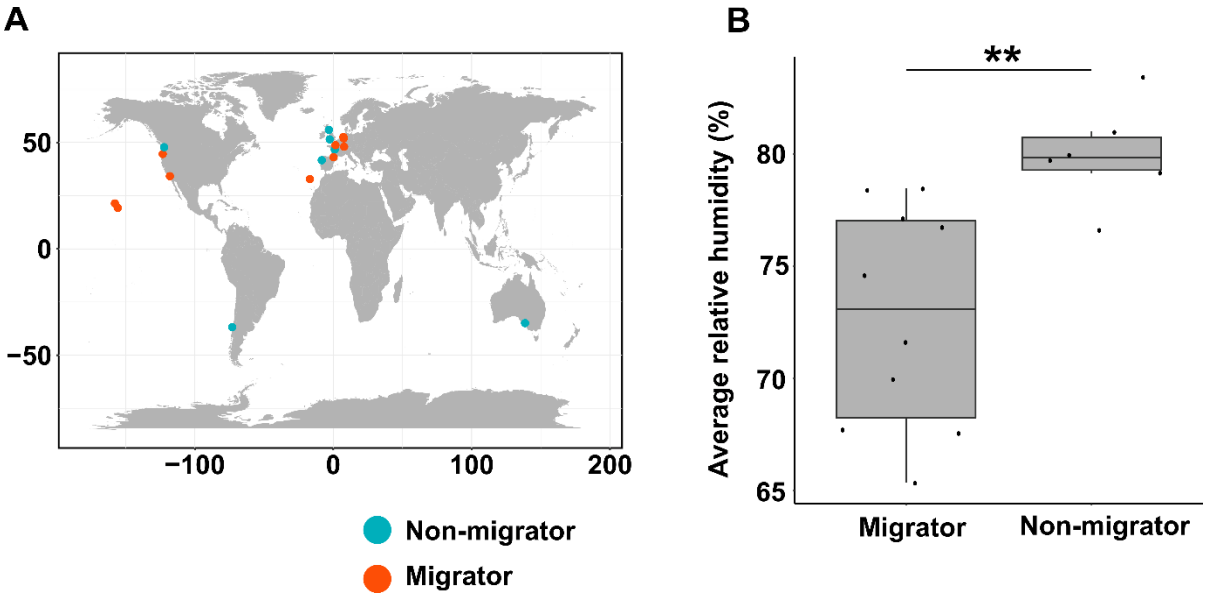

Figure 5.12: Natural variation in niche-associated migratory behavior.
(A) Variation in migratory behavior in a panel of 17 genetically distinct wild isotypes. (B) Boxplots show the three-year average of relative humidity at the location of strain isolation. Each point represents one strain. Migrators tend to be isolated from places with lower relative humidity compared to non-migrators. ** $p \leqslant 0.01$ by two-sample t-test.

Table 5.4: Worm strains used in this study.

Strain	Genotype
N2	Lab reference strain
CB4856	Wild isotype
QX424-427, 434, 441, 442, 444, 450-452, 457, 460, 646, 467, 471-476, 478, 479, 481, 500-511, 514-523, 525-528, 531, 550, 568, 571, 572, 576, 577	QX1430/N2 x CB4856 RIALs
CX11400	*kyIR9 (X, N2>CB4856, ~4745910 - ~4927296) X*
CX11314	Wild isotype
DL226	Wild isotype
DL238	Wild isotype
ED3017	Wild isotype
EG4725	Wild isotype
JT11398	Wild isotype
JU1172	Wild isotype
JU1491	Wild isotype
JU258	Wild isotype
JU440	Wild isotype
JU792	Wild isotype
MY1	Wild isotype
MY16	Wild isotype
RC301	Wild isotype
LSJ1	Wild isotype
AB1	Wild isotype

References

Ajibade, A.A., Wang, H.Y., and Wang, R.F. (2013). Cell type-specific function of TAK1 in innate immune signaling. Trends Immunol. *34*, 307–316.

Alcazar, R.M., Lin, R., and Fire, A.Z. (2008). Transmission dynamics of heritable silencing induced by double-stranded RNA in Caenorhabditis elegans. Genetics *180*, 1275–1288.

Amrit, F.R.G., Steenkiste, E.M., Ratnappan, R., Chen, S.-W., McClendon, T.B., Kostka, D., Yanowitz, J., Olsen, C.P., and Ghazi, A. (2016). DAF-16 and TCER-1 Facilitate Adaptation to Germline Loss by Restoring Lipid Homeostasis and Repressing Reproductive Physiology in C. elegans. PLOS Genet. *12*, e1005788.

An, J.H., and Blackwell, T.K. (2003). SKN-1 links C. elegans mesendodermal specification to a conserved oxidative stress response. Genes Dev. *17*, 1882–1893.

An, J.H., Vranas, K., Lucke, M., Inoue, H., Hisamoto, N., Matsumoto, K., and Blackwell, T.K. (2005). Regulation of the Caenorhabditis elegans oxidative stress defense protein SKN-1 by glycogen synthase kinase-3. Proc. Natl. Acad. Sci. U. S. A. *102*, 16275–16280.

Andersen, E.C., and Horvitz, H.R. (2007). Two C. elegans histone methyltransferases repress lin-3 EGF transcription to inhibit vulval development. Development *134*, 2991–2999.

Andersen, E.C., and Rockman, M. V (2022). Natural genetic variation as a tool for discovery in Caenorhabditis nematodes. Genetics *220*.

Andersen, E.C., Gerke, J.P., Shapiro, J.A., Crissman, J.R., Ghosh, R., Bloom, J.S., Félix, M.-A., and Kruglyak, L. (2012). Chromosome-scale selective sweeps shape Caenorhabditis elegans genomic diversity. Nat. Genet. *44*, 285–290.

Andersen, E.C., Shimko, T.C., Crissman, J.R., Ghosh, R., Bloom, J.S., Seidel, H.S., Gerke, J.P., and Kruglyak, L. (2015). A Powerful New Quantitative Genetics Platform, Combining Caenorhabditis elegans High-Throughput Fitness Assays with a Large Collection of Recombinant Strains. G3 Genes|Genomes|Genetics *5*, 911.

Arsenovic, P.T., Maldonado, A.T., Colleluori, V.D., and Bloss, T.A. (2012). Depletion of the C. elegans NAC engages the unfolded protein response, resulting in increased chaperone expression and apoptosis. PLoS One *7*, e44038.

Artiles, K.L., Fire, A.Z., and Frøkjær-Jensen, C. (2019). Assessment and Maintenance of Unigametic Germline Inheritance for C. elegans. Dev. Cell.

Ashe, A., Sapetschnig, A., Weick, E.-M., Mitchell, J., Bagijn, M.P., Cording, A.C., Doebley, A.-L., Goldstein, L.D., Lehrbach, N.J., Le Pen, J., et al. (2012). piRNAs Can Trigger a Multigenerational Epigenetic Memory in the Germline of C. elegans. Cell *150*, 88–99.

Baird, L., Tsujita, T., Kobayashi, E.H., Funayama, R., Nagashima, T., Nakayama, K., and Yamamoto, M. (2017). A Homeostatic Shift Facilitates Endoplasmic Reticulum Proteostasis through Transcriptional Integration of Proteostatic Stress Response Pathways. Mol. Cell. Biol. *37*.

Bansal, A., Kwon, E.-S., Conte, D., Liu, H., Gilchrist, M.J., MacNeil, L.T., and Tissenbaum, H.A. (2014). Transcriptional regulation of Caenorhabditis

elegansFOXO/DAF-16 modulates lifespan. Longev. Heal. *3*, 5.

Bar-Lavan, Y., Shemesh, N., Dror, S., Ofir, R., Yeger-Lotem, E., and Ben-Zvi, A. (2016). A Differentiation Transcription Factor Establishes Muscle-Specific Proteostasis in Caenorhabditis elegans. PLoS Genet. *12*.

Baugh, L.R., Hill, A.A., Slonim, D.K., Brown, E.L., and Hunter, C.P. (2003). Composition and dynamics of the Caenorhabditis elegans early embryonic transcriptome. Development *130*, 889–900.

Baugh, L.R., Hill, A.A., Claggett, J.M., Hill-Harfe, K., Wen, J.C., Slonim, D.K., Brown, E.L., and Hunter, C.P. (2005). The homeodomain protein PAL-1 specifies a lineage-specific regulatory network in the C. elegans embryo. Development *132*, 1843–1854.

Bean, C.J., Schaner, C.E., and Kelly, W.G. (2004). Meiotic pairing and imprinted X chromatin assembly in Caenorhabditis elegans. Nat. Genet. *36*, 100–105.

Bei, Y., Hogan, J., Berkowitz, L.A., Soto, M., Rocheleau, C.E., Pang, K.M., Collins, J., and Mello, C.C. (2002). SRC-1 and Wnt signaling act together to specify endoderm and to control cleavage orientation in early C. elegans embryos. Dev. Cell *3*, 113–125.

Ben-David, E., Burga, A., and Kruglyak, L. (2017). A maternal-effect selfish genetic element in Caenorhabditis elegans. Science (80-.). *356*, 1051–1055.

Berkowitz, L.A., and Strome, S. (2000). MES-1, a protein required for unequal divisions of the germline in early C. elegans embryos, resembles receptor tyrosine kinases and is localized to the boundary between the germline and gut cells. Development *127*, 4419.

Besseling, J., and Bringmann, H. (2016). Engineered non-Mendelian inheritance of entire parental genomes in C. elegans. Nat. Biotechnol. *34*, 982–986.

Bishop, N.A., and Guarente, L. (2007). Two neurons mediate diet-restriction-induced longevity in C. elegans. Nature *447*, 545–549.

Blackwell, T.K., Steinbaugh, M.J., Hourihan, J.M., Ewald, C.Y., and Isik, M. (2015). SKN-1/Nrf, stress responses, and aging in Caenorhabditis elegans. Free Radic. Biol. Med. *88*, 290–301.

Block, D.H.S., Twumasi-Boateng, K., Kang, H.S., Carlisle, J.A., Hanganu, A., Lai, T.Y.-J., and Shapira, M. (2015). The Developmental Intestinal Regulator ELT-2 Controls p38-Dependent Immune Responses in Adult C. elegans. PLOS Genet. *11*, e1005265.

Bloss, T.A., Witze, E.S., and Rothman, J.H. (2003). Suppression of CED-3-independent apoptosis by mitochondrial βNAC in Caenorhabditis elegans. Nature *424*, 1066–1071.

Bock, M.J., Jarvis, G.C., Corey, E.L., Stone, E.E., and Gribble, K.E. (2019). Maternal age alters offspring lifespan, fitness, and lifespan extension under caloric restriction. Sci. Rep. *9*, 1–16.

Boeck, M.E., Boyle, T., Bao, Z., Murray, J., Mericle, B., and Waterston, R. (2011). Specific roles for the GATA transcription factors end-1 and end-3 during C. elegans E-lineage development. Dev. Biol. *358*, 345–355.

Boveri, T. (1899). Die Entwickelung von Ascaris megalocephala mit besonderer

Rücksicht auf die Kernverhältnisse (Jena, Gustav Fischer (Opitz Library)).

Bowerman, B., Eaton, B.A., and Priess, J.R. (1992). skn-1, a maternally expressed gene required to specify the fate of ventral blastomeres in the early C. elegans embryo. Cell *68*, 1061–1075.

Bowerman, B., Draper, B.W., Mello, C.C., and Priess, J.R. (1993). The maternal gene skn-1 encodes a protein that is distributed unequally in early C. elegans embryos. Cell *74*, 443–452.

Boyle, M.J., and Seaver, E.C. (2008). Developmental expression of foxA and gata genes during gut formation in the polychaete annelid, Capitella sp. I. Evol. Dev. *10*, 89–105.

Brack, A.S., Conboy, M.J., Roy, S., Lee, M., Kuo, C.J., Keller, C., and Rando, T.A. (2007). Increased Wnt signaling during aging alters muscle stem cell fate and increases fibrosis. Science (80-.). *317*, 807–810.

Braendle, C., and Félix, M.-A.A. (2008). Plasticity and Errors of a Robust Developmental System in Different Environments. Dev. Cell *15*, 714–724.

Brenner, S. (1974). The genetics of Caenorhabditis elegans. Genetics *77*, 71–94.

Broitman-Maduro, G., Maduro, M.F., and Rothman, J.H. (2005). The Noncanonical Binding Site of the MED-1 GATA Factor Defines Differentially Regulated Target Genes in the C. elegans Mesendoderm. Dev. Cell *8*, 427–433.

Broitman-Maduro, G., Lin, K.T.-H., Hung, W.W.K., and Maduro, M.F. (2006). Specification of the C. elegans MS blastomere by the T-box factor TBX-35.

Development *133*, 3097–3106.

Broman, K.W., Wu, H., Sen, S., and Churchill, G.A. (2003). R/qtl: QTL mapping in experimental crosses. Bioinformatics *19*, 889–890.

Buckley, B.A., Burkhart, K.B., Gu, S.G., Spracklin, G., Kershner, A., Fritz, H., Kimble, J., Fire, A., and Kennedy, S. (2012). A nuclear Argonaute promotes multigenerational epigenetic inheritance and germline immortality. Nature *489*, 447–451.

Burkhart, K.B., Guang, S., Buckley, B.A., Wong, L., Bochner, A.F., and Kennedy, S. (2011). A Pre-mRNA–Associating Factor Links Endogenous siRNAs to Chromatin Regulation. PLoS Genet. *7*, e1002249.

Burnell, A.M., Houthoofd, K., O'Hanlon, K., and Vanfleteren, J.R. (2005). Alternate metabolism during the dauer stage of the nematode Caenorhabditis elegans. Exp. Gerontol. *40*, 850–856.

Burton, N.O., Riccio, C., Dallaire, A., Price, J., Jenkins, B., Koulman, A., and Miska, E.A. (2020). Cysteine synthases CYSL-1 and CYSL-2 mediate *C. elegans* heritable adaptation to *P. vranovensis* infection. Nat. Commun. *11*, 1–13.

Bygren, L.O., Kaati, G., and Edvinsson, S. (2001). Longevity determined by paternal ancestors' nutrition during their slow growth period. Acta Biotheor. *49*, 53–59.

Cassada, R.C., and Russell, R.L. (1975). The dauerlarva, a post-embryonic developmental variant of the nematode Caenorhabditis elegans. Dev. Biol. *46*, 326–342.

Charest, J., Daniele, T., Wang, J., Bykov, A., Mandlbauer, A., Asparuhova, M.,

Röhsner, J., Gutiérrez-Pérez, P., and Cochella, L. (2020). Combinatorial Action of Temporally Segregated Transcription Factors. Dev. Cell *55*, 483-499.e7.

Chen, Q., Yan, W., and Duan, E. (2016). Epigenetic inheritance of acquired traits through sperm RNAs and sperm RNA modifications. Nat. Rev. Genet. *17*, 733–743.

Chen, Y.W., Ko, W.C., Chen, C.S., and Chen, P.L. (2018). RIOK-1 is a suppressor of the p38 MAPK innate immune pathway in Caenorhabditis elegans. Front. Immunol. *9*, 774.

Chepyala, S.R., Chen, Y.C., Yan, C.C.S., Lu, C.Y.D., Wu, Y.C., and Hsu, C.P. (2016). Noise propagation with interlinked feed-forward pathways. Sci. Rep. *6*, 1–15.

Choe, K.P., Przybysz, A.J., and Strange, K. (2009). The WD40 Repeat Protein WDR-23 Functions with the CUL4/DDB1 Ubiquitin Ligase To Regulate Nuclear Abundance and Activity of SKN-1 in Caenorhabditis elegans. Mol. Cell. Biol. *29*, 2704–2715.

Choi, H., Broitman-Maduro, G., and Maduro, M.F. (2017). Partially compromised specification causes stochastic effects on gut development in C. elegans. Dev. Biol. *427*, 49–60.

Choi, Y.J., Hwang, M.S., Park, J.S., Bae, S.K., Kim, Y.S., and Yoo, M.A. (2008). Age-related upregulation of Drosophila caudal gene via NF-κB in the adult posterior midgut. Biochim. Biophys. Acta - Gen. Subj. *1780*, 1093–1100.

Clokey, G. V, and Jacobson, L.A. (1986). The autofluorescent “lipofuscin granules” in the intestinal cells of Caenorhabditis elegans are secondary lysosomes. Mech. Ageing Dev. *35*, 79–94.

Cortijo, S., Wardenaar, R., Colomé-Tatché, M., Gilly, A., Etcheverry, M., Labadie, K., Caillieux, E., Hospital, F., Aury, J.-M., Wincker, P., et al. (2014). Mapping the epigenetic basis of complex traits. Science *343*, 1145–1148.

Costa, R., Peruzzo, R., Bachmann, M., Montà, G.D., Vicario, M., Santinon, G., Mattarei, A., Moro, E., Quintana-Cabrera, R., Scorrano, L., et al. (2019). Impaired Mitochondrial ATP Production Downregulates Wnt Signaling via ER Stress Induction. Cell Rep. *28*, 1949-1960.e6.

Crofton, A.E., Cartwright, E.L., Feitzinger, A.A., and Lott, S.E. (2018). Effect of larval nutrition on maternal mRNA contribution to the Drosophila Egg. G3 Genes, Genomes, Genet. *8*, 1933–1941.

Cullinan, S.B., Gordan, J.D., Jin, J., Harper, J.W., and Diehl, J.A. (2004). The Keap1-BTB Protein Is an Adaptor That Bridges Nrf2 to a Cul3-Based E3 Ligase: Oxidative Stress Sensing by a Cul3-Keap1 Ligase. Mol. Cell. Biol. *24*, 8477–8486.

Cutter, A.D. (2008). Divergence Times in Caenorhabditis and Drosophila Inferred from Direct Estimates of the Neutral Mutation Rate. Mol. Biol. Evol. *25*, 778–786.

Daniel, D.C., and Johnson, E.M. (2018). PURA , the gene encoding Pur-alpha, member of an ancient nucleic acid-binding protein family with mammalian neurological functions. Gene *643*, 133–143.

Davidson, E.H. (2010). Emerging properties of animal gene regulatory networks. Nature *468*, 911–920.

Davidson, E.H., and Levine, M.S. (2008). Properties of developmental gene regulatory

networks. Proc. Natl. Acad. Sci. U. S. A. *105*, 20063–20066.

Davidson, E.H., Rast, J.P., Oliveri, P., Ransick, A., Calestani, C., Yuh, C.H., Minokawa, T., Amore, G., Hinman, V., Arenas-Mena, C., et al. (2002). A genomic regulatory network for development. Science (80-.). *295*, 1669–1678.

Dejima, K., Hori, S., Iwata, S., Suehiro, Y., Yoshina, S., Motohashi, T., and Mitani, S. (2018). An Aneuploidy-Free and Structurally Defined Balancer Chromosome Toolkit for Caenorhabditis elegans. Cell Rep. *22*, 232–241.

Denver, D.R., Morris, K., Lynch, M., and Thomas, W.K. (2004). High mutation rate and predominance of insertions in the Caenorhabditis elegans nuclear genome. Nature *430*, 679–682.

Dias, B.G., and Ressler, K.J. (2014). Parental olfactory experience influences behavior and neural structure in subsequent generations. Nat. Neurosci. *17*, 89–96.

Dichtel-Danjoy, M.L., and Félix, M.A. (2004). The two steps of vulval induction in Oscheius tipulae CEW1 recruit common regulators including a MEK kinase. Dev. Biol. *265*, 113–126.

Dineen, A., Osborne Nishimura, E., Goszczynski, B., Rothman, J.H., and McGhee, J.D. (2018). Quantitating transcription factor redundancy: The relative roles of the ELT-2 and ELT-7 GATA factors in the C. elegans endoderm. Dev. Biol. *435*, 150–161.

Dirksen, P., Assié, A., Zimmermann, J., Zhang, F., Tietje, A.M., Marsh, S.A., Félix, M.A., Shapira, M., Kaleta, C., Schulenburg, H., et al. (2020). CeMbio - The Caenorhabditis elegans microbiome resource. G3 Genes, Genomes, Genet. *10*,

3025–3039.

Dobzhansky, T. (1949). Towards a Modern Synthesis. Evolution (N. Y). *3*, 376–377.

Dresen, A., Finkbeiner, S., Dottermusch, M., Beume, J.S., Li, Y., Walz, G., and Neumann-Haefelin, E. (2015). Caenorhabditis elegans OSM-11 signaling regulates SKN-1/Nrf during embryonic development and adult longevity and stress response. Dev. Biol. *400*, 118–131.

Du, L., Tracy, S., and Rifkin, S.A. (2016). Mutagenesis of GATA motifs controlling the endoderm regulator elt-2 reveals distinct dominant and secondary cis-regulatory elements. Dev. Biol. *412*, 160–170.

Duveau, F., and Félix, M.-A. (2012). Role of Pleiotropy in the Evolution of a Cryptic Developmental Variation in Caenorhabditis elegans. PLoS Biol. *10*, e1001230.

Eisenmann, D.M. (2005). Wnt signaling. WormBook 1–17.

Elliott, S.L., Sturgeon, C.R., Travers, D.M., and Montgomery, M.C. (2011). Mode of bacterial pathogenesis determines phenotype in elt-2 and elt-7 RNAi Caenorhabditis elegans. Dev. Comp. Immunol. *35*, 521–524.

Evans, K.S., Zhao, Y., Brady, S.C., Long, L., McGrath, P.T., and Andersen, E.C. (2017). Correlations of genotype with climate parameters suggest Caenorhabditis elegans niche adaptations. G3 Genes, Genomes, Genet. *7*, 289–298.

Evans, K.S., Wijk, M.H. van, McGrath, P.T., Andersen, E.C., and Sterken, M.G. (2021). From QTL to gene: C. elegans facilitates discoveries of the genetic mechanisms underlying natural variation. Trends Genet. *37*, 933–947.

Ewe, C.K., Cleuren, Y.N.T., Alok, G., and Rothman, J.H. (2019). ICD-1 / BTF3 antagonizes SKN-1-mediated endoderm specification in Caenorhabditis elegans. MicroPublication Biol.

Ewe, C.K., Torres Cleuren, Y.N., and Rothman, J.H. (2020a). Evolution and developmental system drift in the endoderm gene regulatory network of Caenorhabditis and other nematodes. Front. Cell Dev. Biol. *8*, 170.

Ewe, C.K., Torres Cleuren, Y.N., Flowers, S.E., Alok, G., Snell, R.G., and Rothman, J.H. (2020b). Natural cryptic variation in epigenetic modulation of an embryonic gene regulatory network. Proc. Natl. Acad. Sci. *117*, 201920343.

Ewe, C.K., Alok, G., and Rothman, J.H. (2021a). Stressful development: integrating endoderm development, stress, and longevity. Dev. Biol. *471*, 34–48.

Ewe, C.K., Sommermann, E.M., Kenchel, J., Flowers, S.E., Maduro, M.F., and Rothman, J.H. (2021b). Feedforward regulatory logic underlies robustness of the specification-to-differentiation transition and fidelity of terminal cell fate during C. elegans endoderm development. BioRxiv 2021.08.24.457588.

Ezcurra, M., Benedetto, A., Sornda, T., Gilliat, A.F., Au, C., Zhang, Q., van Schelt, S., Petrache, A.L., Wang, H., de la Guardia, Y., et al. (2018). C. elegans Eats Its Own Intestine to Make Yolk Leading to Multiple Senescent Pathologies. Curr. Biol. *28*, 2544-2556.e5.

Fakhouri, T.H.I., Stevenson, J., Chisholm, A.D., and Mango, S.E. (2010). Dynamic Chromatin Organization during Foregut Development Mediated by the Organ Selector Gene PHA-4/FoxA. PLOS Genet. *6*, e1001060.

Fay, D.S. (2013). Classical genetic methods. WormBook 1–58.

Félix, M.-A. (2007). Cryptic Quantitative Evolution of the Vulva Intercellular Signaling Network in Caenorhabditis. Curr. Biol. *17*, 103–114.

Félix, M.-A., and Wagner, A. (2008). Robustness and evolution: concepts, insights and challenges from a developmental model system. Heredity (Edinb). *100*, 132–140.

Félix, M.A., and Duveau, F. (2012). Population dynamics and habitat sharing of natural populations of Caenorhabditis elegans and C. briggsae. BMC Biol. *10*, 1–19.

Félix, M.-A., Ashe, A., Piffaretti, J., Wu, G., Nuez, I., Bélicard, T., Jiang, Y., Zhao, G., Franz, C.J., Goldstein, L.D., et al. (2011). Natural and Experimental Infection of Caenorhabditis Nematodes by Novel Viruses Related to Nodaviruses. PLoS Biol. *9*, e1000586.

Félix, M.A., De Ley, P., Sommer, R.J., Frisse, L., Nadler, S.A., Thomas, W.K., Vanfleteren, J., and Sternberg, P.W. (2000). Evolution of vulva development in the Cephalobina (Nematoda). Dev. Biol. *221*, 68–86.

Ferguson-Smith, A.C. (2011). Genomic imprinting: the emergence of an epigenetic paradigm. Nat. Rev. Genet. *12*, 565–575.

Fire, A., Xu, S., Montgomery, M.K., Kostas, S.A., Driver, S.E., and Mello, C.C. (1998). Potent and specific genetic interference by double-stranded RNA in Caenorhabditis elegans. Nature *391*, 806–811.

Florez-Mcclure, M.L., Hohsfield, L.A., Fonte, G., Bealor, M.T., and Link, C.D. (2007). Decreased Insulin-Receptor Signaling Promotes the Autophagic Degradation of β-

Amyloid Peptide in C. elegans. Autophagy *3*, 569–580.

Frézal, L., and Félix, M.A. (2015). C. elegans outside the Petri dish. Elife *4*.

Frézal, L., Demoinet, E., Braendle, C., Miska, E., and Félix, M.-A. (2018). Natural Genetic Variation in a Multigenerational Phenotype in C. elegans. Curr. Biol. *28*, 2588-2596.e8.

Fukushige, T., Hawkins, M.G., and McGhee, J.D. (1998). The GATA-factor elt-2 is essential for formation of the Caenorhabditis elegans intestine. Dev. Biol. *198*, 286–302.

Gaudet, J., Muttumu, S., Horner, M., and Mango, S.E. (2004). Whole-Genome Analysis of Temporal Gene Expression during Foregut Development. PLOS Biol. *2*, e352.

Gilbert, S.P.R., Mullan, T.W., Poole, R.J., and Woollard, A. (2020). Caudal-dependent cell positioning directs morphogenesis of the C. elegans ventral epidermis. Dev. Biol. *461*, 31–42.

Gilleard, J.S., and McGhee, J.D. (2001). Activation of Hypodermal Differentiation in the Caenorhabditis elegans Embryo by GATA Transcription Factors ELT-1 and ELT-3 . Mol. Cell. Biol. *21*, 2533–2544.

Gilst, M.R. Van, Hadjivassiliou, H., Jolly, A., and Yamamoto, K.R. (2005). Nuclear Hormone Receptor NHR-49 Controls Fat Consumption and Fatty Acid Composition in C. elegans. PLoS Biol. *3*, e53.

Gissendanner, C.R., Crossgrove, K., Kraus, K.A., Maina, C. V., and Sluder, A.E.

(2004). Expression and function of conserved nuclear receptor genes in Caenorhabditis elegans. Dev. Biol. *266*, 399–416.

Glover-Cutter, K.M., Lin, S., and Blackwell, T.K. (2013). Integration of the Unfolded Protein and Oxidative Stress Responses through SKN-1/Nrf. PLoS Genet. *9*, e1003701.

Goszczynski, B., Captan, V. V., Danielson, A.M., Lancaster, B.R., and McGhee, J.D. (2016). A 44 bp intestine-specific hermaphrodite-specific enhancer from the C. elegans vit-2 vitellogenin gene is directly regulated by ELT-2, MAB-3, FKH-9 and DAF-16 and indirectly regulated by the germline, by daf-2/insulin signaling and by the TGF-β/Sma/Mab pathway. Dev. Biol. *413*, 112–127.

Graebsch, A., Roche, S., and Niessing, D. (2009). X-ray structure of Pur-α reveals a Whirly-like fold and an unusual nucleic-acid binding surface. Proc. Natl. Acad. Sci. U. S. A. *106*, 18521–18526.

Grimbert, S., and Braendle, C. (2014). Cryptic genetic variation uncovers evolution of environmentally sensitive parameters in *Caenorhabditis* vulval development. Evol. Dev. *16*, 278–291.

Guang, S., Bochner, A.F., Pavelec, D.M., Burkhart, K.B., Harding, S., Lachowiec, J., and Kennedy, S. (2008). An Argonaute Transports siRNAs from the Cytoplasm to the Nucleus. Science (80-.). *321*, 537–541.

Guang, S., Bochner, A.F., Burkhart, K.B., Burton, N., Pavelec, D.M., and Kennedy, S. (2010). Small regulatory RNAs inhibit RNA polymerase II during the elongation phase of transcription. Nature *465*, 1097–1101.

Gui, R., Liu, Q., Yao, Y., Deng, H., Ma, C., Jia, Y., and Yi, M. (2016). Noise decomposition principle in a coherent feed-forward transcriptional regulatory loop. Front. Physiol. *7*, 600.

Guillaume, F., and Otto, S.P. (2012). Gene functional trade-offs and the evolution of pleiotropy. Genetics *192*, 1389–1409.

Gumienny, T.L., Lambie, E., Hartwieg, E., Horvitz, H.R., and Hengartner, M.O. (1999). Genetic control of programmed cell death in the Caenorhabditis elegans hermaphrodite germline. Development *126*, 1011–1022.

Haack, H., and Hodgkin, J. (1991). Tests for parental imprinting in the nematode Caenorhabditis elegans. MGG Mol. Gen. Genet. *228*, 482–485.

Haag, E.S., Fitch, D.H.A., and Delattre, M. (2018). From “the Worm” to “the Worms” and Back Again: The Evolutionary Developmental Biology of Nematodes. Genetics *210*, 397–433.

Hahn, G.D. (1991). A modified Euler method for dynamic analyses. Int. J. Numer. Methods Eng. *32*, 943–955.

Hall, S.E., Chirn, G.-W., Lau, N.C., and Sengupta, P. (2013). RNAi pathways contribute to developmental history-dependent phenotypic plasticity in C. elegans. RNA *19*, 306–319.

Van Ham, T.J., Thijssen, K.L., Breitling, R., Hofstra, R.M.W., Plasterk, R.H.A., and Nollen, E.A.A. (2008). C. elegans model identifies genetic modifiers of α-synuclein inclusion formation during aging. PLoS Genet. *4*.

Hansen, M., Chandra, A., Mitic, L.L., Onken, B., Driscoll, M., and Kenyon, C. (2008). A Role for Autophagy in the Extension of Lifespan by Dietary Restriction in C. elegans. PLoS Genet. *4*, e24.

Hashimshony, T., Feder, M., Levin, M., Hall, B.K., and Yanai, I. (2015). Spatiotemporal transcriptomics reveals the evolutionary history of the endoderm germ layer. Nature *519*, 219–222.

Heestand, B., Simon, M., Frenk, S., Titov, D., and Ahmed, S. (2018). Transgenerational Sterility of Piwi Mutants Represents a Dynamic Form of Adult Reproductive Diapause. Cell Rep. *23*, 156–171.

Hermann, G.J., Schroeder, L.K., Hieb, C.A., Kershner, A.M., Rabbitts, B.M., Fonarev, P., Grant, B.D., and Priess, J.R. (2005). Genetic Analysis of Lysosomal Trafficking in Caenorhabditis elegans. Mol. Biol. Cell *16*, 3273–3288.

Hertweck, M., Göbel, C., and Baumeister, R. (2004). C. elegans SGK-1 is the critical component in the Akt/PKB kinase complex to control stress response and life span. Dev. Cell *6*, 577–588.

Hibshman, J.D., Hung, A., and Baugh, L.R. (2016). Maternal Diet and Insulin-Like Signaling Control Intergenerational Plasticity of Progeny Size and Starvation Resistance. PLOS Genet. *12*, e1006396.

Ho, D.S.W., Schierding, W., Wake, M., Saffery, R., and O'Sullivan, J. (2019). Machine learning SNP based prediction for precision medicine. Front. Genet. *10*, 267.

Holterman, M., Van Der Wurff, A., Van Den Elsen, S., Van Megen, H., Bongers, T.,

Holovachov, O., Bakker, J., and Helder, J. (2006). Phylum-wide analysis of SSU rDNA reveals deep phylogenetic relationships among nematodes and accelerated evolution toward crown clades. Mol. Biol. Evol. *23*, 1792–1800.

Horner, M.A., Quintin, S., Domeier, M.E., Kimble, J., Labouesse, M., and Mango, S.E. (1998). pha-4, an HNF-3 homolog, specifies pharyngeal organ identity in Caenorhabditis elegans. Genes Dev. *12*, 1947.

Houri-Ze'evi, L., and Rechavi, O. (2016). Plastic germline reprogramming of heritable small RNAs enables maintenance or erasure of epigenetic memories. RNA Biol. *13*, 1212–1217.

Houri-Zeevi, L., and Rechavi, O. (2017). A Matter of Time: Small RNAs Regulate the Duration of Epigenetic Inheritance. Trends Genet. *33*, 46–57.

Houri-Zeevi, L., Teichman, G., Gingold, H., and Rechavi, O. (2021). Stress resets ancestral heritable small RNA responses. Elife *10*.

Hryniuk, A., Grainger, S., Savory, J.G.A., and Lohnes, D. (2012). Cdx function is required for maintenance of intestinal identity in the adult. Dev. Biol. *363*, 426–437.

Hu, Q., D'Amora, D.R., Macneil, L.T., Walhout, A.J.M., and Kubiseski, T.J. (2017). The oxidative stress response in caenorhabditis elegans requires the GATA transcription factor ELT-3 and SKN-1/Nrf2. Genetics *206*, 1909–1922.

Huang, S., Shetty, P., Robertson, S.M., and Lin, R. (2007). Binary cell fate specification during C. elegans embryogenesis driven by reiterated reciprocal asymmetry of TCF POP-1 and its coactivator β-catenin SYS-1. Development *134*,

2685–2695.

Hunter, C.P., and Kenyon, C. (1996). Spatial and temporal controls target pal-1 blastomere-specification activity to a single blastomere lineage in C. elegans embryos. Cell *87*, 217–226.

Ilil, C., JB, K., and BJ, M. (1998). The nuclear hormone receptor SEX-1 is an X-chromosome signal that determines nematode sex. Nature *396*, 168–173.

Inoue, A., Jiang, L., Lu, F., Suzuki, T., and Zhang, Y. (2017). Maternal H3K27me3 controls DNA methylation-independent imprinting. Nature *547*, 419–424.

Inoue, H., Hisamoto, N., An, J.H., Oliveira, R.P., Nishida, E., Blackwell, T.K., and Matsumoto, K. (2005). The C. elegans p38 MAPK pathway regulates nuclear localization of the transcription factor SKN-1 in oxidative stress response. Genes Dev. *19*, 2278–2283.

Itoh, K., Wakabayashi, N., Katoh, Y., Ishii, T., Igarashi, K., Engel, J.D., and Yamamoto, M. (1999). Keap1 represses nuclear activation of antioxidant responsive elements by Nrf2 through binding to the amino-terminal Neh2 domain. Genes Dev. *13*, 76–86.

Jamil, M., Wang, W., Xu, M., and Tu, J. (2015). Exploring the roles of basal transcription factor 3 in eukaryotic growth and development. Biotechnol. Genet. Eng. Rev. *31*, 21–45.

Jia, K., Chen, D., and Riddle, D.L. (2004). The TOR pathway interacts with the insulin signaling pathway to regulate C. elegans larval development, metabolism and life

span. Development *131*, 3897–3906.

Jordan, J.M., Hibshman, J.D., Webster, A.K., Kaplan, R.E.W., Leinroth, A., Guzman, R., Maxwell, C.S., Chitrakar, R., Bowman, E.A., Fry, A.L., et al. (2019). Insulin/IGF Signaling and Vitellogenin Provisioning Mediate Intergenerational Adaptation to Nutrient Stress. Curr. Biol. *29*, 2380-2388.e5.

Kaati, G., Bygren, L., and Edvinsson, S. (2002). Cardiovascular and diabetes mortality determined by nutrition during parents' and grandparents' slow growth period. Eur. J. Hum. Genet. *10*, 682–688.

Kalb, J.M., Lau, K.K., Goszczynski, B., Fukushige, T., Moons, D., Okkema, P.G., and McGhee, J.D. (1998). pha-4 is Ce-fkh-1, a fork head/HNF-3alpha,beta,gamma homolog that functions in organogenesis of the C. elegans pharynx. Development *125*, 2171–2180.

Kaletta, T., Schnabel, H., and Schnabel, R. (1997). Binary specification of the embryonic lineage in Caenorhabditis elegans. Nature *390*, 294–298.

Kamath, R.S., and Ahringer, J. (2003). Genome-wide RNAi screening in Caenorhabditis elegans. Methods *30*, 313–321.

Kamath, R.S., Fraser, A.G., Dong, Y., Poulin, G., Durbin, R., Gotta, M., Kanapin, A., Le Bot, N., Moreno, S., Sohrmann, M., et al. (2003). Systematic functional analysis of the Caenorhabditis elegans genome using RNAi. Nature *421*, 231–237.

Katz, D.J., Edwards, T.M., Reinke, V., and Kelly, W.G. (2009). A C. elegans LSD1 demethylase contributes to germline immortality by reprogramming epigenetic

memory. Cell *137*, 308–320.

Keith, S.A., Maddux, S.K., Zhong, Y., Chinchankar, M.N., Ferguson, A.A., Ghazi, A., and Fisher, A.L. (2016). Graded Proteasome Dysfunction in Caenorhabditis elegans Activates an Adaptive Response Involving the Conserved SKN-1 and ELT-2 Transcription Factors and the Autophagy-Lysosome Pathway. PLOS Genet. *12*, e1005823.

Kelly, W.G. (2014). Transgenerational epigenetics in the germline cycle of Caenorhabditis elegans. Epigenetics Chromatin *7*, 6.

Keum, Y.-S. (2012). Regulation of Nrf2-Mediated Phase II Detoxification and Anti-oxidant Genes. Biomol. Ther. (Seoul). *20*, 144–151.

Kirstein-Miles, J., Scior, A., Deuerling, E., and Morimoto, R.I. (2013). The nascent polypeptide-associated complex is a key regulator of proteostasis. EMBO J. *32*, 1451–1468.

Kishimoto, S., Uno, M., Okabe, E., Nono, M., and Nishida, E. (2017). Environmental stresses induce transgenerationally inheritable survival advantages via germline-to-soma communication in Caenorhabditis elegans. Nat. Commun. *8*, 1–12.

Köppen, M., Simske, J.S., Sims, P.A., Firestein, B.L., Hall, D.H., Radice, A.D., Rongo, C., and Hardin, J.D. (2001). Cooperative regulation of AJM-1 controls junctional integrity in Caenorhabditis elegans epithelia. Nat. Cell Biol. *3*, 983–991.

Korswagen, H.C., Coudreuse, D.Y.M., Betist, M.C., Van De Water, S., Zivkovic, D., and Clevers, H.C. (2002). The Axin-like protein PRY-1 is a negative regulator of a

canonical Wnt pathway in C. elegans. Genes Dev. *16*, 1291–1302.

Ladstätter, S., and Tachibana, K. (2019). Genomic insights into chromatin reprogramming to totipotency in embryos. J Cell Biol *218*, 70–82.

Lange, A., Mills, R.E., Lange, C.J., Stewart, M., Devine, S.E., and Corbett, A.H. (2007). Classical nuclear localization signals: definition, function, and interaction with importin alpha. J. Biol. Chem. *282*, 5101–5105.

Lapierre, L.R., Gelino, S., Meléndez, A., and Hansen, M. (2011). Autophagy and lipid metabolism coordinately modulate life span in germline-less C. elegans. Curr. Biol. *21*, 1507–1514.

Lee, H., Choi, M.K., Lee, D., Kim, H.S., Hwang, H., Kim, H., Park, S., Paik, Y.K., and Lee, J. (2011). Nictation, a dispersal behavior of the nematode Caenorhabditis elegans, is regulated by IL2 neurons. Nat. Neurosci. 2011 151 *15*, 107–112.

Lee, S.H., Wong, R.R., Chin, C.Y., Lim, T.Y., Eng, S.A., Kong, C., Ijap, N.A., Lau, M.S., Lim, M.P., Gan, Y.H., et al. (2013). Burkholderia pseudomallei suppresses Caenorhabditis elegans immunity by specific degradation of a GATA transcription factor. Proc. Natl. Acad. Sci. U. S. A. *110*, 15067–15072.

Lehrbach, N.J., and Ruvkun, G. (2016). Proteasome dysfunction triggers activation of SKN-1A/Nrf1 by the aspartic protease DDI-1. Elife *5*.

Lehrbach, N.J., and Ruvkun, G. (2019). Endoplasmic reticulum-associated SKN-1A/Nrf1 mediates a cytoplasmic unfolded protein response and promotes longevity. Elife *8*.

Lev, I., Seroussi, U., Gingold, H., Bril, R., Anava, S., and Rechavi, O. (2017). MET-2-Dependent H3K9 Methylation Suppresses Transgenerational Small RNA Inheritance. Curr. Biol. *27*, 1138–1147.

Lev, I., Gingold, H., and Rechavi, O. (2019). H3K9me3 is required for inheritance of small RNAs that target a unique subset of newly evolved genes. Elife *8*.

Lezzerini, M., and Budovskaya, Y. (2014). A dual role of the Wnt signaling pathway during aging in Caenorhabditis elegans. Aging Cell *13*, 8–18.

Li, H., Liu, X., Wang, D., Su, L., Zhao, T., Li, Z., Lin, C., Zhang, Y., Huang, B., Lu, J., et al. (2017). O-GlcNAcylation of SKN-1 modulates the lifespan and oxidative stress resistance in Caenorhabditis elegans. Sci. Rep. *7*, 43601.

Li, W., Wang, D., and Wang, D. (2018). Regulation of the Response of Caenorhabditis elegans to Simulated Microgravity by p38 Mitogen-Activated Protein Kinase Signaling. Sci. Rep. *8*, 857.

Li, X., Zhao, Z., Xu, W., Fan, R., Xiao, L., Ma, X., and Du, Z. (2019). Systems Properties and Spatiotemporal Regulation of Cell Position Variability during Embryogenesis. Cell Rep. *26*, 313-321.e7.

Libina, N., Berman, J.R., and Kenyon, C. (2003). Tissue-Specific Activities of C. elegans DAF-16 in the Regulation of Lifespan. Cell *115*, 489–502.

Lin, K., Hsin, H., Libina, N., and Kenyon, C. (2001). Regulation of the Caenorhabditis elegans longevity protein DAF-16 by insulin/IGF-1 and germline signaling. Nat. Genet. *28*, 139–145.

Lin, K.T.-H., Broitman-Maduro, G., Hung, W.W.K., Cervantes, S., and Maduro, M.F. (2009). Knockdown of SKN-1 and the Wnt effector TCF/POP-1 reveals differences in endomesoderm specification in C. briggsae as compared with C. elegans. Dev. Biol. *325*, 296–306.

Lin, R., Thompson, S., and Priess, J.R. (1995). pop-1 Encodes an HMG box protein required for the specification of a mesoderm precursor in Early C. elegans embryos. Cell *83*, 599–609.

Lin, R., Hill, R.J., and Priess, J.R. (1998). POP-1 and anterior-posterior fate decisions in C. elegans embryos. Cell *92*, 229–239.

Liro, M.J., Morton, D.G., and Rose, L.S. (2018). The kinases PIG-1 and PAR-1 act in redundant pathways to regulateasymmetric division in the EMS blastomere of C.elegans. Dev. Biol. *444*, 9.

Liu, Q., and Haag, E.S. (2014). Evolutionarily dynamic roles of a PUF RNA-binding protein in the somatic development of *Caenorhabditis briggsae*. J. Exp. Zool. Part B Mol. Dev. Evol. *322*, 129–141.

Liu, C., Li, Y., Semenov, M., Han, C., Baeg, G.H., Tan, Y., Zhang, Z., Lin, X., and He, X. (2002). Control of β-catenin phosphorylation/degradation by a dual-kinase mechanism. Cell *108*, 837–847.

Liu, H., Fergusson, M.M., Castilho, R.M., Liu, J., Cao, L., Chen, J., Malide, D., Rovira, I.I., Schimel, D., Kuo, C.J., et al. (2007). Augmented Wnt signaling in a mammalian model of accelerated aging. Science (80-.). *317*, 803–806.

Liu, Q., Stumpf, C., Thomas, C., Wickens, M., and Haag, E.S. (2012). Context-dependent function of a conserved translationalregulatory module. Development *139*, 1509–1521.

Livak, K.J., and Schmittgen, T.D. (2001). Analysis of relative gene expression data using real-time quantitative PCR and the 2-ΔΔCT method. Methods *25*, 402–408.

Lo, J.Y., Spatola, B.N., and Curran, S.P. (2017). WDR23 regulates NRF2 independently of KEAP1. PLoS Genet. *13*.

Lo, M.C., Gay, F., Odom, R., Shi, Y., and Lin, R. (2004). Phosphorylation by the β-catenin/MAPK complex promotes 14-3-3-mediated nuclear export of TCF/POP-1 in signal-responsive cells in C. elegans. Cell *117*, 95–106.

Lu, R., Maduro, M., Li, F., Li, H.W., Broitman-Maduro, G., Li, W.X., and Ding, S.W. (2005). Animal virus replication and RNAi-mediated antiviral silencing in Caenorhabditis elegans. Nature *436*, 1040–1043.

Lynn, D.A., Dalton, H.M., Sowa, J.N., Wang, M.C., Soukas, A.A., Curran, S.P., and Ruvkun, G. (2015). Omega-3 and -6 fatty acids allocate somatic and germline lipids to ensure fitness during nutrient and oxidative stress in Caenorhabditis elegans. Proc. Natl. Acad. Sci. U. S. A. *112*, 15378–15383.

Lyons, L.C., and Hecht, R.M. (1997). Acute Ethanol Exposure Induces Nondisjunction of the X Chromosome During Spermatogenesis. Worm Breeder's Gaz. *14*.

MacQueen, A.J., Baggett, J.J., Perumov, N., Bauer, R.A., Januszewski, T., Schriefer, L., and Waddle, J.A. (2005). ACT-5 is an essential Caenorhabditis elegans actin

required for intestinal microvilli formation. Mol. Biol. Cell *16*, 3247–3259.

Maduro, M.F. (2015). Developmental robustness in the *Caenorhabditis elegans* embryo. Mol. Reprod. Dev. *82*, 918–931.

Maduro, M.F. (2017). Gut development in C. elegans. Semin. Cell Dev. Biol. *66*, 3–11.

Maduro, M.F. (2020). Evolutionary dynamics of the Skn-1/Med/end-1,3 regulatory gene cascade in Caenorhabditis endoderm specification. G3 Genes, Genomes, Genet. *10*, 333–356.

Maduro, M.F., and Rothman, J.H. (2002). Making Worm Guts: The Gene Regulatory Network of the Caenorhabditis elegans Endoderm. Dev. Biol. *246*, 68–85.

Maduro, M.F., Meneghini, M.D., Bowerman, B., Broitman-Maduro, G., and Rothman, J.H. (2001). Restriction of mesendoderm to a single blastomere by the combined action of SKN-1 and a GSK-3beta homolog is mediated by MED-1 and -2 in C. elegans. Mol. Cell *7*, 475–485.

Maduro, M.F., Lin, R., and Rothman, J.H. (2002). Dynamics of a Developmental Switch: Recursive Intracellular and Intranuclear Redistribution of Caenorhabditis elegans POP-1 Parallels Wnt-Inhibited Transcriptional Repression. Dev. Biol. *248*, 128–142.

Maduro, M.F., Kasmir, J.J., Zhu, J., and Rothman, J.H. (2005a). The Wnt effector POP-1 and the PAL-1/Caudal homeoprotein collaborate with SKN-1 to activate C. elegans endoderm development. Dev. Biol. *285*, 510–523.

Maduro, M.F., Hill, R.J., Heid, P.J., Newman-Smith, E.D., Zhu, J., Priess, J.R., and Rothman, J.H. (2005b). Genetic redundancy in endoderm specification within the genus Caenorhabditis. Dev. Biol. *284*, 509–522.

Maduro, M.F., Broitman-Maduro, G., Mengarelli, I., and Rothman, J.H. (2007). Maternal deployment of the embryonic SKN-1 → MED-1,2 cell specification pathway in C. elegans. Dev. Biol. *301*, 590–601.

Maduro, M.F., Broitman-Maduro, G., Choi, H., Carranza, F., Wu, A.C.-Y., and Rifkin, S.A. (2015). MED GATA factors promote robust development of the C. elegans endoderm. Dev. Biol. *404*, 66–79.

Maeshima, K., Kaizu, K., Tamura, S., Nozaki, T., Kokubo, T., and Takahashi, K. (2015). The physical size of transcription factors is key to transcriptional regulation in chromatin domains. J. Phys. Condens. Matter *27*.

Makova, K.D., and Hardison, R.C. (2015). The effects of chromatin organization on variation in mutation rates in the genome. Nat. Rev. Genet. *16*, 213–223.

Mangan, S., and Alon, U. (2003). Structure and function of the feed-forward loop network motif. Proc. Natl. Acad. Sci. U. S. A. *100*, 11980–11985.

Mango, S.E., Lambie, E.J., and Kimble, J. (1994). The pha-4 gene is required to generate the pharyngeal primordium of Caenorhabditis elegans. Development *120*, 3019–3031.

Mann, F.G., Van Nostrand, E.L., Friedland, A.E., Liu, X., and Kim, S.K. (2016). Deactivation of the GATA Transcription Factor ELT-2 Is a Major Driver of Normal

Aging in C. elegans. PLoS Genet. *12*.

Markesich, D.C., Gajewski, K.M., Nazimiec, M.E., and Beckingham, K. (2000). bicaudal encodes the Drosophila beta NAC homolog, a component of the ribosomal translational machinery. Development *127*.

Marré, J., Traver, E.C., and Jose, A.M. (2016). Extracellular RNA is transported from one generation to the next in *Caenorhabditis elegans*. Proc. Natl. Acad. Sci. *113*, 12496–12501.

Martindale, M.Q., Pang, K., and Finnerty, J.R. (2004). Investigating the origins of triploblasty: “mesodermal” gene expression in a diploblastic animal, the sea anemone Nematostella vectensis (phylum, Cnidaria; class, Anthozoa). Development *131*, 2463–2474.

McGhee, J. (2007). The C. elegans intestine. WormBook 1–36.

McGhee, J.D., Fukushige, T., Krause, M.W., Minnema, S.E., Goszczynski, B., Gaudet, J., Kohara, Y., Bossinger, O., Zhao, Y., Khattra, J., et al. (2009). ELT-2 is the predominant transcription factor controlling differentiation and function of the C. elegans intestine, from embryo to adult. Dev. Biol. *327*, 551–565.

McGrath, P.T., Rockman, M. V, Zimmer, M., Jang, H., Macosko, E.Z., Kruglyak, L., and Bargmann, C.I. (2009). Quantitative mapping of a digenic behavioral trait implicates globin variation in C. elegans sensory behaviors. Neuron *61*, 692–699.

Meneghini, M.D., Ishitani, T., Carter, J.C., Hisamoto, N., Ninomiya-Tsuji, J., Thorpe, C.J., Hamill, D.R., Matsumoto, K., and Bowerman, B. (1999). MAP kinase and Wnt

pathways converge to downregulate an HMG-domain repressor in Caenorhabditis elegans. Nature *399*, 793–797.

Milloz, J., Duveau, F., Nuez, I., and Felix, M.-A. (2008). Intraspecific evolution of the intercellular signaling network underlying a robust developmental system. Genes Dev. *22*, 3064–3075.

Miyata, S., Begun, J., Troemel, E.R., and Ausubel, F.M. (2008). DAF-16-dependent suppression of immunity during reproduction in Caenorhabditis elegans. Genetics *178*, 903–918.

Mizunuma, M., Neumann-Haefelin, E., Moroz, N., Li, Y., and Blackwell, T.K. (2014). mTORC2-SGK-1 acts in two environmentally responsive pathways with opposing effects on longevity. Aging Cell *13*, 869–878.

Moilanen, L.H., Fukushige, T., and Freedman, J.H. (1999). Regulation of metallothionein gene transcription. Identification fo upstream regulatory elements and transcription factors responsible for cell- specific expression of the metallothionein genes from Caenorhabditis elegans. J. Biol. Chem. *274*, 29655–29665.

Moore, R.S., Kaletsky, R., and Murphy, C.T. (2019). Piwi/PRG-1 Argonaute and TGF-β Mediate Transgenerational Learned Pathogenic Avoidance. Cell *177*, 1827-1841.e12.

Much, J.W., Slade, D.J., Klampert, K., Garriga, G., and Wightman, B. (2000). The fax-1 nuclear hormone receptor regulates axon pathfinding and neurotransmitter expression. Development *127*, 703–712.

Murakami, R., Okumura, T., and Uchiyama, H. (2005). GATA factors as key regulatory molecules in the development of Drosophila endoderm. Dev. Growth Differ. *47*, 581–589.

Nakamura, K., Kim, S., Ishidate, T., Bei, Y., Pang, K., Shirayama, M., Trzepacz, C., Brownell, D.R., and Mello, C.C. (2005). Wnt signaling drives WRM-1/beta-catenin asymmetries in early C. elegans embryos. Genes Dev. *19*, 1749–1754.

Nakanishi, N., Sogabe, S., and Degnan, B.M. (2014). Evolutionary origin of gastrulation: Insights from sponge development. BMC Biol. *12*.

Natarajan, L., Witwer, N.E., and Eisenmann, D.M. (2001). The divergent Caenorhabditis elegans beta-catenin proteins BAR-1, WRM-1 and HMP-2 make distinct protein interactions but retain functional redundancy in vivo. Genetics *159*, 159–172.

Ninomiya-Tsuji, J., Kishimoto, K., Hiyama, A., Inoue, J.I., Cao, Z., and Matsumoto, K. (1999). The kinase TAK1 can activate the NIK-IκB as well as the MAP kinase cascade in the IL-1 signalling pathway. Nature *398*, 252–256.

Nishi, Y., and Lin, R. (2005). DYRK2 and GSK-3 phosphorylate and promote the timely degradation of OMA-1, a key regulator of the oocyte-to-embryo transition in C. elegans. Dev. Biol. *288*, 139–149.

Nono, M., Kishimoto, S., Sato-Carlton, A., Carlton, P.M., Nishida, E., and Uno, M. (2020). Intestine-to-Germline Transmission of Epigenetic Information Intergenerationally Ensures Systemic Stress Resistance in C. elegans. Cell Rep. *30*, 3207-3217.e4.

Notredame, C., Higgins, D.G., and Heringa, J. (2000). T-Coffee: A novel method for fast and accurate multiple sequence alignment. J. Mol. Biol. *302*, 205–217.

Nuzhdin, S. V., Tufts, D.M., and Hahn, M.W. (2008). Abundant genetic variation in transcript level during early Drosophila development. Evol. Dev. *10*, 683–689.

Okumura, T., Matsumoto, A., Tanimura, T., and Murakami, R. (2005). An endoderm-specific GATA factor gene, dGATAe, is required for the terminal differentiation of the Drosophila endoderm. Dev. Biol. *278*, 576–586.

Olofsson, H., Ripa, J., and Jonzén, N. (2009). Bet-hedging as an evolutionary game: The trade-off between egg size and number. Proc. R. Soc. B Biol. Sci. *276*, 2963–2969.

van Otterdijk, S.D., and Michels, K.B. (2016). Transgenerational epigenetic inheritance in mammals: how good is the evidence? FASEB J. *30*, 2457–2465.

Owraghi, M., Broitman-Maduro, G., Luu, T., Roberson, H., and Maduro, M.F. (2010). Roles of the Wnt effector POP-1/TCF in the C. elegans endomesoderm specification gene network. Dev. Biol. *340*, 209–221.

Paaby, A.B., White, A.G., Riccardi, D.D., Gunsalus, K.C., Piano, F., and Rockman, M. V (2015). Wild worm embryogenesis harbors ubiquitous polygenic modifier variation. Elife *4*, e09178.

Panowski, S.H., Wolff, S., Aguilaniu, H., Durieux, J., and Dillin, A. (2007). PHA-4/Foxa mediates diet-restriction-induced longevity of C. elegans. Nature *447*, 550–555.

Papadopoli, D., Boulay, K., Kazak, L., Pollak, M., Mallette, F.A., Topisirovic, I., and

Hulea, L. (2019). mTOR as a central regulator of lifespan and aging. F1000Research *8*.

Papp, D., Csermely, P., and Sőti, C. (2012). A Role for SKN-1/Nrf in Pathogen Resistance and Immunosenescence in Caenorhabditis elegans. PLoS Pathog. *8*, e1002673.

Papsdorf, K., and Brunet, A. (2019). Linking Lipid Metabolism to Chromatin Regulation in Aging. Trends Cell Biol. *29*, 97–116.

Pedregosa, F., Michel, V., Grisel, O., Blondel, M., Prettenhofer, P., Weiss, R., Vanderplas, J., Cournapeau, D., Pedregosa, F., Varoquaux, G., et al. (2011). Scikit-learn: Machine Learning in Python. J. Mach. Learn. Res. *12*, 2825–2830.

Perez, C.L., and Van Gilst, M.R. (2008). A 13C Isotope Labeling Strategy Reveals the Influence of Insulin Signaling on Lipogenesis in C. elegans. Cell Metab. *8*, 266–274.

Perez, M.F., and Lehner, B. (2019a). Intergenerational and Transgenerational Epigenetic Inheritance in Animals. Nat. Cell Biol. *21*, 143–151.

Perez, M.F., and Lehner, B. (2019b). Vitellogenins - Yolk Gene Function and Regulation in Caenorhabditis elegans. Front. Physiol. *10*, 1067.

Perez, M.F., Francesconi, M., Hidalgo-Carcedo, C., and Lehner, B. (2017). Maternal age generates phenotypic variation in Caenorhabditis elegans. Nature *552*, 106.

Peter, I.S. (2020). The function of architecture and logic in developmental gene regulatory networks. In Current Topics in Developmental Biology, (Academic Press Inc.), pp. 267–295.

Peter, I.S., and Davidson, E.H. (2011). Evolution of gene regulatory networks controlling body plan development. Cell *144*, 970–985.

Phillips, B.T., Kidd, A.R., King, R., Hardin, J., and Kimble, J. (2007). Reciprocal asymmetry of SYS-1/beta-catenin and POP-1/TCF controls asymmetric divisions in Caenorhabditis elegans. Proc. Natl. Acad. Sci. *104*, 3231–3236.

Prall, O.W.J., Menon, M.K., Solloway, M.J., Watanabe, Y., Zaffran, S., Bajolle, F., Biben, C., McBride, J.J., Robertson, B.R., Chaulet, H., et al. (2007). An Nkx2-5/Bmp2/Smad1 Negative Feedback Loop Controls Heart Progenitor Specification and Proliferation. Cell *128*, 947–959.

Putzke, A.P., and Rothman, J.H. (2010). Repression of Wnt signaling by a Fer-type nonreceptor tyrosine kinase. Proc. Natl. Acad. Sci. *107*, 16154–16159.

Radhakrishnan, S.K., den Besten, W., and Deshaies, R.J. (2014). p97-dependent retrotranslocation and proteolytic processing govern formation of active Nrf1 upon proteasome inhibition. Elife *3*.

Raj, A., Rifkin, S.A., Andersen, E., and van Oudenaarden, A. (2010). Variability in gene expression underlies incomplete penetrance. Nature *463*, 913–918.

Raposo, G., and Stoorvogel, W. (2013). Extracellular vesicles: Exosomes, microvesicles, and friends. J. Cell Biol. *200*, 373–383.

Rasmussen, J.P., Feldman, J.L., Reddy, S.S., and Priess, J.R. (2013). Cell Interactions and Patterned Intercalations Shape and Link Epithelial Tubes in C. elegans. PLoS Genet. *9*, 1003772.

Ratnappan, R., Amrit, F.R.G., Chen, S.-W., Gill, H., Holden, K., Ward, J., Yamamoto, K.R., Olsen, C.P., and Ghazi, A. (2014). Germline Signals Deploy NHR-49 to Modulate Fatty-Acid β-Oxidation and Desaturation in Somatic Tissues of C. elegans. PLoS Genet. *10*, e1004829.

Rechavi, O., and Lev, I. (2017). Principles of Transgenerational Small RNA Inheritance in Caenorhabditis elegans. Curr. Biol. *27*, R720–R730.

Rechavi, O., Minevich, G., and Hobert, O. (2011). Transgenerational inheritance of an acquired small RNA-based antiviral response in C. elegans. Cell *147*, 1248–1256.

Rechavi, O., Houri-Ze'evi, L., Anava, S., Goh, W.S.S., Kerk, S.Y., Hannon, G.J., and Hobert, O. (2014). Starvation-induced transgenerational inheritance of small RNAs in C. elegans. Cell *158*, 277–287.

Reinke, S.N., Hu, X., Sykes, B.D., and Lemire, B.D. (2010). Caenorhabditis elegans diet significantly affects metabolic profile, mitochondrial DNA levels, lifespan and brood size. Mol. Genet. Metab. *100*, 274–282.

Riddle, M.R., Spickard, E.A., Jevince, A., Nguyen, K.C.Q., Hall, D.H., Joshi, P.M., and Rothman, J.H. (2016). Transorganogenesis and transdifferentiation in C. elegans are dependent on differentiated cell identity. Dev. Biol. *420*, 136–147.

Robida-Stubbs, S., Glover-Cutter, K., Lamming, D.W., Mizunuma, M., Narasimhan, S.D., Neumann-Haefelin, E., Sabatini, D.M., and Blackwell, T.K. (2012). TOR signaling and rapamycin influence longevity by regulating SKN-1/Nrf and DAF-16/FoxO. Cell Metab. *15*, 713–724.

Rocheleau, C.E., Yasuda, J., Shin, T.H., Lin, R., Sawa, H., Okano, H., Priess, J.R., Davis, R.J., and Mello, C.C. (1999). WRM-1 Activates the LIT-1 Protein Kinase to Transduce Anterior/Posterior Polarity Signals in C. elegans. Cell *97*, 717–726.

Rodaway, A., and Patient, R. (2001). Mesendoderm: An Ancient Germ Layer? Cell *105*, 169–172.

Rohlfing, A.K., Miteva, Y., Hannenhalli, S., and Lamitina, T. (2010). Genetic and physiological activation of osmosensitive gene expression mimics transcriptional signatures of pathogen infection in C. elegans. PLoS One *5*.

Romney, S.J., Thacker, C., and Leibold, E.A. (2008). An Iron Enhancer Element in the FTN-1 gene directs iron-dependent expression in Caenorhabditis elegans intestine. J. Biol. Chem. *283*, 716–725.

Rual, J.-F., Ceron, J., Koreth, J., Hao, T., Nicot, A.-S., Hirozane-Kishikawa, T., Vandenhaute, J., Orkin, S.H., Hill, D.E., van den Heuvel, S., et al. (2004). Toward Improving Caenorhabditis elegans Phenome Mapping With an ORFeome-Based RNAi Library. Genome Res. *14*, 2162–2168.

Ruf, V., Holzem, C., Peyman, T., Walz, G., Blackwell, T.K., and Neumann-Haefelin, E. (2013). TORC2 signaling antagonizes SKN-1 to induce C. elegans mesendodermal embryonic development. Dev. Biol. *384*, 214–227.

Ruhe, A. (1979). Accelerated Gauss-Newton algorithms for nonlinear least squares problems. BIT Numer. Math. 1979 193 *19*, 356–367.

Russell, J.C., Merrihew, G.E., Robbins, J.E., Postupna, N., Kim, T.-K., Golubeva, A.,

Noori, A., Wang, K., Keene, C.D., MacCoss, M.J., et al. (2018). Isolation and characterization of extracellular vesicles from Caenorhabditis elegans for multi-omic analysis. BioRxiv 476226.

Ryu, J.H., Kim, S.H., Lee, H.Y., Jin, Y.B., Nam, Y. Do, Bae, J.W., Dong, G.L., Seung, C.S., Ha, E.M., and Lee, W.J. (2008). Innate immune homeostasis by the homeobox gene Caudal and commensal-gut mutualism in Drosophila. Science (80-.). *319*, 777–782.

Sala, A.J., Bott, L.C., Brielmann, R.M., and Morimoto, R.I. (2020). Embryo integrity regulates maternal proteostasis and stress resilience. Genes Dev.

Schieber, M., and Chandel, N.S. (2014). TOR signaling couples oxygen sensing to lifespan in C.elegans. Cell Rep. *9*, 9–15.

Schiffer, P.H., Nsah, N.A., Grotehusmann, H., Kroiher, M., Loer, C., and Schierenberg, E. (2014). Developmental variations among Panagrolaimid nematodes indicate developmental system drift within a small taxonomic unit. Dev. Genes Evol. *224*, 183–188.

Schiffer, P.H., Polsky, A.L., Cole, A.G., Camps, J.I.R., Kroiher, M., Silver, D.H., Grishkevich, V., Anavy, L., Koutsovoulos, G., Hashimshony, T., et al. (2018). The gene regulatory program of Acrobeloides nanus reveals conservation of phylum-specific expression. Proc. Natl. Acad. Sci. U. S. A. *115*, 4459–4464.

Schlesinger, A., Shelton, C.A., Maloof, J.N., Meneghini, M., and Bowerman, B. (1999). Wnt pathway components orient a mitotic spindle in the early Caenorhabditis elegans embryo without requiring gene transcription in the responding cell. Genes Dev. *13*,

2028–2038.

Schmid, M.W., Heichinger, C., Coman Schmid, D., Guthörl, D., Gagliardini, V., Bruggmann, R., Aluri, S., Aquino, C., Schmid, B., Turnbull, L.A., et al. (2018). Contribution of epigenetic variation to adaptation in Arabidopsis. Nat. Commun. *9*, 4446.

Schott, D.H., Cureton, D.K., Whelan, S.P., and Hunter, C.P. (2005). An antiviral role for the RNA interference machinery in Caenorhabditis elegans. Proc. Natl. Acad. Sci. U. S. A. *102*, 18420–18424.

Schulenburg, H., and Félix, M.-A. (2017). The Natural Biotic Environment of Caenorhabditis elegans. Genetics *206*, 55–86.

Schuster, E., McElwee, J.J., Tullet, J.M.A., Doonan, R., Matthijssens, F., Reece-Hoyes, J.S., Hope, I.A., Vanfleteren, J.R., Thornton, J.M., and Gems, D. (2010). DamID in *C. elegans* reveals longevity-associated targets of DAF-16/FoxO. Mol. Syst. Biol. *6*, 399.

Seidel, H.S., Rockman, M. V, and Kruglyak, L. (2008). Widespread genetic incompatibility in C. elegans maintained by balancing selection. Science *319*, 589–594.

Seydoux, G., and Fire, A. (1994). Soma-germline asymmetry in the distributions of embryonic RNAs in Caenorhabditis elegans. Development *120*, 2823–2834.

Sha, K., and Fire, A. (2005). Imprinting capacity of gamete lineages in Caenorhabditis elegans. Genetics *170*, 1633–1652.

Sha, Z., and Goldberg, A.L. (2014). Proteasome-mediated processing of Nrf1 is essential for coordinate induction of all proteasome subunits and p97. Curr. Biol. *24*, 1573–1583.

Shapira, M., Hamlin, B.J., Rong, J., Chen, K., Ronen, M., and Tan, M.W. (2006). A conserved role for a GATA transcription factor in regulating epithelial innate immune responses. Proc. Natl. Acad. Sci. U. S. A. *103*, 14086–14091.

Sheaffer, K.L., Updike, D.L., and Mango, S.E. (2008). The Target of Rapamycin Pathway Antagonizes pha-4/FoxA to Control Development and Aging. Curr. Biol. *18*, 1355–1364.

Shen, K., Gamerdinger, M., Chan, R., Gense, K., Martin, E.M., Sachs, N., Knight, P.D., Schlömer, R., Calabrese, A.N., Stewart, K.L., et al. (2019). Dual Role of Ribosome-Binding Domain of NAC as a Potent Suppressor of Protein Aggregation and Aging-Related Proteinopathies. Mol. Cell *74*, 729-741.e7.

Shetty, P., Lo, M.-C., Robertson, S.M., and Lin, R. (2005). C. elegans TCF protein, POP-1, converts from repressor to activator as a result of Wnt-induced lowering of nuclear levels. Dev. Biol. *285*, 584–592.

Shin, T.H., Yasuda, J., Rocheleau, C.E., Lin, R., Soto, M., Bei, Y., Davis, R.J., and Mello, C.C. (1999). MOM-4, a MAP kinase kinase kinase-related protein, activates WRM-1/LIT-1 kinase to transduce anterior/posterior polarity signals in C. elegans. Mol. Cell *4*, 275–280.

Shirayama, M., Seth, M., Lee, H.-C., Gu, W., Ishidate, T., Conte, D., and Mello, C.C. (2012). piRNAs initiate an epigenetic memory of nonself RNA in the C. elegans

germline. Cell *150*, 65–77.

Shoichet, S.A., Malik, T.H., Rothman, J.H., and Shivdasani, R.A. (2000). Action of the Caenorhabditis elegans GATA factor END-1 in Xenopus suggests that similar mechanisms initiate endoderm development in ecdysozoa and vertebrates. Proc. Natl. Acad. Sci. U. S. A. *97*, 4076–4081.

Simon, M., Sarkies, P., Ikegami, K., Doebley, A.-L., Goldstein, L.D., Mitchell, J., Sakaguchi, A., Miska, E.A., and Ahmed, S. (2014). Reduced Insulin/IGF-1 Signaling Restores Germ Cell Immortality to Caenorhabditis elegans Piwi Mutants. Cell Rep. *7*, 762–773.

Singh, K.D., Roschitzki, B., Snoek, L.B., Grossmann, J., Zheng, X., Elvin, M., Kamkina, P., Schrimpf, S.P., Poulin, G.B., Kammenga, J.E., et al. (2016). Natural genetic variation influences protein abundances in C. elegans developmental signalling pathways. PLoS One *11*.

Sommer, R.J. (2020). Phenotypic Plasticity: From Theory and Genetics to Current and Future Challenges. Genetics *215*, 1–13.

Sommer, R.J., and Sternberg, P.W. (1994). Changes of induction and competence during the evolution of vulva development in nematodes. Science (80-.). *265*, 114–118.

Sommermann, E.M., Strohmaier, K.R., Maduro, M.F., and Rothman, J.H. (2010). Endoderm development in Caenorhabditis elegans: The synergistic action of ELT-2 and -7 mediates the specification→differentiation transition. Dev. Biol. *347*, 154–166.

Spracklin, G., Fields, B., Wan, G., Becker, D., Wallig, A., Shukla, A., and Kennedy, S. (2017). The RNAi Inheritance Machinery of Caenorhabditis elegans. Genetics *206*, 1403–1416.

van Steenwyk, G., Roszkowski, M., Manuella, F., Franklin, T.B., and Mansuy, I.M. (2018). Transgenerational inheritance of behavioral and metabolic effects of paternal exposure to traumatic stress in early postnatal life: evidence in the 4th generation. Environ. Epigenetics *4*.

Steinbaugh, M.J., Narasimhan, S.D., Robida-Stubbs, S., Moronetti Mazzeo, L.E., Dreyfuss, J.M., Hourihan, J.M., Raghavan, P., Operaña, T.N., Esmaillie, R., and Blackwell, T.K. (2015). Lipid-mediated regulation of SKN-1/Nrf in response to germ cell absence. Elife *4*.

Sterken, M.G., Snoek, L.B., Kammenga, J.E., and Andersen, E.C. (2015). The laboratory domestication of Caenorhabditis elegans. Trends Genet. *31*, 224–231.

Suh, E., Chen, L., Taylor, J., and Traber, P.G. (1994). A homeodomain protein related to caudal regulates intestine-specific gene transcription. Mol. Cell. Biol. *14*, 7340–7351.

Sullivan-Brown, J.L., Tandon, P., Bird, K.E., Dickinson, D.J., Tintori, S.C., Heppert, J.K., Meserve, J.H., Trogden, K.P., Orlowski, S.K., Conlon, F.L., et al. (2016). Identifying regulators of morphogenesis common to vertebrate neural tube closure and Caenorhabditis elegans gastrulation. Genetics *202*, 123–139.

Sulston, J.E., Schierenberg, E., White, J.G., and Thomson, J.N. (1983). The embryonic cell lineage of the nematode Caenorhabditis elegans. Dev. Biol. *100*, 64–

119.

Sumiyoshi, E., Takahashi, S., Obata, H., Sugimoto, A., and Kohara, Y. (2011). The β-catenin HMP-2 functions downstream of Src in parallel with the Wnt pathway in early embryogenesis of C. elegans. Dev. Biol. *355*, 302–312.

Surkova, S., Kosman, D., Kozlov, K., Manu, Myasnikova, E., Samsonova, A.A., Spirov, A., Vanario-Alonso, C.E., Samsonova, M., and Reinitz, J. (2008). Characterization of the Drosophila segment determination morphome. Dev. Biol. *313*, 844–862.

Tabet, F., Vickers, K.C., Cuesta Torres, L.F., Wiese, C.B., Shoucri, B.M., Lambert, G., Catherinet, C., Prado-Lourenco, L., Levin, M.G., Thacker, S., et al. (2014). HDL-transferred microRNA-223 regulates ICAM-1 expression in endothelial cells. Nat. Commun. *5*, 3292.

Taubert, S., Ward, J.D., and Yamamoto, K.R. (2011). Nuclear hormone receptors in nematodes: Evolution and function. Mol. Cell. Endocrinol. *334*, 49–55.

Thorpe, C.J., Schlesinger, A., Carter, J.C., and Bowerman, B. (1997). Wnt signaling polarizes an early C. elegans blastomere to distinguish endoderm from mesoderm. Cell *90*, 695–705.

Timmons, L., and Fire, A. (1998). Specific interference by ingested dsRNA. Nature *395*, 854.

Tintori, S.C., Osborne Nishimura, E., Golden, P., Lieb, J.D., and Goldstein, B. (2016). A Transcriptional Lineage of the Early C. elegans Embryo. Dev. Cell *38*, 430–444.

Torres Cleuren, Y.N., Ewe, C.K., Chipman, K.C., Mears, E.R., Wood, C.G., Al-Alami, C.E.A., Alcorn, M.R., Turner, T.L., Joshi, P.M., Snell, R.G., et al. (2019). Extensive intraspecies cryptic variation in an ancient embryonic gene regulatory network. Elife *8*.

True, J.R., and Haag, E.S. (2001). Developmental system drift and flexibility in evolutionary trajectories. Evol. Dev. *3*, 109–119.

Tullet, J.M.A., Hertweck, M., An, J.H., Baker, J., Hwang, J.Y., Liu, S., Oliveira, R.P., Baumeister, R., and Blackwell, T.K. (2008). Direct Inhibition of the Longevity-Promoting Factor SKN-1 by Insulin-like Signaling in C. elegans. Cell *132*, 1025–1038.

Vågerö, D., Pinger, P.R., Aronsson, V., and van den Berg, G.J. (2018). Paternal grandfather's access to food predicts all-cause and cancer mortality in grandsons. Nat. Commun. *9*, 5124.

Vastenhouw, N.L., Brunschwig, K., Okihara, K.L., Müller, F., Tijsterman, M., and Plasterk, R.H.A. (2006). Gene expression: long-term gene silencing by RNAi. Nature *442*, 882–882.

Vickers, K.C., Palmisano, B.T., Shoucri, B.M., Shamburek, R.D., and Remaley, A.T. (2011). MicroRNAs are transported in plasma and delivered to recipient cells by high-density lipoproteins. Nat. Cell Biol. *13*, 423–435.

Vishnupriya, R., Thomas, L., Wahba, L., Fire, A., and Subramaniam, K. (2020). PLP-1 is essential for germ cell development and germline gene silencing in Caenorhabditis elegans. Dev. *147*.

Visser, J.A.G.M., Hermisson, J., Wagner, G.P., Meyers, L.A., Bagheri-Chaichian, H., Blanchard, J.L., Chao, L., Cheverud, J.M., Elena, S.F., Fontana, W., et al. (2003). Evolution and detection of genetic robustness. Evolution (N. Y). *57*, 1959–1972.

Vu, V., Verster, A.J., Schertzberg, M., Chuluunbaatar, T., Spensley, M., Pajkic, D., Hart, G.T., Moffat, J., and Fraser, A.G. (2015). Natural Variation in Gene Expression Modulates the Severity of Mutant Phenotypes. Cell *162*, 391–402.

Waddington, C. (1957). The strategy of the genes (London: Volume George Allen and Unwin).

Waddington, C.H. (1942). Canalization of development and the inheritance of acquired characters. Nature *150*, 563–565.

Waddington, C.H. (1953). Genetic Assimilation of an Acquired Character. Evolution (N. Y). *7*, 118–126.

Walston, T., Tuskey, C., Edgar, L., Hawkins, N., Ellis, G., Bowerman, B., Wood, W., and Hardin, J. (2004). Multiple Wnt Signaling Pathways Converge to Orient the Mitotic Spindle in Early C. elegans Embryos. Dev. Cell *7*, 831–841.

Walther, D.M., Kasturi, P., Zheng, M., Pinkert, S., Vecchi, G., Ciryam, P., Morimoto, R.I., Dobson, C.M., Vendruscolo, M., Mann, M., et al. (2015). Widespread proteome remodeling and aggregation in aging C. elegans. Cell *161*, 919–932.

Wang, W., and Chan, J.Y. (2006). Nrf1 is targeted to the endoplasmic reticulum membrane by an N-terminal transmembrane domain: Inhibition of nuclear translocation and transacting function. J. Biol. Chem. *281*, 19676–19687.

Wang, Z., Stoltzfus, J., You, Y., Ranjit, N., Tang, H., Xie, Y., Lok, J.B., Mangelsdorf, D.J., and Kliewer, S.A. (2015). The Nuclear Receptor DAF-12 Regulates Nutrient Metabolism and Reproductive Growth in Nematodes. PLOS Genet. *11*, e1005027.

Ward, J.D., Mullaney, B., Schiller, B.J., He, L.D., Petnic, S.E., Couillault, C., Pujol, N., Bernal, T.U., Van Gilst, M.R., Ashrafi, K., et al. (2014). Defects in the C. elegans acyl-CoA Synthase, acs-3, and Nuclear Hormone Receptor, nhr-25, Cause Sensitivity to Distinct, but Overlapping Stresses. PLoS One *9*, e92552.

Waring, D.A., and Kenyon, C. (1991). Regulation of cellular responsiveness to inductive signals in the developing C. elegans nervous system. Nature *350*, 712–715.

Webster, A.K., Jordan, J.M., Hibshman, J.D., Chitrakar, R., and Baugh, R. (2018). Transgenerational Effects of Extended Dauer Diapause on Starvation Survival and Gene Expression Plasticity in Caenorhabditis elegans.

Weick, E.-M., Sarkies, P., Silva, N., Chen, R.A., Moss, S.M.M., Cording, A.C., Ahringer, J., Martinez-Perez, E., and Miska, E.A. (2014). PRDE-1 is a nuclear factor essential for the biogenesis of Ruby motif-dependent piRNAs in C. elegans. Genes Dev. *28*, 783–796.

Wen, Y.A., Xiong, X., Scott, T., Li, A.T., Wang, C., Weiss, H.L., Tan, L., Bradford, E., Fan, T.W.M., Chandel, N.S., et al. (2019). The mitochondrial retrograde signaling regulates Wnt signaling to promote tumorigenesis in colon cancer. Cell Death Differ. 2019 2610 *26*, 1955–1969.

Widmayer, S.J., Evans, K., Zdraljevic, S., and Andersen, E.C. (2021). Evaluating the power and limitations of genome-wide association mapping in C. elegans. BioRxiv

2021.09.09.459688.

Wiegner, O., and Schierenberg, E. (1998). Specification of gut cell fate differs significantly between the nematodes Acrobeloides nanus and Caenorhabditis elegans. Dev. Biol. *204*, 3–14.

Wiesenfahrt, T., Berg, J.Y., Osborne Nishimura, E., Robinson, A.G., Goszczynski, B., Lieb, J.D., and McGhee, J.D. (2016). The function and regulation of the GATA factor ELT-2 in the *C. elegans* endoderm. Development *143*, 483–491.

Winston, W.M., Sutherlin, M., Wright, A.J., Feinberg, E.H., and Hunter, C.P. (2007). Caenorhabditis elegans SID-2 is required for environmental RNA interference. Proc. Natl. Acad. Sci. U. S. A. *104*, 10565–10570.

Witten, T.M., and Bonchev, D. (2007). Predicting aging/longevity-related genes in the nematode Caenorhabditis elegans. Chem. Biodivers. *4*, 2639–2655.

Witze, E.S., Field, E.D., Hunt, D.F., and Rothman, J.H. (2009). C. elegans pur alpha, an activator of end-1, synergizes with the Wnt pathway to specify endoderm. Dev. Biol. *327*, 12–23.

Wu, L.H., and Lengyel, J.A. (1998). Role of caudal in hindgut specification and gastrulation suggests homology between Drosophila amnioproctodeal invagination and vertebrate blastopore. Development *125*.

Wu, J., Jiang, X., Li, Y., Zhu, T., Zhang, J., Zhang, Z., Zhang, L., Zhang, Y., Wang, Y., Zou, X., et al. (2018). PHA-4/FoxA senses nucleolar stress to regulate lipid accumulation in Caenorhabditis elegans. Nat. Commun. *9*, 1–17.

Wu, Q., Cao, X., Yan, D., Wang, D., and Aballay, A. (2015). Genetic screen reveals link between the maternal effect sterile gene mes-1 and pseudomonas aeruginosa-induced neurodegeneration in caenorhabditis elegans. J. Biol. Chem. *290*, 29231–29239.

Xu, A., Shi, G., Liu, F., and Ge, B. (2013). Caenorhabditis elegans mom-4 is required for the activation of the p38 MAPK signaling pathway in the response to Pseudomonas aeruginosa infection. Protein Cell *4*, 53–61.

Xu, Y., He, Z., Song, M., Zhou, Y., and Shen, Y. (2019). A microRNA switch controls dietary restriction-induced longevity through Wnt signaling. EMBO Rep. *20*.

Yang, X.D., Huang, S., Lo, M.C., Mizumoto, K., Sawa, H., Xu, W., Robertson, S., and Lin, R. (2011). Distinct and mutually inhibitory binding by two divergent β-catenins coordinates TCF levels and activity in C. elegans. Development *138*, 4255–4265.

Yang, X.D., Karhadkar, T.R., Medina, J., Robertson, S.M., and Lin, R. (2015). β-Cateninrelated protein WRM-1 is a multifunctional regulatory subunit of the LIT-1 MAPK complex. Proc. Natl. Acad. Sci. U. S. A. *112*, E137–E146.

Yip, K.Y., Alexander, R.P., Yan, K.-K., and Gerstein, M. (2010). Improved Reconstruction of In Silico Gene Regulatory Networks by Integrating Knockout and Perturbation Data. PLoS One *5*, e8121.

Yuan, H.-X., Xiong, Y., and Guan, K.-L. (2013). Nutrient Sensing, Metabolism, and Cell Growth Control. Mol. Cell *49*, 379–387.

Yuh, C.H., Dorman, E.R., Howard, M.L., and Davidson, E.H. (2004). An otx cis-

regulatory module: a key node in the sea urchin endomesoderm gene regulatory network. Dev. Biol. *269*, 536–551.

Zaret, K. (1999). Developmental competence of the gut endoderm: Genetic potentiation by GATA and HNF3/fork head proteins. Dev. Biol. *209*, 1–10.

Zhang, Y. (2008). I-TASSER server for protein 3D structure prediction. BMC Bioinformatics *9*, 40.

Zhang, N., Mendieta-Esteban, J., Magli, A., Lilja, K.C., Perlingeiro, R.C.R., Marti-Renom, M.A., Tsirigos, A., and Dynlacht, B.D. (2020). Muscle progenitor specification and myogenic differentiation are associated with changes in chromatin topology. Nat. Commun. *11*, 1–18.

Zhang, P., Judy, M., Lee, S.J., and Kenyon, C. (2013). Direct and indirect gene regulation by a life-extending foxo protein in C. elegans: Roles for GATA factors and lipid gene regulators. Cell Metab. *17*, 85–100.

Zheng, M., Messerschmidt, D., Jungblut, B., and Sommer, R.J. (2005). Conservation and diversification of Wnt signaling function during the evolution of nematode vulva development. Nat. Genet. *37*, 300–304.

Zhong, M., Niu, W., Lu, Z.J., Sarov, M., Murray, J.I., Janette, J., Raha, D., Sheaffer, K.L., Lam, H.Y.K., Preston, E., et al. (2010). Genome-Wide Identification of Binding Sites Defines Distinct Functions for Caenorhabditis elegans PHA-4/FOXA in Development and Environmental Response. PLoS Genet. *6*, e1000848.

Zhou, H.M., and Walthall, W.W. (1998). UNC-55, an orphan nuclear hormone

receptor, orchestrates synaptic specificity among two classes of motor neurons in Caenorhabditis elegans. J. Neurosci. *18*, 10438–10444.

Zhou, Y., Wang, X., Song, M., He, Z., Cui, G., Peng, G., Dieterich, C., Antebi, A., Jing, N., and Shen, Y. (2019). A secreted microRNA disrupts autophagy in distinct tissues of Caenorhabditis elegans upon ageing. Nat. Commun. *10*, 1–14.

Zhu, X., and Rosenfeld, M.G. (2004). Transcriptional control of precursor proliferation in the early phases of pituitary development. Curr. Opin. Genet. Dev. *14*, 567–574.

Zhu, J., Hill, R.J., Heid, P.J., Fukuyama, M., Sugimoto, A., Priess, J.R., and Rothman, J.H. (1997). end-1 encodes an apparent GATA factor that specifies the endoderm precursor in Caenorhabditis elegans embryos. Genes Dev. *11*, 2883–2896.